NAVAL POSTGRADUATE SCHOOL
Monterey, California

DTIC
ELECTE
FEB 28 1992
S
B
D

THESIS

RADAR TARGET IDENTIFICATION
BY NATURAL RESONANCES :
EVALUATION OF SIGNAL PROCESSING ALGORITHMS

by

Gregory A. Lazarakos

September, 1991

Thesis Advisor: Michael A. Morgan

Approved for public release; distribution is unlimited

92-04982

92 2 25 209

REPORT DOCUMENTATION PAGE

1a. REPORT SECURITY CLASSIFICATION UNCLASSIFIED	1b. RESTRICTIVE MARKINGS
2a. SECURITY CLASSIFICATION AUTHORITY	3. DISTRIBUTION/AVAILABILITY OF REPORT
2b. DECLASSIFICATION/DOWNGRADING SCHEDULE	Approved for public release; distribution is unlimited.

4. PERFORMING ORGANIZATION REPORT NUMBER(S)	5 MONITORING ORGANIZATION REPORT NUMBER(S)

6a. NAME OF PERFORMING ORGANIZATION Naval Postgraduate School	6b. OFFICE SYMBOL (If applicable) 3A	7a. NAME OF MONITORING ORGANIZATION Naval Postgraduate School
6c. ADDRESS (City, State, and ZIP Code) Monterey, CA 93943-5000		7b. ADDRESS (City, State, and ZIP Code) Monterey, CA 93943-5000

8a. NAME OF FUNDING/SPONSORING ORGANIZATION	8b. OFFICE SYMBOL (If applicable)	9 PROCUREMENT INSTRUMENT IDENTIFICATION NUMBER
8c. ADDRESS (City, State, and ZIP Code)		10 SOURCE OF FUNDING NUMBERS

Program Element No	Project No	Task No	Work Unit Accession Number

11. TITLE (Include Security Classification)
RADAR TARGET IDENTIFICATION BY NATURAL RESONANCES: EVALUATION OF SIGNAL PROCESSING ALGORITHMS

12. PERSONAL AUTHOR(S) Gregory A. Lazarakos

13a. TYPE OF REPORT Master's Thesis	13b. TIME COVERED From To	14. DATE OF REPORT (year, month, day) September 1991	15. PAGE COUNT 109

16. SUPPLEMENTARY NOTATION
The views expressed in this thesis are those of the author and do not reflect the official policy or position of the Department of Defense or the U.S. Government.

17. COSATI CODES			18. SUBJECT TERMS (continue on reverse if necessary and identify by block number)
FIELD	GROUP	SUBGROUP	Natural Resonances, Noncooperative Target Recognition, Pole Extraction, Kumaresan-Tufts Algorithm, Cadzow-Solomon Algorithm

19. ABSTRACT (continue on reverse if necessary and identify by block number)

When a radar pulse impinges upon a target, the resultant scattering process can be solved as a linear time-invariant (LTI) system problem. The system has a transfer function with poles and zeros. Previous work has shown that these poles are independent of the exciting waveform and target's aspect, but they are dependent on the target's structure and geometry. This thesis evaluates the resonance estimation performance of two signal processing techniques: the Kumaresan-Tufts algorithm and the Cadzow-Solomon algorithm. Both algorithms are programmed using MATLAB. Test data used to evaluate these algorithms includes synthetic and integral equation generated signals, with and without additive noise, in addition to new experimental scattering data from a thin-wire, aluminum spheres and scale model aircraft.

20. DISTRIBUTION/AVAILABILITY OF ABSTRACT ☒ UNCLASSIFIED/UNLIMITED ☐ SAME AS REPORT ☐ DTIC USERS	21 ABSTRACT SECURITY CLASSIFICATION UNCLASSIFIED
22a. NAME OF RESPONSIBLE INDIVIDUAL M. A. Morgan	22b. TELEPHONE (Include Area code) (408) 646-2677	22c OFFICE SYMBOL EC/Mw

DD FORM 1473, 84 MAR   83 APR edition may be used until exhausted   SECURITY CLASSIFICATION OF THIS PAGE
All other editions are obsolete   UNCLASSIFIED

i

Radar Target Identification
by Natural Resonances:
Evaluation of Signal Processing Algorithms

by

Gregory A. Lazarakos
Lieutenant JG, Hellenic Navy

Submitted in partial fulfillment
of the requirements for the degree of

MASTER OF SCIENCE IN SYSTEMS ENGINEERING
(ELECTRONIC WARFARE)

from the
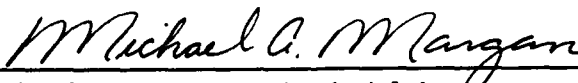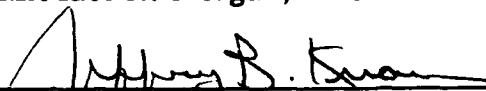
NAVAL POSTGRADUATE SCHOOL
September 1991

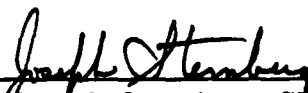Author: _____
Gregory A. Lazarakos

Approved by: _____
Michael A. Morgan, Thesis Advisor

_____
Jeffrey B. Knorr, Second Reader

_____
Joseph Sternberg, Chairman
Electronic Warfare Academic Group

ii

ABSTRACT

When a radar pulse impinges upon a target, the resultant scattering process can be solved as a linear time-invariant (LTI) system problem. The system has a transfer function with poles and zeros. Previous work has shown that the poles are independent of the exciting waveform and target's aspect, but they are dependent on the target's structure and geometry. This thesis evaluates the resonance estimation performance of two signal processing techniques: the Kumaresan-Tufts algorithm and the Cadzow-Solomon algorithm. Improvements are made to the Cadzow-Solomon algorithm. Both algorithms are programmed using MATLAB. Test data used to evaluate these algorithms includes synthetic and integral equation generated signals, with and without additive noise, in addition to new experimental scattering data from a thin wire, aluminum spheres and scale model aircraft.

iii

TABLE OF CONTENTS

LIST OF FIGURES

I. INTRODUCTION

When a radar pulse impinges upon a target, the resultant scattering process can be solved as a linear time-invariant (LTI) system problem. The system has a transfer function with poles and zeros. This description is provided by the Singularity Expansion Method (SEM) developed by Dr. Carl Baum [Ref. 1], of the Air Force Weapons Laboratory at Kirtland Air Force Base. Baum's SEM describes the induced current and scattered field using damped sinusoidal waveforms which resonate with complex natural frequencies unique to the object. These frequencies are determined by the object's composition and structural geometry. Natural frequencies are also the complex poles of the transfer function. These poles are independent of the incident electromagnetic excitation, including aspect and polarization, as initially postulated by Moffatt and Mains [Ref. 2]. Morgan [Ref. 3] has shown that a target scattering response (following illumination) can be represented as a weighted expansion of complex natural resonances whose poles are independent of the incident electromagnetic excitation. The problem of classifying a radar target can be solved, in principle, by determining the pole positions of the target's response.

1

Although this idea is not new, early attempts to demonstrate the practicability of such an identification system have produced poor results due to the presence of noise in the system. Two separate signal processing algorithms have been developed by Kumaresan-Tufts [Ref. 4] and Cadzow-Solomon [Ref. 5] to locate target poles with a high degree of accuracy, in the presence of noise. The Kumaresan-Tufts algorithm is intended for purely auto-regressive (AR) signals, while the Cadzow-Solomon algorithm is intended for auto-regressive moving-average (ARMA) signals. This thesis evaluates the viability of these two signal processing techniques by using new experimental electromagnetic scattering data. The use of this method improves identification of natural resonances in noisy signals with the correct selection of problem parameters.

A. THE PROBLEM

The approach employed to classify radar targets is comprised of two steps, based on natural resonances. The first step locates the position of the poles of the targets of interest. Numerical analysis of integral equation techniques will derive the poles for simple targets, e.g., a thin wire. For more complicated targets such as aircraft, the poles must be extracted from actual measurements of the target's response to incident electromagnetic excitation. The information

2

collected can then be used to form a database for comparison to the data *obtained in actual field use.*

The second step for target classification is the comparison of the data obtained in field measurements with the data contained in the database. The target is classified based on the closest data match. One method of accomplishing the classification is to use the same signal processing technique that was used to form the database initially. Speed is an important factor in the classification process, as the time required to achieve classification must be less than the time for the target to become a threat. Another, more efficient way to perform the comparison is to employ the use of annihilation filters, as proposed by Morgan and Dunavin [Ref. 6]. This approach employs energy cancellation based upon the location of the target's poles. For example, a total target response (including early-time and late-time) may be subjected to a bank of annihilation filters. The filter that corresponds to the proper target will exhibit, in theory, a response coincident with the driven portion of the target response while annihilating the signal during the late-time portion of the response.

A system used for classification of radar targets would require a bank of annihilation filters corresponding to each class of target. The system could then determine the class of target, based on the filter producing the minimal amount of output energy.

3

B. BACKGROUND

Transient electromagnetic scattering can be described by showing an incident field in free space illuminating a perfectly conductive finite-sized object. Figure 1 depicts induced current on a scattering body. The magnetic field integral equation (MFIE)
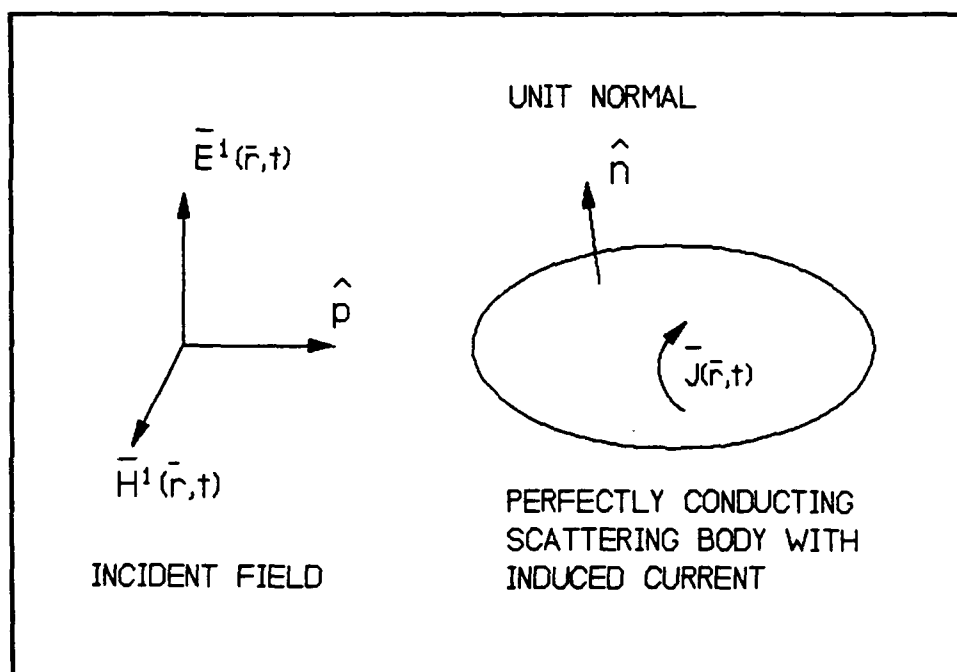
Figure 1   Transient electromagnetic scattering

describes induced current on the surface of a scattering body as:

$$\mathcal{J}(\bar{r}, t) = 2\hat{n} \times \bar{H}^i(\bar{r}, t) + \iint_{S_{PV}} \bar{\bar{K}}(\bar{r}, \bar{r}', t) \cdot \mathcal{J}(\bar{r}, t - \frac{|\bar{r} - \bar{r}'|}{c}) \cdot \overline{dS} \qquad (1)$$

where,

- $\mathcal{J}$ is the electric current density,

- $\hat{n}$ is the unit normal vector outward to the surface,

4

- $\overline{H}^i$ is the incident magnetic field intensity at the surface,

- $\overline{\overline{K}}$ is the dyadic Green's function kernel

and, the principal-value (PV) type integral excludes the point $\overline{r}=\overline{r}'$. The cross product, $2\hat{n}\times\overline{H}^i$, represents the physical optics portion of the induced current. The principal-value surface integral, S_{PV}, represents the contribution due to induced physical optics currents other than the contribution from the cross product. This current represents "feedback" effects from currents at other points on the object.

When $\overline{H}^i=0$, Equation (1) solutions become the source-free ("natural") current modes of the scattering problem. These modes may be described by the sum of the exponentially damped sinusoids, or: $\overline{J}_n(\overline{r})\exp(s_nt)$, where s_n are the poles or natural resonance frequencies in complex conjugate pairs of the form

$$s_n=\sigma_n+j\cdot\omega_n. \qquad (2)$$

where,

- σ_n = the damping rate in Nepers/sec,

- ω_n = the frequency in radians/sec.

These resonance frequencies are functions of the geometry and composition of the scattering object. Although the number of poles is, in theory, infinite for any given object, only a

finite subset will be excited, due to the finite bandwidth of the incident field.

Figure 2 represents a plane wave impulse illumination, in which part of the object has been illuminated from the
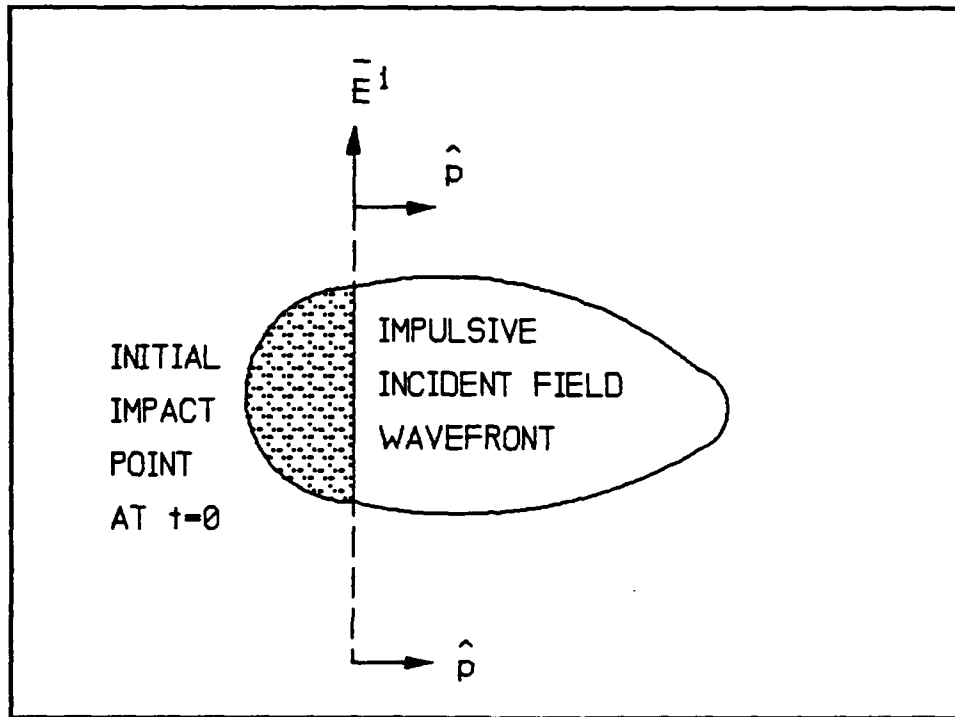
Figure 2 Plane wave impulse illumination

incident field wavefront. The scattered field is composed of two parts: the early-time driven response and the late-time natural mode response. The early-time driven response occurs as the excitation wavefront travels over the object and each point becomes excited. The late-time natural mode response occurs, by definition, when the excitation has been completed over the complete body. Throughout the early-time phase, the impulsive plane wave incident field will be identically zero at all points on the surface except on the conformal ring

6

where the intersection with the wavefront occurs. This area is indicated by the dotted line in Figure 2. This conformal ring changes cross-sectional shape and position as the wavefront moves. The induced surface current on the ring is therefore composed of the physical optics term plus the feedback current, as described in Equation (1). Thus, no induced current is present at the area of the object ahead of the wavefront.

The back-scattered far-field, resulting from the surface current on the object, will be of the form

$$\overline{H}^s(-r\hat{p}, t) = \frac{1}{4\pi cr} \cdot \frac{\partial}{\partial t} \iint\limits_{S} \hat{p} \times \overline{J}(\overline{r}', t - \frac{|\overline{r} - \overline{r}'|}{c}) \cdot \overline{dS'}. \qquad (3)$$

The unit vector $\hat{p}$ indicates the direction of the plane wave's propagation. The back-scattered far-field for a fixed point is then a result of integrating the current at every point on the object's surface. Thus, the back-scattered far-field will be of the form

$$\overline{H}^s(-r\hat{p}, t) = u(t - \frac{r}{c}) \cdot [\overline{H}_{po}(-r\hat{p}, t) + \sum_{\substack{n=-\infty \\ n\neq 0}}^{\infty} \overline{H}_n(-r\hat{p}, t) \exp(s_n t)]. \qquad (4)$$

Two individual terms emerge from these calculations. The first term in Equation (4) represents the physical optics scattered field generated by the $2\hat{n} \times \overline{H}^i$ driven current. The second term represents the scattered field produced by the

7

source-free wake current or "feedback" current. The physical optics scattered field is highly aspect dependent.

During the early-time portion of the target's response, the scattered field produced by the "feedback" current term in Equation (4) contains exponential resonance terms with time-varying coefficients $\overline{H}_n$, as described by the Singularity Expansion Method (SEM) [Ref. 1]. This form of the SEM expansion is termed "Class 2" and is presented analytically by Morgan [Ref. 7]. For the monostatic scattering case, the transition from early-time to late-time in the target's response will occur at

$$\Delta t = \tau + (1 + \cos\alpha) \cdot \frac{D}{c}, \tag{5}$$

after the leading edge of the scattered pulse returns to the radar antenna, where,

- τ is the incident pulse width,
- D is the target's largest dimension, and
- α is the aspect of the target.

The term α also represents the angle between the target's largest dimension and the direction of wave propagation, where c is the velocity of propagation or speed of light. At this transition time, the physical optics field vanishes. During the late-time portion of the target's response only the second term in Equation (4) remains. However, it is now comprised of

8

constant coefficients, $\overline{H}_n$. This form of the late-time SEM expansion is termed "Class 1".

The early-time scattered field is therefore constituted of both a physical optics term and a "Class 2" SEM expansion with time-varying coefficients, while the late-time scattered field is described by a simple "Class 1" SEM expansion with constant coefficients.

II. POLE EXTRACTION ALGORITHMS

Obtaining the target response is the first step to be completed in a Non-Cooperative Target Recognition (NCTR) system. Once the response is obtained in time domain, the target's poles may be located. Numerically, these poles may be described by the damping rate σ and the radian frequency ω or, in other words, the complex number indicating the pole's location in the s-plane or z-plane. The location of the poles may also be described analytically by solving the boundary-value electromagnetic problem. This may be easily done only for simple shape targets like thin wires and spheres. However, for general targets, detailed knowledge of the target's composition (dimensions and materials) and, also, access to a large amount of computing power is required.

The next section of this thesis discusses the analytical method which is used to compare the poles extracted from measurements taken with a thin wire. The viability of the Cadzow-Solomon algorithm will also be tested.

A. EARLY METHODS

The NCTR system is used to discriminate and to classify targets with relatively similar shapes and dimensions. In

such cases, the location of the poles from these targets will be relatively close, requiring a high degree of precision in measurement and estimation. A basic method in signal processing is to obtain the signal's spectrum using the Fast Fourier Transform (FFT). The FFT algorithm yields results in a short amount of time. However, the FFT may be used only as a tool to add information to the basic methodology when locating radar target natural resonances. This is because the frequency resolution, equal to the reciprocal of the time interval between the samples, is of the order of several MHz or higher. Another limitation of the FFT is that it provides only real frequencies within a signal, while both the damping rate and the frequency of the poles are required for target classification.

Thus, other methods providing more accurate results needed to be developed.

1. Direct Minimization

As previously described, the transient scattered signal waveform will have the form

$$y(t) = y_E(t) \, [u(t) - u(t - T_0)] + y_L(t) \cdot u(t - T_0) + N(t) \qquad (6)$$

where,

- $y_E(t)$ is the early-time portion,

- $y_L(t)$ is the late-time portion and

- $N(t)$ is the undesirable noise and clutter.

11

Morgan [Ref. 7] presents the way to determine the natural resonance parameters by modeling the late-time scattering response as a sum of damped sinusoids,

$$\hat{y}_L(t) = \sum_{n=1}^{\infty} A_n \cdot \exp(\sigma_n t) \cdot \cos(\omega_n t + \phi_n) \tag{7}$$

where $\hat{y}$ represents the modeled signal and $A_n \cdot \exp(j\phi_n)$ represents the aspect dependent residues. The digital domain form of the model is

$$\hat{y}(k \cdot \Delta t) = \hat{y}_k = \sum_{n=1}^{N} A_n \cdot \exp(\sigma_n \cdot k\Delta t) \cdot \cos(\omega_n \cdot k\Delta t + \phi_n) \tag{8}$$

where,

- A_n is the amplitude,

- σ_n is the damping rate,

- ω_n is the radial frequency, and

- ϕ_n is the phase.

After comparing the modeled signal $\hat{y}_n$ to the actual received discrete signal y_n, the mean square error may be obtained as $e_n^2 = (y_n - \hat{y}_n)^2$. The four parameters of the model $(A_n, \phi_n, \sigma_n, \omega_n)$ may then be adjusted in order to derive the mean square error minimum. As this is a multi-dimensional, highly non-linear minimization problem, it is computationally inefficient.

12

2. Prony's Method

Blaricum and Mittra [Ref. 8] present a novel approach for systematically deriving the complex poles and residues of a target from a set of time domain data. The method is based on Prony's algorithm, used to model the late-time response of a radar target. The set of time domain data is the discrete set of sampled transient values of the impulse response $I(t_n)$ or I_n. The method is based on the fact that I_n must satisfy a difference equation of order N, written as

$$\sum_{p=0}^{N-1} a_p \cdot I_{p+k} = -I_{N+k} , \qquad (9)$$

where $p+k=0,1,\ldots,2N-1$ and $2N$ are the data samples used. This leads to the solution of a matrix equation

$$\begin{bmatrix} I_1 & I_2 & \cdots & I_N \\ I_2 & I_3 & \cdots & I_{N+1} \\ \vdots & \vdots & \ddots & \vdots \\ I_N & I_{N+1} & \cdots & I_{2N-1} \end{bmatrix} \cdot \begin{bmatrix} a_N \\ a_{N-1} \\ \vdots \\ a_1 \end{bmatrix} = \begin{bmatrix} I_{N+1} \\ I_{N+2} \\ \vdots \\ I_{2N} \end{bmatrix} . \qquad (10)$$

After the coefficients a_i are found, the method solves the roots of a polynomial as

$$z^N - a_1 z^{N-1} - \cdots - a_N = 0 . \qquad (11)$$

If d_m ($m=1,2,\ldots,N$) represents those roots, then the poles of the system model in the z-plane are the roots d_m. The poles in the s-plane may be found using the formula

13

$$s_m = \frac{\ln(d_m)}{\Delta t},$$ (12)

where Δt is the time-stepping interval used in obtaining the sampled data. The matrix in Equation (10) is in the form of a transposed Vandermonde matrix, whose inverse can be computed in closed form. This method requires at least 2N equally spaced transient data samples to find N poles. If greater than 2N samples are desired, then one may obtain a least squares type fit to the matrix in Equation (10). Since the system order is not known **a priori** in the NCTR problem, Blaricum and Mittra [Ref. 9] present two schemes for determining the number of poles contained in the transient response. The first is the Householder orthogonalization method, and the second is an eigenvalue method. When the data are noisy, Blaricum and Mittra [Ref. 9] indicate that the eigenvalue method is the better method. This method will be discussed in Section 3 of this chapter when a bias compensation method is examined.

3. Kumaresan-Tufts Algorithm

Kumaresan and Tufts [Ref. 4] modified Prony's method by using the "backward linear prediction" technique and "singular value decomposition" (SVD) to alleviate the sensitivity to noise and the need for **a priori** knowledge of the system order.

14

Analytically, Kumaresan-Tufts algorithm modifies Prony's method as follows:

- The system order is intentionally overestimated. The excess order provides the flexibility to the system to model the noise, improving the estimation of parameters of exponentially damped sinusoidal signals in noise.

- Singular value decomposition alleviates severe ill-conditioning of the data matrix.

- The causality of the system is used to separate the computed signal's poles from the spurious computed noise poles introduced by the overestimated system order.

The separation of the signal poles from the noise poles is the result of the "backward prediction" that causes the signal poles to fall outside the unit circle in the z-plane, while the extraneous "noise poles" fall inside the unit circle.

Moderately large values of system order are essential in improving the accuracy of the pole location estimates.

a. System Model

Suppose that the N samples of the observed time domain data of a response signal $y(n)$ consists of samples of M exponentially damped signals in white Gaussian noise $w(n)$, as represented by

$$y(n) = \sum_{k=1}^{M} a_k \cdot \exp(s_k n) + w(n), \quad n=0,1,\ldots,N-1. \tag{13}$$

The following linear prediction equations can be formed, using real time domain data in the backward direction.

15

$$
\begin{bmatrix}
y(2) & y(3) & \dots & y(L+1) \\
y(3) & y(4) & \dots & y(L+2) \\
\vdots & \vdots & \ddots & \vdots \\
y(N-L+1) & \dots & \dots & y(N)
\end{bmatrix}
\begin{bmatrix}
a(1) \\
a(2) \\
\vdots \\
a(L)
\end{bmatrix}
= -
\begin{bmatrix}
y(1) \\
y(2) \\
\vdots \\
y(N-L)
\end{bmatrix}
\tag{14}
$$

The terms of the above equation may be also represented by

$$
D \cdot a = -h \tag{14a}
$$

where,

- D is the data matrix $(N-L) \times L$,

- a is the vector of backward prediction coefficients $(L \times 1)$, and

- h the data vector $(N-L) \times 1$.

In the above matrix equation, L represents the overestimated system order, chosen to satisfy the inequality M≤L≤N-M. The matrix equation is solved with the SVD method, using the pseudoinverse matrix D^+, as $a = D^+ \cdot (-h)$. Here the coefficients a_i correspond to those in Equation (11), where the roots of the polynomial define the poles of the system model in the z-plane.

As with Prony's method, the Kumaresan-Tufts method is intended for purely auto-regressive (AR) signals. Both methods, therefore, use the late-time portion of the response signal when addressing the target classification problem.

b. Singular Value Decomposition

Singular value decomposition (SVD) is the basic technique on which the Kumaresan-Tufts algorithm is based. There are two main advantages with SVD:

- It helps to alleviate the effects of ill-conditioning of the data matrix.

- It separates the signal poles from the noise poles.

The following discussion of SVD is a synopsis of material taken from Strang [Ref. 10].

The SVD is closely associated with the eigenvalue-eigenvector factorization of a symmetric matrix : $A=Q \cdot \Lambda \cdot Q^T$. SVD makes a similar factorization, but for any ($m{\times}n$) matrix A, as follows:

$$A=Q_1 \cdot \Sigma \cdot Q_2^T \qquad\qquad (15)$$

where Q_1, Q_2 are two orthogonal matrices and Σ is the diagonal (but rectangular) matrix with its positive entries (also called sigma, in the form of $\sigma_1, \sigma_2, \ldots, \sigma_r$). These entries are the singular values of A, filling the first r places on the main diagonal of Σ, where r is the rank of A. These entries sigma are also the square roots of the nonzero eigenvalues of both AA^T and A^TA. The columns of Q_1 ($m{\times}m$) are eigenvectors of AA^T, and the columns of Q_2 ($n{\times}n$) are eigenvectors of A^TA.

The SVD works well for numerically stable computations. An initial reason is that Q_1 and Q_2 are orthogonal matrices that never change the length of a vector. Since $||Qx||^2 = x^T Q^T Q x = ||x||^2$, multiplication by Q cannot destroy the scaling. A second reason is that SVD gives a more stable measure of the rank of A.

The prime use of SVD is to solve every linear system in the form of $Ax = b$. For every matrix A (m × n), which can be factored into $A = Q_1 \cdot \Sigma \cdot Q_2^T$, another matrix can be defined. This matrix will be the pseudoinverse of A, as follows:

$$A^+ = Q_2 \cdot \Sigma^+ \cdot Q_1^T \qquad (16)$$

where, Q_1, Q_2 are the same orthogonal matrices found with the SVD. The value Σ^+ is the diagonal (n × m) matrix, with its entries on the main diagonal being $\frac{1}{\sigma_1}, \frac{1}{\sigma_2}, \ldots, \frac{1}{\sigma_r}$. The optimal solution of $Ax = b$ is

$$x^+ = A^+ \cdot b \qquad (17)$$

that is, the minimum length solution to the nearest equation, $A\bar{x} = p$. As the column space of A^+ is in the row space of A, then x^+ is always in the row space of A.

18

To solve the system of equations in Equation (14), the pseudoinverse of matrix D may be found as in Equation (16) in the form $D^+ = V \cdot \Sigma^+ \cdot U^T$, where Σ^+ will be a $(L \times (N-L))$ matrix, whose L singular values are the reciprocals of those found in the Σ matrix. The minimum length least squares solution of $D \cdot a = -h$ is $a = D^+ \cdot (-h) = V \cdot \Sigma^+ \cdot U^T \cdot (-h)$.

c. Bias Compensation

In the discussion of the SVD above, Σ is a $(N-L) \times L$ diagonal matrix, with its entries being the square roots of the nonzero eigenvalues of both DD^T and D^TD. In the noiseless case, the prediction equations are satisfied exactly. If the system order has been overestimated as L, when M is the actual order of the system, the diagonal of Σ splits into a signal subspace with M positive singular values of $\sigma_1, \sigma_2, \ldots, \sigma_M$ and a subspace with L-M zero values. For the noisy signal case, the first M positive signal values are perturbed into a noisy signal subspace

$$\sigma_1, \sigma_2, \ldots, \sigma_M \text{ with eigenvalues } \lambda_1' \geq \lambda_2' \geq \ldots \geq \lambda_M', \qquad (18)$$

and a noise subspace with L-M values

$$\sigma_{M+1}, \sigma_{M+2}, \ldots, \sigma_L \text{ with eigenvalues } \lambda_{M+1}' \geq \lambda_{M+2}' \geq \ldots \geq \lambda_L'. \qquad (19)$$

Kumaresan and Tufts noticed [Ref. 4] that the noise perturbed the signal's singular values, the reason for the

bias towards the unit circle in the z-plane in the pole position estimates. Kumaresan and Tufts proposed a compensation method which moves the poles back towards the center of the z-plane. This method is based on averaging the smallest L-M singular values, $\sigma_{M+1}, \sigma_{M+2}, \ldots, \sigma_L$, and then subtracting this average value from each of the first M singular values, $\sigma_1, \sigma_2, \ldots, \sigma_M$. The smallest L-M values are then set to zero and a new matrix, Σ, is used to compute the pseudoinverse D^+. Although Kumaresan and Tufts claim that this method gives better results, the testing completed for this thesis shows that the bias towards the center of the z-plane is greater than the bias error that the noise makes. This result causes much more perturbation on the pole position estimates.

Norton [Ref. 11] proposed another compensation method based on the Eigenvalue Shifting Theorem. The noisy data matrix may be described by $D=S+N$, where S is the noiseless signal data matrix and N is the noise data matrix of the wide-sense stationary white noise process, v_i, written as

$$N = \begin{bmatrix} v_1 & \cdots & v_L \\ \vdots & \ddots & \vdots \\ v_{N-L} & \cdots & v_N \end{bmatrix}.$$

(20)

The expected value of DD^T may be found from

$$DD^T = E[(S+N)(S+N)^T] = E[SS^T] + E[SN^T] + E[NS^T] + E[NN^T]. \quad (21)$$

As white noise has a mean of zero, the two terms $E[SN^T]$ and $E[NS^T]$ become zero. Since the noise is wide-sense stationary, $E[NN^T] = \sigma_v^2 \cdot I$, where σ_v is the noise variance and I is the identity matrix. As S is deterministic, $E[SS^T] = SS^T$. This leads to the formula

$$E[DD^T] = SS^T + \sigma_v^2 \cdot I. \quad (22)$$

The eigenvalue shifting theorem [Ref. 11] describes the case when the eigenvalues of SS^T are λ_i, where the eigenvalues of $E[DD^T]$ are $\lambda_i + \sigma_v^2$. Therefore, the eigenvalues of DD^T, which are the squares of the singular values of D, are increased by the noise variance, σ_v^2.

In the noiseless case, these singular values would be zero. If the noise singular values are squared and averaged, an unbiased estimation of σ_v^2 may be obtained. Norton [Ref. 11] proposed correcting the signal singular values by first subtracting the noise variance σ_v^2 from the squares of the first M diagonal entries of matrix Σ and then taking the square root of the reduced values as the new

21

diagonal entries of matrix Σ (while the noise singular values are set to zero). As in the Kumaresan-Tufts bias compensation method, the pseudoinverse D^+ can be found from the new matrix Σ.

Although Norton's method seems to be a more correct bias compensation method, both methods are based on the fact that a decision has to be made about the actual order of the system. The separation between the signal eigenvalues and the noise eigenvalues is not readily obvious, because the eigenvalues of matrix DD^T or D^TD appear to steadily decrease.

d. Performance and Earlier Results

Kumaresan and Tufts tested the algorithm, obtaining good results using synthetic data with various levels of white Gaussian noise, as low as 15 dB SNR. Norton [Ref. 11] developed the algorithm as a computer subroutine and tested it with various sets and types of data. Synthetic data were tested at various SNR values, ranging from 90 dB to 7 dB. When the SNR decreased, the error in pole position estimates increased. Norton claimed that the algorithm gave good results for SNR≥20 dB. Norton also used simulations of thin wires produced by Morgan's Time-Domain thin wire integral equation (TDIE) computer program to test the algorithm. The results of those tests illustrated the aspect independence on estimated poles of the target, [Ref. 11].

Larison [Ref. 12] programmed the algorithm using Fortran and tested synthetic and thin wire integral equation data at various SNR's ranging from 90 dB to 7 dB. Like Norton, he claimed good results in extracting the low frequency poles position with SNR as low as 20 dB by using Norton's bias compensation method. Larison maintained that the two most critical parameters are:

- to select the appropriate starting point to begin the data processing

- to select the appropriate system order to provide the best possible results.

The algorithm has been tested by the author of this thesis, after developing the algorithm using MATLAB. The algorithm was tested using synthetic data at various SNR's ranging from 30 dB to 10 dB, without using the bias compensation method. The synthetic signal response is based on ten pole pairs within a frequency range of 1-10 GHz, with a medium Q damping factor using k=0.7. This chosen value of k simulates typical expected levels of damping from measured scattering responses of real targets (e.g., the thin wire). Damping factor and SNR level are discussed, in detail, in Chapter III, Section A, of this thesis. Table I shows the poles and residues used for the testing.

Figures 3 to 10 illustrate the evaluation of the Kumaresan-Tufts algorithm. Figures 3 to 6 illustrate the synthetic signal waveform for various SNR's. Figures 7 and 8 illustrate the spectrum of the synthetic signal for SNR=30 dB

23

and SNR=10 dB. Figures 9 and 10 illustrate the true and the algorithm poles in both the s-plane and z-plane, for various SNR's. For the above simulation, the values used for N and L were 300 and 60, respectively, while M (actual order) was 20. The simulation revealed that as the noise increases relative to the signal, there is a bias of all the poles towards the unit circle, specially the higher frequency poles.

Table I MEDIUM Q SYNTHETIC POLES

f_n [GHz]	σ_n [GNp/s]	ω_n [Grad/s]	A_n	ϕ_n
1	-0.3562	6.2752	1	0
2	-0.7124	12.5504	1	0
3	-1.0687	18.8256	1	0
4	-1.4249	25.1007	1	0
5	-1.7811	31.3759	1	0
6	-2.1373	37.6511	1	0
7	-2.4935	43.9263	1	0
8	-2.8498	50.2015	1	0
9	-3.2060	56.4767	1	0
10	-3.5622	62.7518	1	0
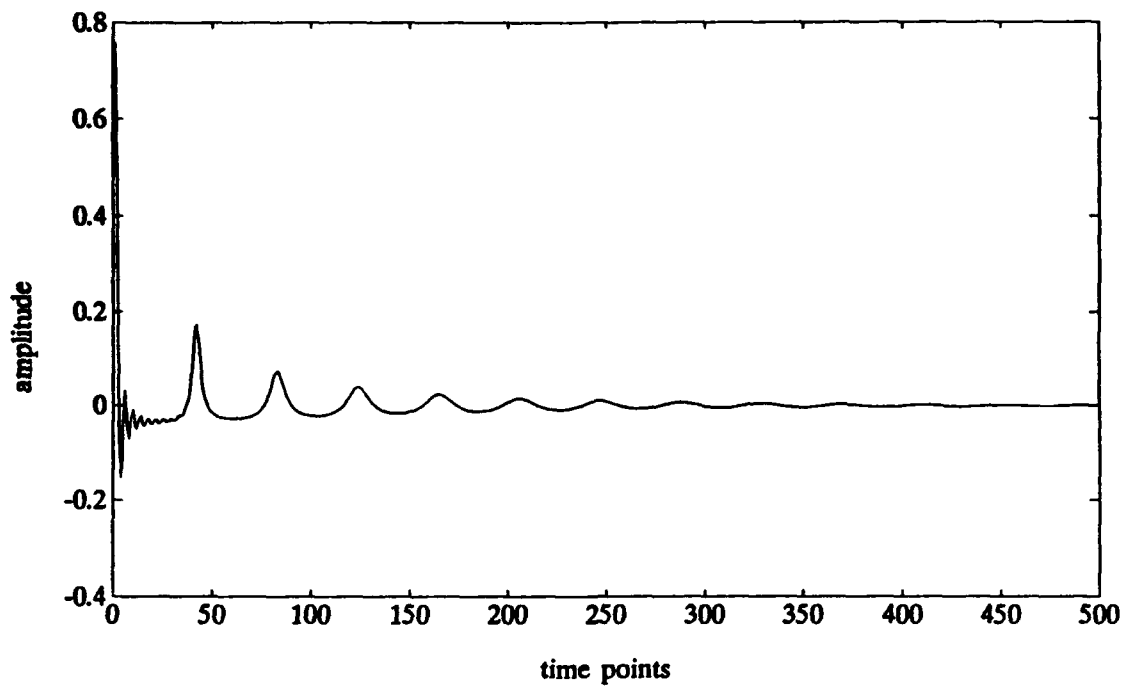
Figure 3   Generated synthetic signal without noise
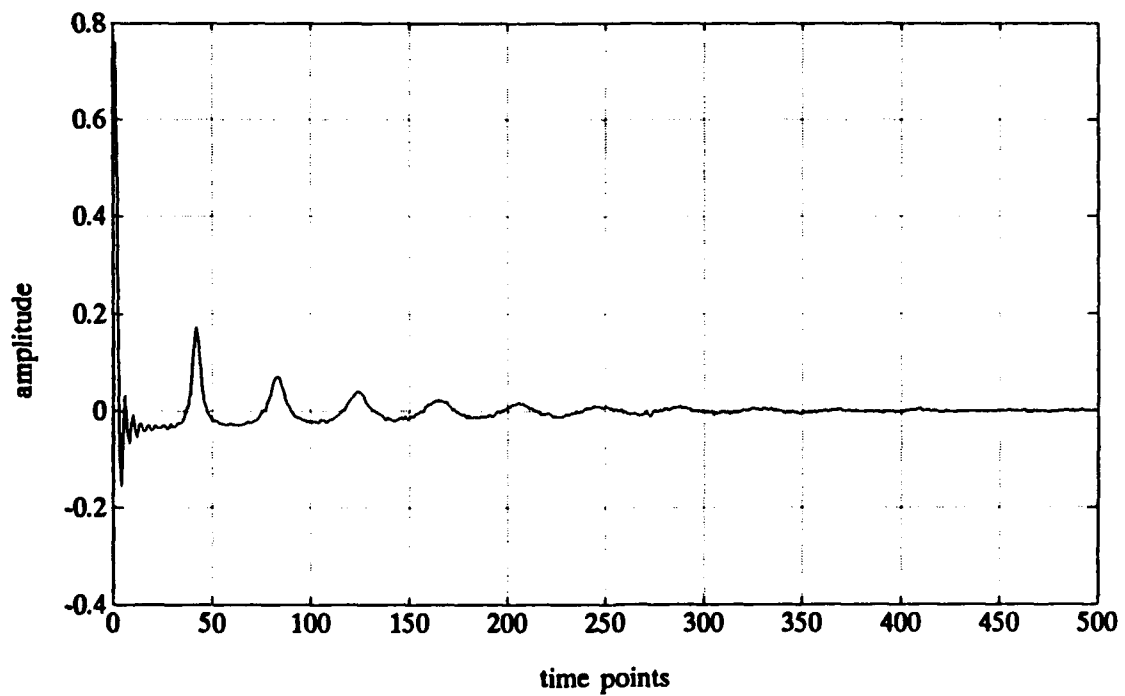
Figure 4   Generated synthetic signal with 30 dB SNR

25
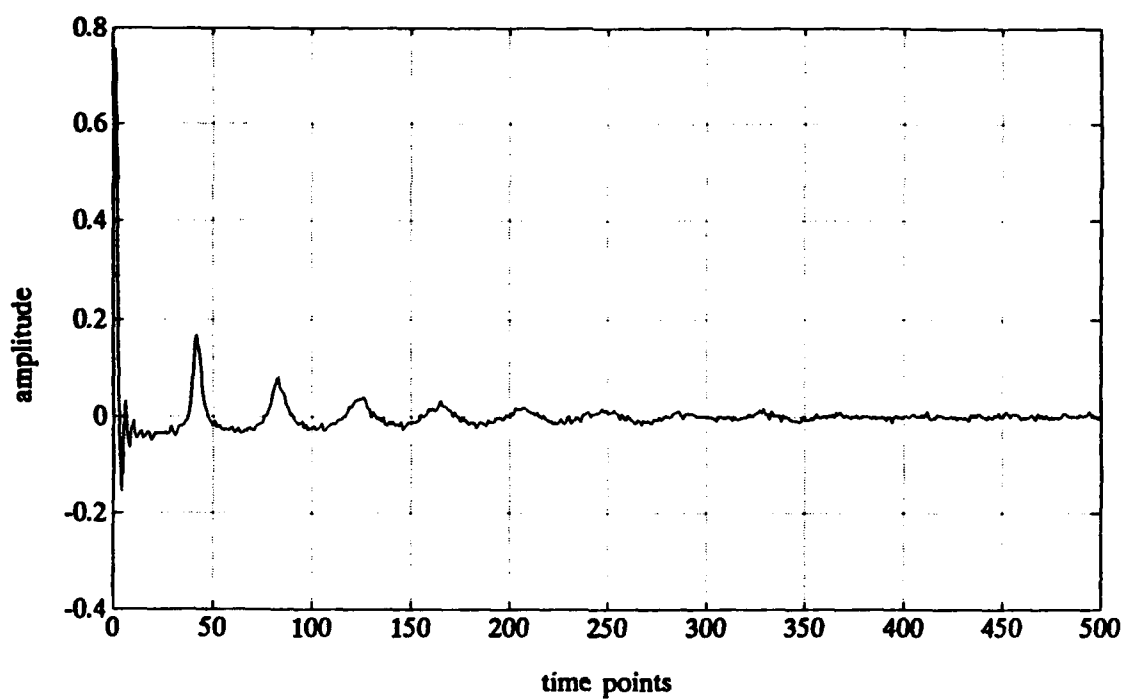
Figure 5   Generated synthetic signal with 20 dB SNR
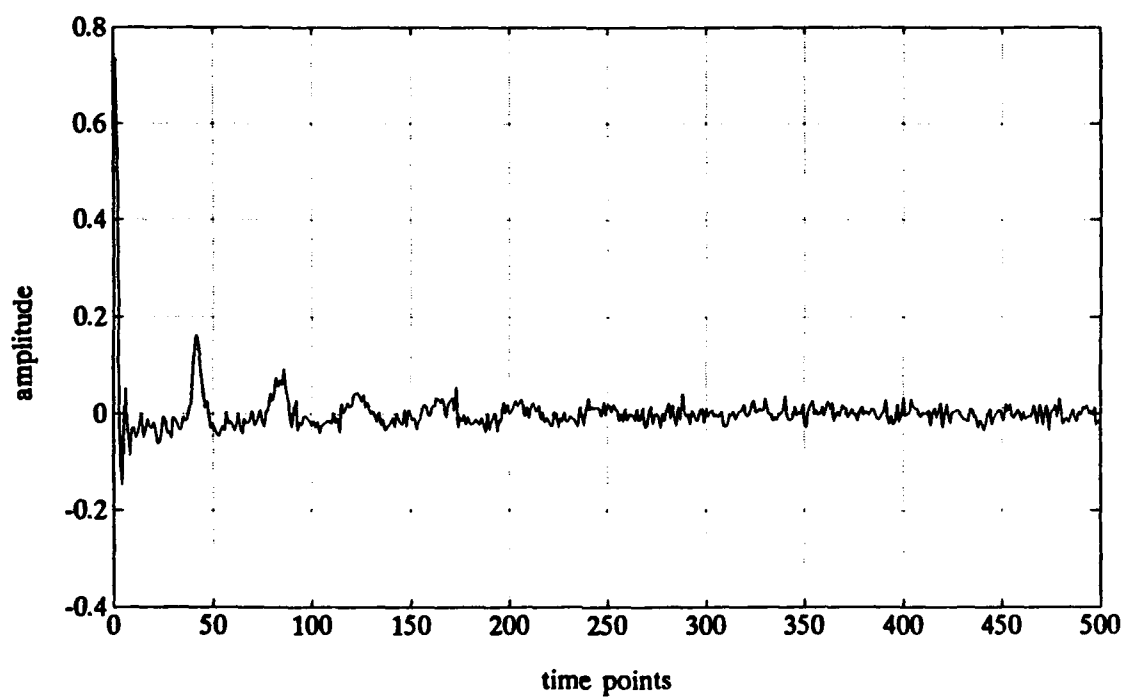
Figure 6   Generated synthetic signal with 10 dB SNR

26
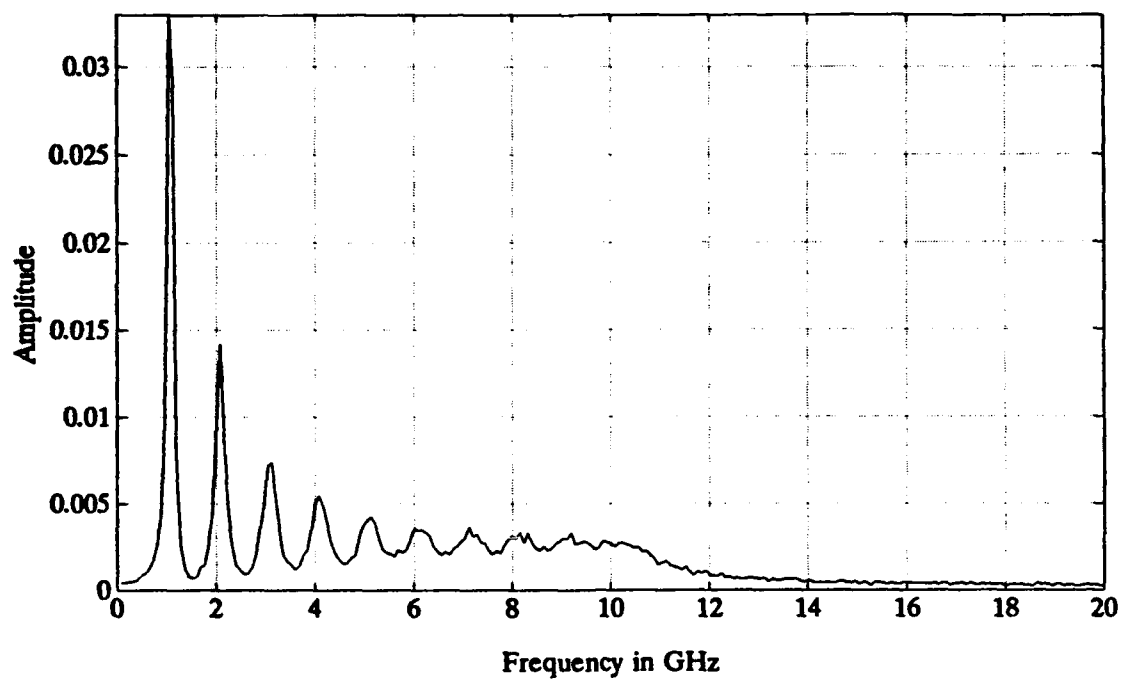
Figure 7   Spectrum of the SNR=30 dB synthetic signal
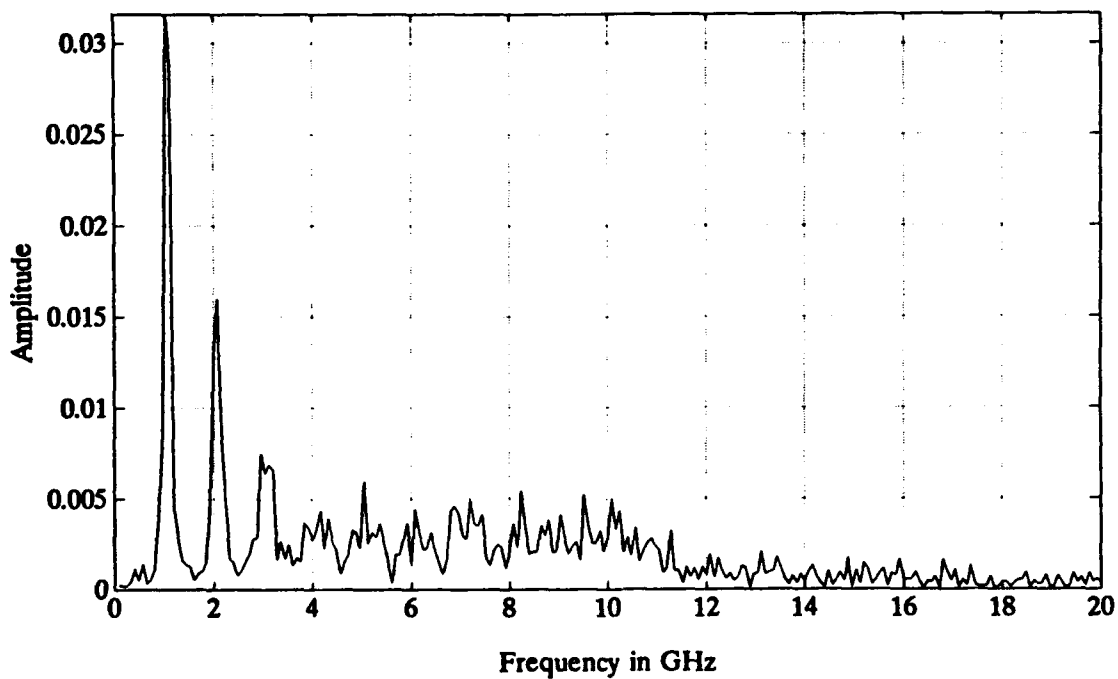
Figure 8   Spectrum of the SNR=10 dB synthetic signal
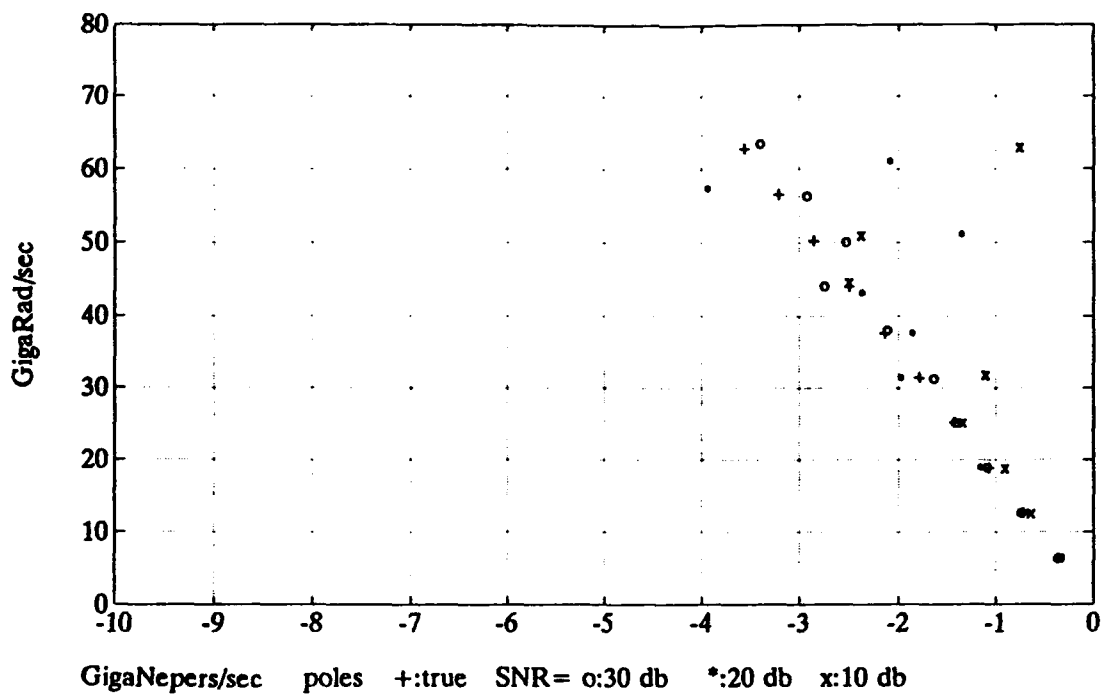
Figure 9   Kumaresan-Tufts poles in the s-plane

+:true poles   SNR= o:30 db   *:20 db   x:10 db
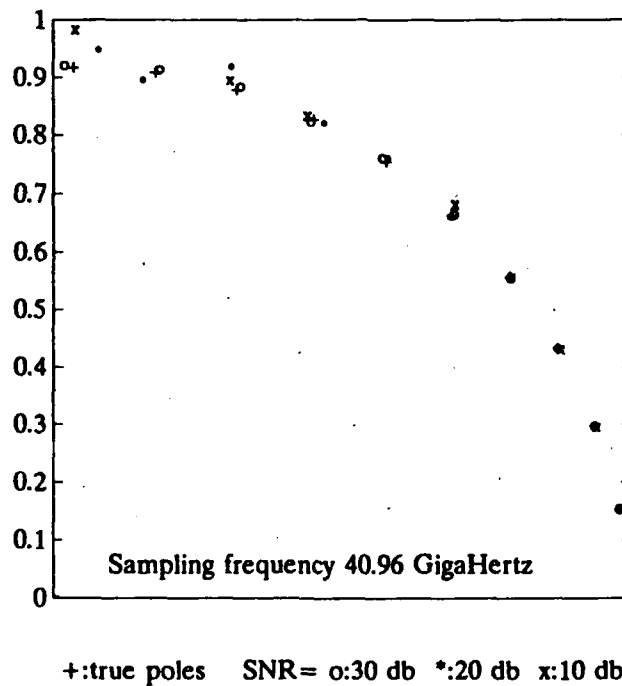
Figure 10   Kumaresan-Tufts poles in the z-plane

B. CADZOW-SOLOMON ALGORITHM

Many investigators have used both excitation and response data to identify linear systems. Cadzow and Solomon [Ref. 5] proposed an identification procedure in which both the excitation and response are contaminated by white noise. This method is based upon the null space characterization of an associated "data matrix". The Cadzow-Solomon algorithm is used in this thesis to simulate and demonstrate the identification problem.

1. System Model

The Cadzow-Solomon algorithm is based upon the Auto-Regressive Moving-Average (ARMA) model. In an ideal modeling situation, the assumption may be made that the excitation signal $x(n)$ and the response signal $y(n)$ are perfectly related by means of an ARMA relationship, such that

$$y(n) = \sum_{i=1}^{L} a_i y(n-i) + \sum_{i=0}^{K} b_i x(n-i), \tag{23}$$

as associated with the transfer function

$$H(z) = \frac{b_0 + b_1 z^{-1} + \ldots + b_K z^{-K}}{1 - a_1 z^{-1} - \ldots - a_L z^{-L}} \tag{24}$$

where,

- a_i are the coefficients which correspond to the poles of the transfer function, and

29

- b_i are the coefficients which correspond to the zeros of the transfer function.

The order of the numerator of the system's transfer function is K and the order of the denominator is L. The classic modeling problem is to identify the system's coefficients, a_i and b_i, from a finite set of observations of the excitation, $x(n)$, and response, $y(n)$, time series.

Cadzow-Solomon present the set of equations for the algorithm in matrix form as follows:

$$\begin{bmatrix} y(0) & y(-1) & \dots & y(-p) \\ y(1) & y(0) & \dots & y(1-p) \\ \vdots & \vdots & \ddots & \vdots \\ y(N) & y(N-1) & \dots & y(N-p) \end{bmatrix} \cdot \begin{bmatrix} 1 \\ a_1 \\ \vdots \\ a_p \end{bmatrix} = \begin{bmatrix} x(0) & x(-1) & \dots & x(-q) \\ x(1) & x(0) & \dots & x(1-q) \\ \vdots & \vdots & \ddots & \vdots \\ x(N) & x(N-1) & \dots & x(N-q) \end{bmatrix} \cdot \begin{bmatrix} b_0 \\ b_1 \\ \vdots \\ b_q \end{bmatrix} \quad (25)$$

or, more concisely

$$Y_p a_p = X_q b_q \qquad (26)$$

where,

- X_q is the (N+1)×(q+1) "excitation data matrix",

- Y_p is the (N+1)×(p+1) "response data matrix",

- a_p is the (p+1)×1 "auto-regressive parameter vector" and

- b_q is the (q+1)×1 "moving-average parameter vector".

The least squares solution for a causal, real data, overestimated ARMA model ($p \geq \overline{p}, q \geq \overline{q}$) can be found by taking a

30

linear algebraic approach based on the eigenvalue-eigenvector decomposition of the data matrix $D_{p,q} = [Y_p \vdots -X_q]$ as

$$D_{p,q}^T \cdot D_{p,q} \cdot u_k = \lambda_k \cdot u_k, \quad 1 \leq k \leq p+q+2.$$

(27)

The parameter vector is found from the procedure to be

$$\begin{bmatrix} a_p \\ \cdots \\ b_q \end{bmatrix} = \left[\sum_{k=1}^{p+q+2} \frac{|u_k(1)|^2}{\lambda_k} \right]^{-1} \sum_{k=1}^{p+q+2} \frac{u_k(1)}{\lambda_k} \cdot \overline{u_k}$$

(28)

where $\overline{u_k}$ is the eigenvector associated with the eigenvalue λ_k.

If the actual system order is $(\overline{p}, \overline{q})$, then the system order is less than the overestimated order (p, q). At least $s = 1 + \min(p-\overline{p}, q-\overline{q})$ of the eigenvalues in the decomposition, as described in Equation (27), must be identically zero for the noise-free case.

Following the technique of "backward prediction" as used in the Kumaresan-Tufts algorithm, the matrix equation (Equation 25) may be modified as follows:

$$\begin{bmatrix} y(2) & \ldots & y(L+1) \\ y(3) & \ldots & y(L+2) \\ \vdots & \ddots & \vdots \\ y(N-L+1) & \ldots & y(N) \end{bmatrix} \begin{bmatrix} x(1) & \ldots & x(K+1) \\ x(2) & \ldots & x(K+2) \\ \vdots & \ddots & \vdots \\ x(N-L) & \ldots & x(N-L+K) \end{bmatrix} \begin{bmatrix} a_1 \\ \vdots \\ a_L \\ b_0 \\ \vdots \\ b_k \end{bmatrix} = \begin{bmatrix} y(1) \\ y(2) \\ \vdots \\ y(N-L) \end{bmatrix}$$

(29)

or, in matrix notation

$$[D_{yx}] \cdot \begin{bmatrix} a \\ \cdots \\ b \end{bmatrix} = y.$$

(30)

31

This matrix is associated with the coefficients a_i and b_i as shown in Equations (23) and (24). The size of the excitation and response data matrices are $(N-L) \times (K+1)$ and $(N-L) \times L$, respectively, while the size of the ARMA parameter vector is $(L+K+1) \times 1$.

As in the Kumaresan-Tufts case, singular value decomposition can also be used in Cadzow-Solomon's algorithm to provide the minimum-norm solution. Its use reduces ill-conditioning of the data matrix, D_{yx}, and separates the signal poles from the noise poles across the unit circle. The optimal solution of Equation (30) is

$$\begin{bmatrix} a \\ \cdots \\ b \end{bmatrix} = [D_{yx}]^+ \cdot y. \tag{31}$$

2. Bias Compensation

When the system's order, (p,q), exceeds the true order of a noise contaminated system, $(\bar{p},\bar{q})$, for $p > \bar{p}$ and $q > \bar{q}$, Cadzow and Solomon maintain that there will be

$$s = 1 + \min(p - \bar{p}, q - \bar{q}) \tag{32}$$

eigenvalues, which will asymptotically approach $(N+1) \cdot \sigma_w^2$ for large N, where σ_w^2 is the noise variance. The eigenvalues in

the noise-free case are zero, and therefore, the parameter vector may be found from the equation

$$\begin{bmatrix} a_p \\ \cdots \\ (\dfrac{\sigma_v}{\sigma_w}) b_q \end{bmatrix} = \left[\sum_{k=0}^{s} |u_k(1)|^2 \right]^{-1} \cdot \sum_{k=0}^{s} u_k(1) \overline{u_k} \qquad (33)$$

where the $\overline{u_k}$ terms are the eigenvectors associated with the smallest (s) eigenvalues, λ_k.

However, the above method may not be applied exactly as described above because

- the excitation noise, σ_v, is zero for the radar target classification problem, and

- the $q-\overline{q}$, cannot be directly determined since the extraneous zeros cannot be separated from the signal zeros in the same manner as the poles are.

Another problem occuring in the Cadzow-Solomon's algorithm is that additive noise is different for input and output data. Norton [Ref. 11] described that if the input data noise is v_i and the output data noise is w_i, the noisy data matrix may be expressed as

$$D_{yx} = [D_y \vdots D_x] = S_{yx} + N_{yx} \qquad (34)$$

where, $N_{yx} = [N_y \vdots N_x]$, or in matrix form

$$N_x = \begin{bmatrix} v_1 & \cdots & v_{k+1} \\ \vdots & \ddots & \vdots \\ v_{N-L} & \cdots & v_{N+K-L} \end{bmatrix} \qquad (35)$$

33

$$N_y = \begin{bmatrix} w_2 & \cdots & w_{L+1} \\ \vdots & \ddots & \vdots \\ w_{N-L+1} & \cdots & w_N \end{bmatrix}. \qquad (36)$$

Therefore, the correlation product will be

$$E\left[D_{yx} D_{yx}^T\right] = S_{yx} S_{yx}^T + E\left[N_{yx} N_{yx}^T\right] \qquad (37)$$

As the additive noise is different for the input and output data, the noise correlation matrix $E[N_{yx} N_{yx}^T]$ is not of the form $\sigma^2 I$. So, the eigenvalue compensation method that Norton described as being applicable in the Kumaresan-Tufts algorithm is not applicable in the Cadzow-Solomon algorithm.

By examining the diagonal entries of the data matrix product, $D_{p,q}^T \cdot D_{p,q}$, it may be seen that the first (g) entries are close to 1. In the noise-free case, these first (g) diagonal entries are exactly equal to 1. This is a direct consequence of the fact that the diagonal entries of $D_{p,q}^T \cdot D_{p,q}$ contain bias errors proportional to the noise variances σ_v^2 and σ_w^2. Since the excitation data used in radar target classification problems are noise-free, these bias errors are proportional only to σ_w^2. The bias compensation may be obtained by setting the first (g) diagonal entries equal to 1 and then finding the eigenvalues and eigenvectors from the

34

corrected matrix, $D_{p,q}^T \cdot D_{p,q}$. The parameter vector may then be found from

$$\begin{bmatrix} a_p \\ \cdots \\ b_q \end{bmatrix} = \left[\sum_{k=1}^{p+q+2} \frac{|u_k(1)|^2}{\lambda_k} \right]^{-1} \sum_{k=1}^{p+q+2} \frac{u_k(1)}{\lambda_k} \overline{u_k}. \tag{38}$$

3. Earlier Results

Norton [Ref. 11] programmed the Cadzow-Solomon algorithm in Pascal and tested it on various types of data. Using synthetic data, Norton tested the algorithm using three SNR values, 30 dB, 20 dB, and 10 dB. The results were good at the 30 dB level, but as the SNR decreased, the error in the pole position estimates increased. Norton also used simulations of thin wire scattering produced by Morgan's TDIE computer program to test the algorithm, obtaining better results than those obtained from the Kumaresan-Tufts algorithm. These results occured because the Cadzow-Solomon algorithm takes into account only the input and output data and does not require purely late-time data.

Larison [Ref. 12] programmed the Cadzow-Solomon algorithm in Fortran and tested it using synthetic data and TDIE data, at various SNR's, ranging from 90 dB to 7 dB. Using bias compensation, Larison claimed good results in extracting the low frequency pole positions with SNR as low as 20 dB.

Murphy [Ref. 13] tested the Cadzow-Solomon algorithm using Larison's Fortran programs, using synthetic data as well as thin wire integral equation generated data and measured data. Murphy generated three separate signals, each based on ten pole pairs covering the frequency range of 1-10 GHz. Depending on the level of damping for each signal, Murphy obtained an average error between the true and the extracted poles having values on the order of 10^{-2} for the values

- SNR=10 dB and for HIGH Q,

- SNR=20 dB and for MEDIUM Q, and

- SNR=30 dB and for LOW Q.

Murphy made the observations that,

- The best results were obtained by choosing a starting point located within several points of the zero crossing nearest to the first obvious response of the excitation.

- The best results were obtained by using a data matrix in which the overestimated number of poles to the true number of poles was of the order of 2.5, while the number of asking zeros was equal to the number of true zeros.

- The best results were not always obtained when using the bias compensation scheme as proposed by Norton.

When processing the thin wire data, Murphy calculated the feed-forward order of the system by determining the length of early-time as equal to 2L/c. Recent research at NPS, that is as yet unpublished, indicates that this method is not correct, as each excited point along the target excites its adjacent point. This early-time may be described as $(1+\cos\alpha)\cdot L/c$, as shown in Chapter III, where α is the aspect of the target.

36

When processing the TDIE data, Murphy did not obtain good results for SNR=20 dB, in spite of the fact that the poles extracted from thin wire measured responses appeared to give good results for the low frequency poles.

III. ALGORITHM TESTING

The initial objective of this thesis was to evaluate the viability of the Kumaresan-Tufts and the Cadzow-Solomon algorithms. In a radar target classification problem the finite duration excitation signal produces both early-time and late-time response signals. In this situation, the Cadzow-Solomon algorithm is more significant. Thus, the main effort of this thesis was changed to evaluate and improve the Cadzow-Solomon algorithm using both synthetic and real data. The Kumaresan-Tufts algorithm was evaluated and tested only with synthetic data, as presented in Chapter II.

The Cadzow-Solomon algorithm was tested in two phases. The first phase of testing used synthetic data, while the second phase was performed with thin wire measurement data. The synthetic data testing phase attempted to simulate the conditions expected from the response of a simple target during the presence of a stationary white noise. The thin wire data testing phase attempted to evaluate the conditions appearing from a real target response. Those conditions were then compared with those simulated from the computed Time Domain Integral Equation (TDIE) thin wire response.

A. SYNTHETIC SIGNAL MODEL

As the Cadzow-Solomon algorithm is based on the ARMA model, the representation in Equation (23) has been used to produce the synthetic signal response.

This signal response is based on ten pole pairs within a frequency range of 1-10 GHz, with a medium Q damping factor using k=0.7. The poles were developed in accordance with the following equation:

$$\frac{\sigma_n}{\omega_n} = \frac{1}{2\pi} \ln(k) \qquad\qquad (39)$$

Table II lists the s-plane poles used in the synthetic signal.

Table II   MEDIUM Q SYNTHETIC POLES

f_n [GHz]	σ_n [GNp/s]	ω_n [Grad/s]
1	−0.3562	6.2752
2	−0.7124	12.5504
3	−1.0687	18.8256
4	−1.4249	25.1007
5	−1.7811	31.3759
6	−2.1373	37.6511
7	−2.4935	43.9263
8	−2.8498	50.2015
9	−3.2060	56.4767
10	−3.5622	62.7518

The chosen value of k simulates typical expected levels of damping from measured scattering responses of real targets, (e.g., the thin wire and scale model aircraft targets). The sampling frequency used to convert the s-plane poles to z-plane poles was 51 GHz, based on N=256 samples over a time window of t_0=5 nsec:

39

$$f_s = \frac{1}{\Delta t} = \frac{N-1}{t_0} \qquad (40)$$

1. Coefficient Generator and Recursive Signal Generator

The coefficients a_i are obtained by multiplying the terms $(z-z_1)(z-z_2)\ldots(z-z_{20})$, where z_i is the ith z-plane pole associated with the s-plane pole in the relationship

$$z_i = \exp[(\sigma_i + j\omega_i) \cdot \Delta t], \qquad (41)$$

and equal to the product of those terms with the polynomial

$$z^{20} - a_1 z^{19} - a_2 z^{18} - \ldots - a_{20}. \qquad (42)$$

The coefficients b_i are obtained by the inverse partial fraction expansion using the term $\dfrac{R_i}{z-z_i}$, where R_i is the ith residue of amplitude value 1 and phase difference 0 for each of the signal poles. The time domain signal response of the ARMA model is generated via Equation (23) with the values L=20 and K=19. This procedure has been developed in the MATLAB computer program ARMAGEN1.M. The program listing appears in Appendix A.

40

2. Double Gaussian Smoothing Function Generator

The excitation signal chosen for generating the test signal response was the double Gaussian waveform, via the equation

$$x(n) = A_1 \exp(-a_1 t^2) - A_2 \exp(-a_2 t^2), \tag{43}$$

with

$$a_1 = \frac{4\ln(10)}{T_1^2}, \quad T_1 = 0.147 \; nsec \tag{44}$$

$$a_2 = \frac{4\ln(10)}{T_2^2}, \quad T_2 = 0.314 \; nsec \tag{45}$$

where,

$$A_1 = \frac{\sqrt{a_1}}{\sqrt{a_1} - \sqrt{a_2}}, \quad A_2 = A_1 - 1. \tag{46}$$

This waveform is a wide Gaussian pulse with a ten percent width of T_2 nsec subtracted from a narrow Gaussian pulse with a ten percent width of T_1 nsec. This results in a bandwidth of 1 to 10 GHz. Figure 12 illustrates the double Gaussian waveform and Figure 13 illustrates the spectrum of the waveform. This procedure has been developed in the computer program EXCGEN.M in MATLAB. The program listing appears in Appendix B.

41

3. Synthetic Noise Generator

Synthetic noise was generated to contaminate the signal response by adding a time series noise signal to the signal response. The noise was assumed to be wide sense stationary and white. To produce a Gaussian distribution, a normal distribution function was multiplied with a standard deviation value σ, computed via the equation

$$\sigma^2 = variance = \frac{\sum_{k=1}^{N} [y(k)]^2}{N} \cdot \frac{1}{10^{\frac{SNR}{10}}} \qquad (47)$$

where,

- $y(n)$ is the signal response data,

- N is the number of time points and

- SNR is the Signal-to-Noise Ratio in dB.

This procedure was developed in the computer program NOISEGEN.M in MATLAB. The program listing appears in Appendix C.

4. Spectrum Estimation

Estimation of the power spectral density (PSD), also called the spectrum of the sampled signal response, is obtained employing the Fast Fourier Transform (FFT). This spectrum may be computed via the equation

$$S(k) = \frac{1}{N} \cdot |Y(k)|^2 \qquad (48)$$

42

where,

- N is the number of time points (power of 2),

- $Y(k)$ is the FFT of the signal y(t) and

- $S(k)$ is the periodogram spectral estimate of y(t).

This procedure was developed through the computer program SPECTRUM.M in MATLAB. The program listing appears in Appendix D.

B. SYNTHETIC SIGNAL TESTING RESULTS

This procedure shows the weaknesses of the Cadzow-Solomon algorithm by using no bias compensation. Cases were examined for the three different SNR's of 30, 20 and 10 dB. Overestimation varied from 2:1 up to 5:1, e.g., for 20 true poles and 60 asking poles, the ratio is 3:1. The interval processed was composed of 200 points, starting where the excitation began.

Figures 11-23 illustrates the results of this effort. Although the generated SNR's were 30, 20 and 10 dB, the resulting SNR's over the processed window were 2 dB higher. Observations made led to the following factors, thus improving results as previously obtained from the Cadzow-Solomon algorithm.

- The most significant factor is to select the excitation starting point as the point to start the algorithm processing.

43

- The second significant factor is to select the system order or number of asking poles. In the case of 20 true poles, 60 asking poles gives the most accurate results for all SNR's employed.

- A third significant factor is to determine the number of unknown zeros. For synthetic data, the position of the low frequency poles was obtained with better accuracy when this number was equal to the number of asking poles than with the case where the number of asking zeros was equal to the number of true poles.

Figure 23 illustrates the case of $K+1=20$ (as compared to Figure 19 for $K+1=60$), where $(K+1)$ represents the number of asking zeros. In the case where $K+1=20$, more poles were obtained within the unit circle (as compared to the case where $K+1=60$) at the frequencies of the true poles, but with a different damping factor. The experimental data indicates the following result:

- There is a bias of all the poles towards the unit circle that results in the loss of some poles. The bias is so large that it forces the poles to appear on the other side of the unit circle as noise poles.

By examining the spectra of the synthetic signal at different noise levels, as illustrated in Figures 15-16, it may be noticed that the high frequency poles cannot be completely separated from the white noise spectrum when increasing the noise level. This is due to the fact that these high frequency poles carry very little energy.
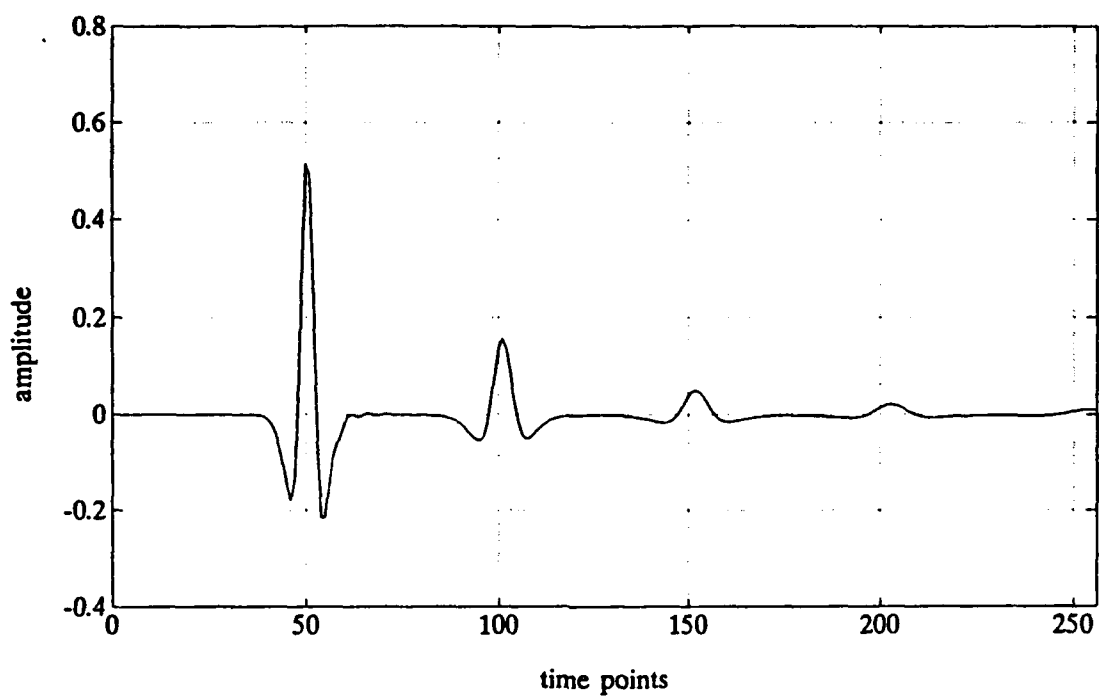
The set of equations in matrix form developed in Equation (29) have been developed in the computer program CADSOL1.M in MATLAB. The program listing appears in Appendix E.
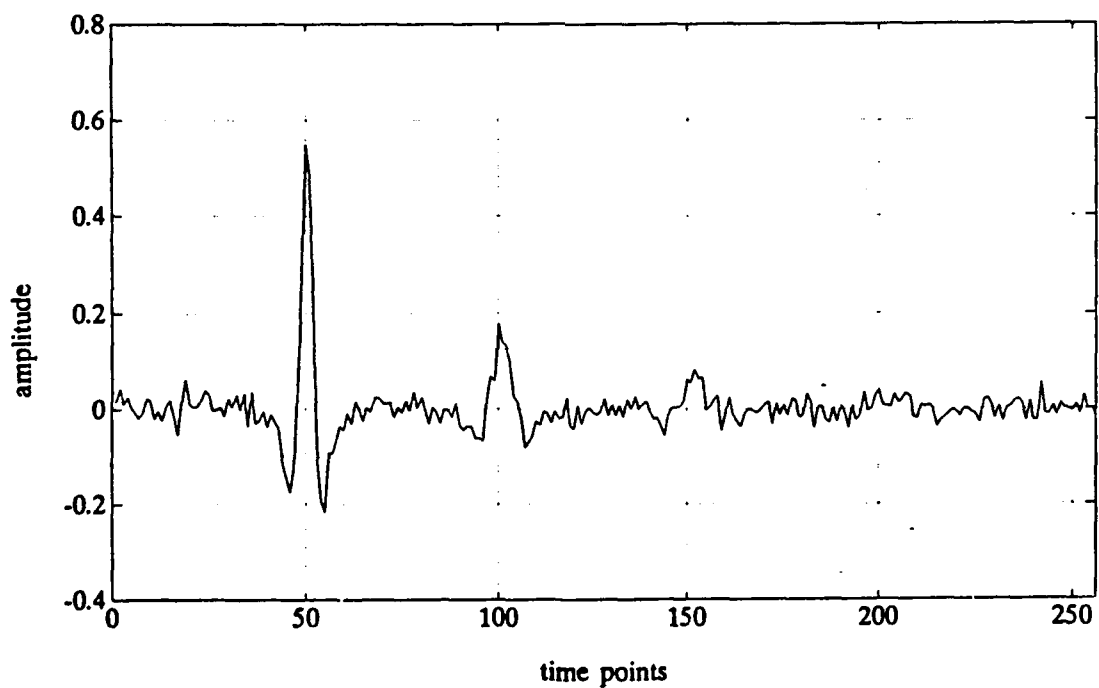
44
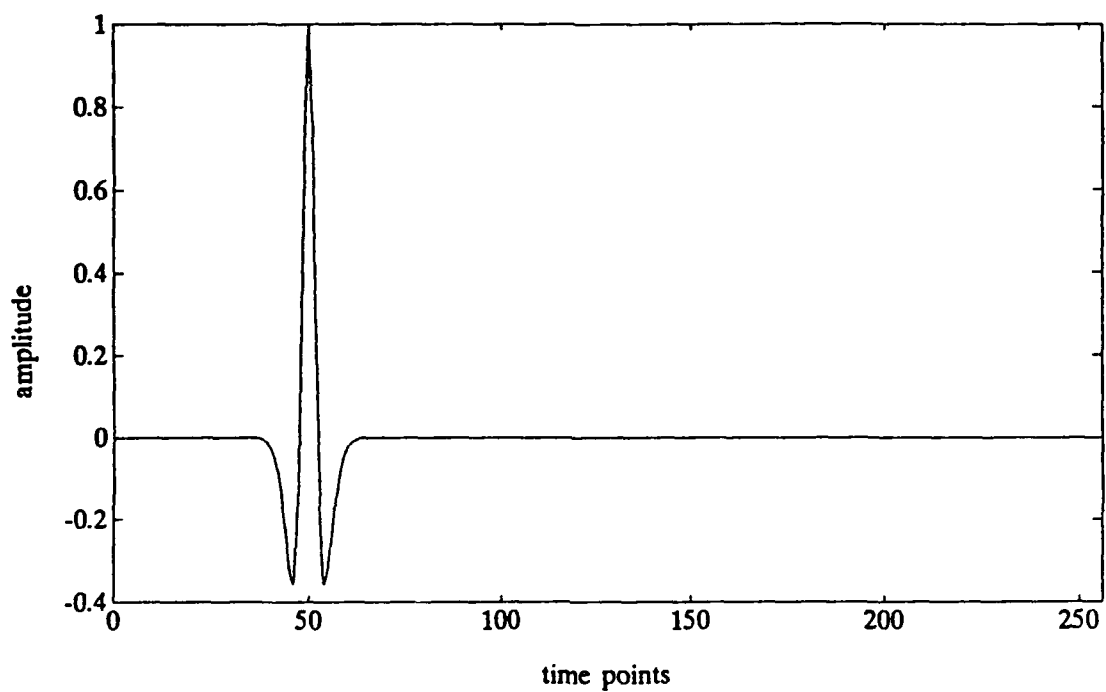
Figure 11   Double-Gaussian Smoothing Function
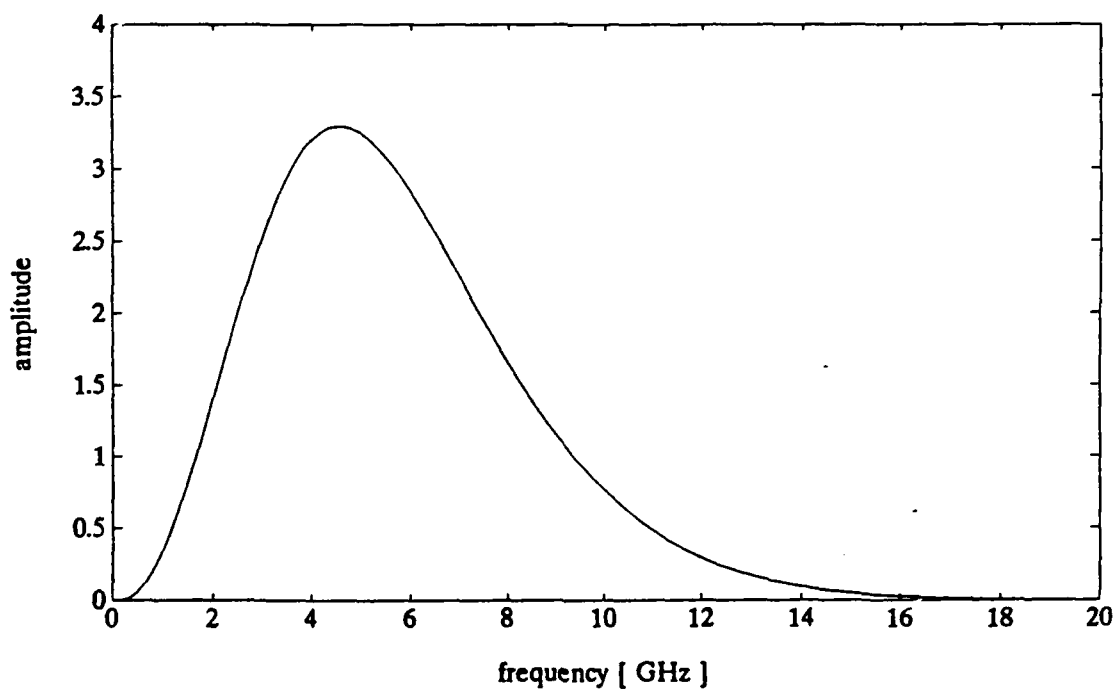
Figure 12   Spectrum of the Double-Gaussian Function

Figure 13   Synthetic signal without noise

Figure 14   Synthetic Signal with SNR=10 dB

46
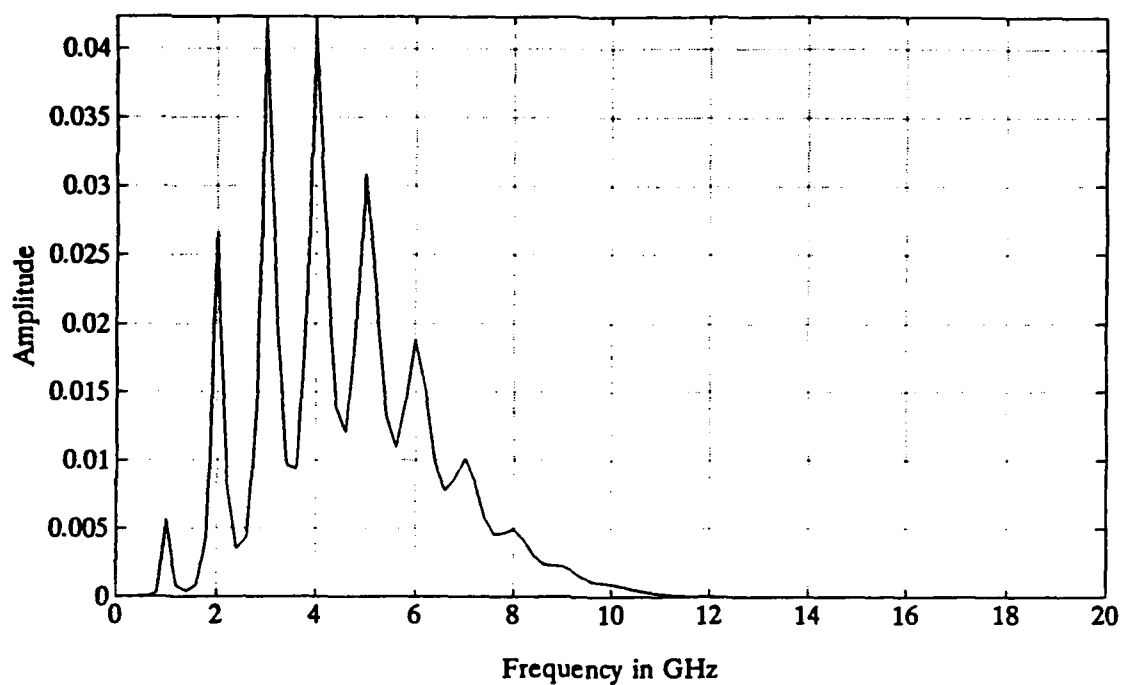
Figure 15   Spectrum of the synthetic signal without noise
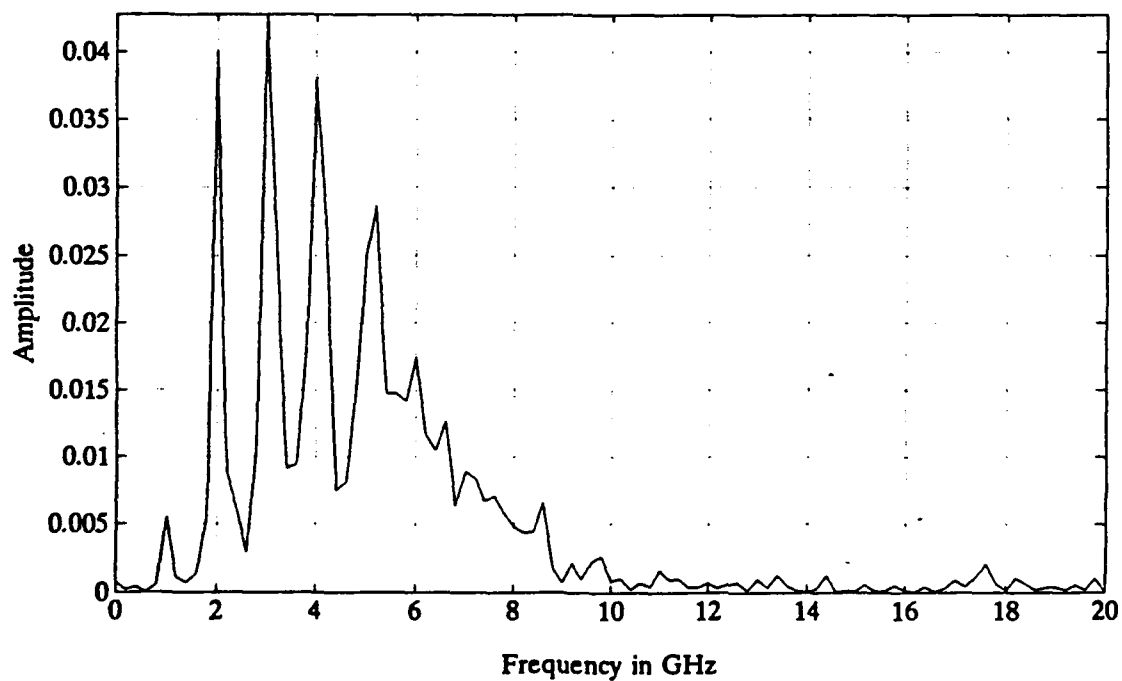
Figure 16   Spectrum of the synthetic signal with SNR=10 dB

GigaRad/sec

GigaNepers/sec   +:true   algorithm: *=60 unk
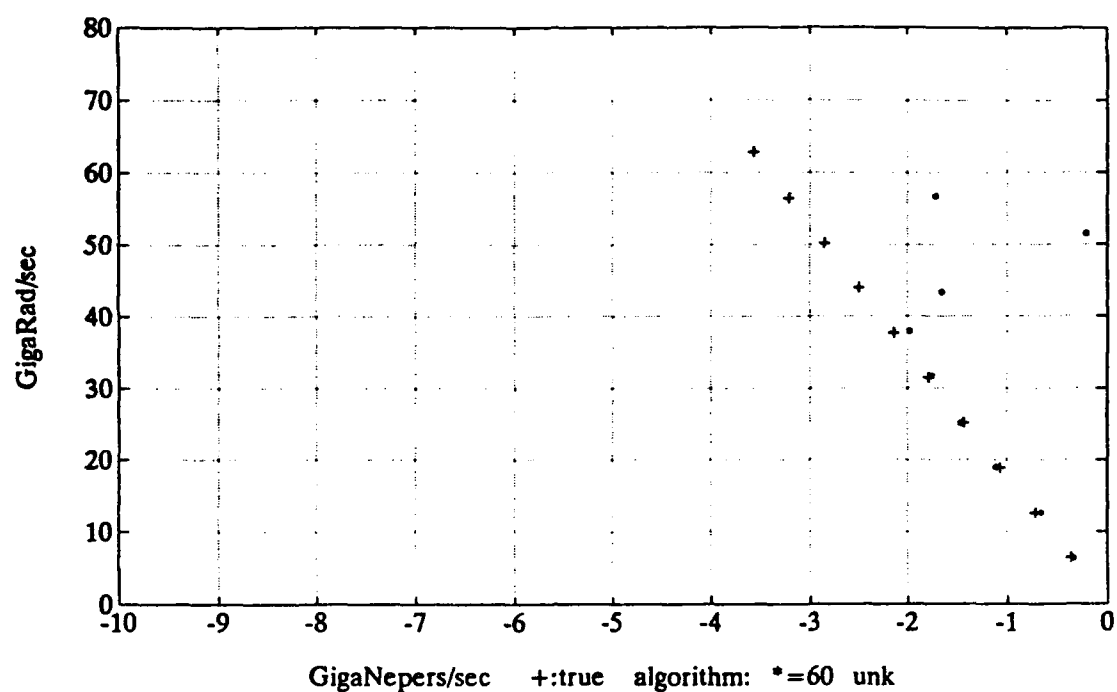
Figure 17   Poles in s-plane, SNR=32 dB, for synthetic signal

+:true   o:algorithm   *:noise   unk poles=60   exp zeros=60
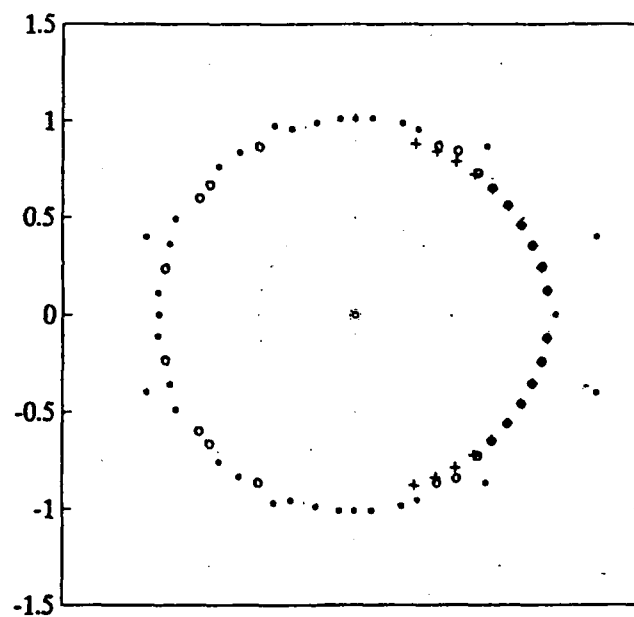
Figure 18   Poles in z-plane, SNR=32 dB, for synthetic signal
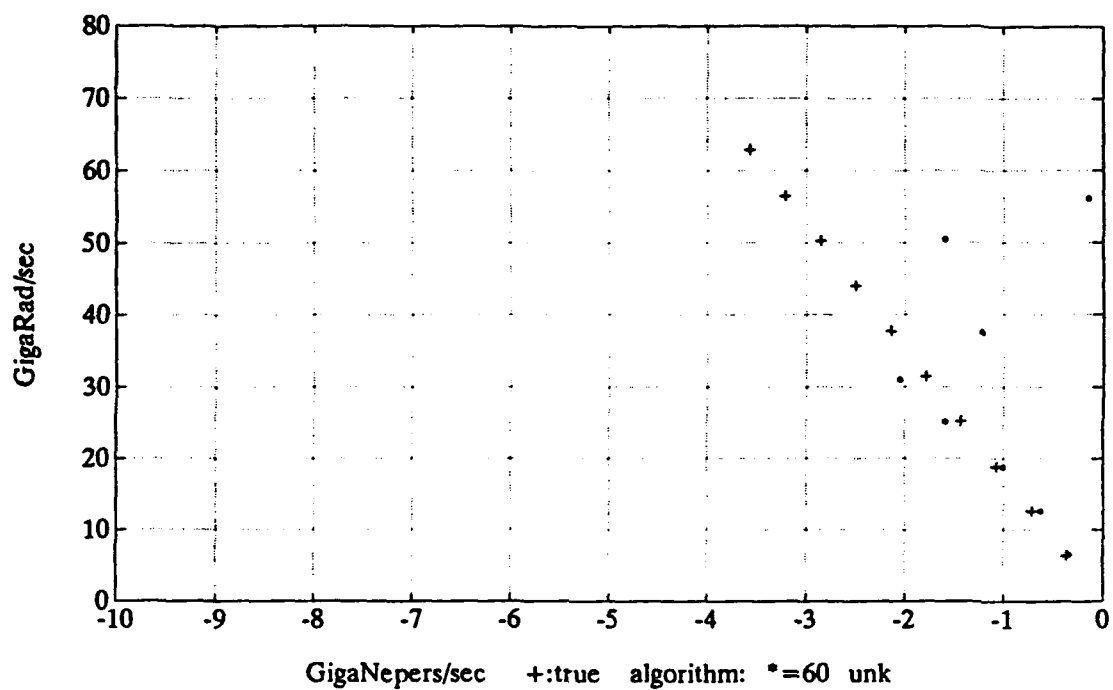
Figure 19   Poles in s-plane, SNR=22 dB, for synthetic signal

+:true   o:algorithm   *:noise   unk poles=60   exp zeros=60

Figure 20   Poles in z-plane, SNR=22 dB, for synthetic signal

Figure 21 Poles in s-plane, SNR=12 dB, for synthetic signal

+:true   o:algorithm   *:noise   unk poles=60   exp zeros=60

Figure 22 Poles in z-plane, SNR=12 dB, for synthetic signal

Figure 23 Poles in s-plane, SNR=22 dB, K+1=20, for synthetic signal

C. THIN WIRE SIGNAL TESTING

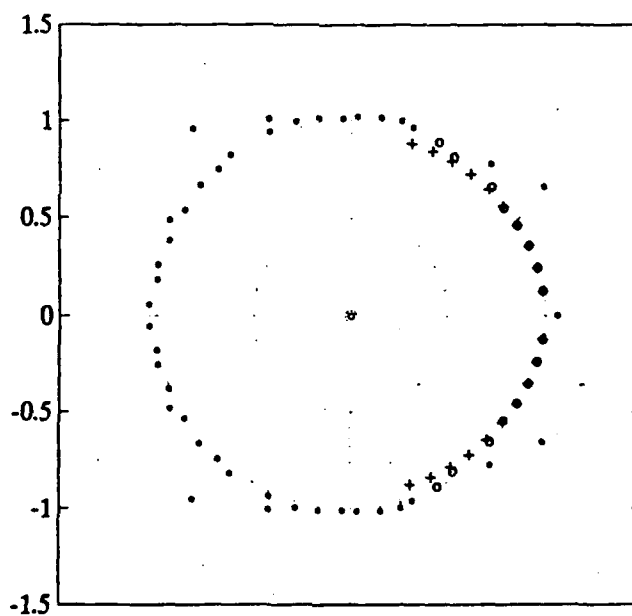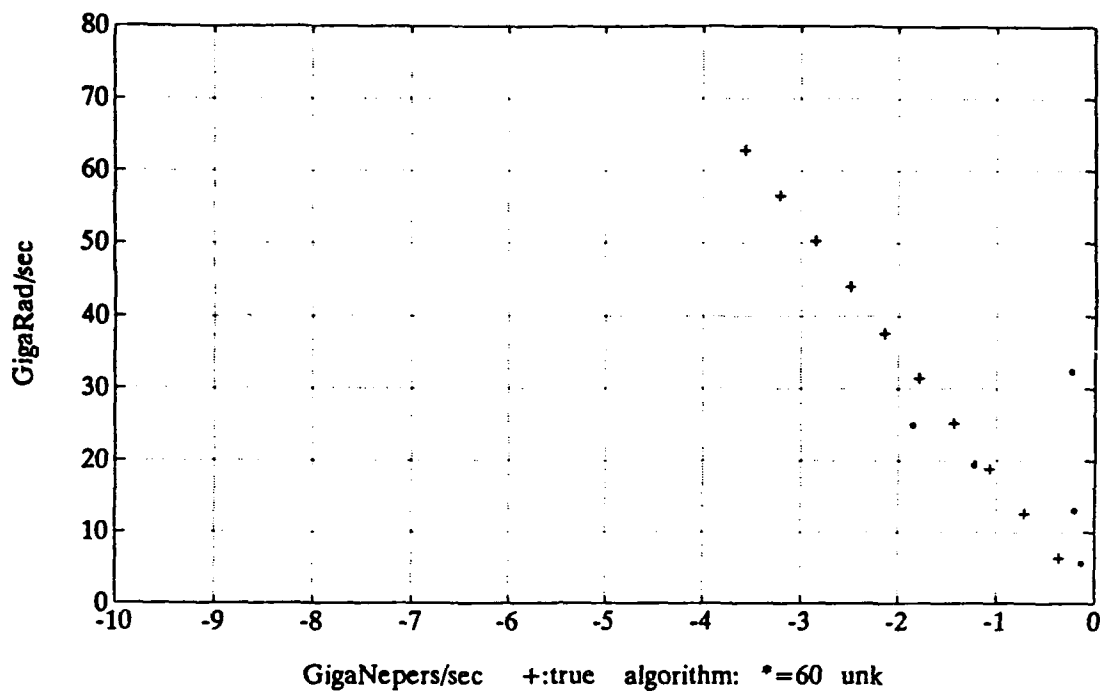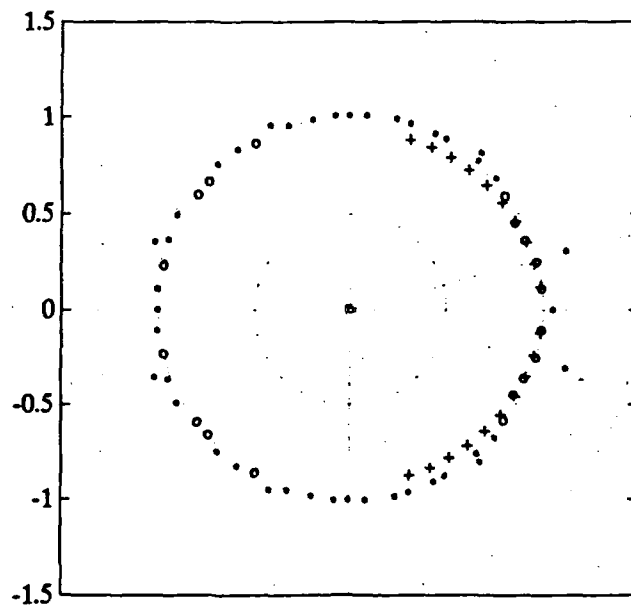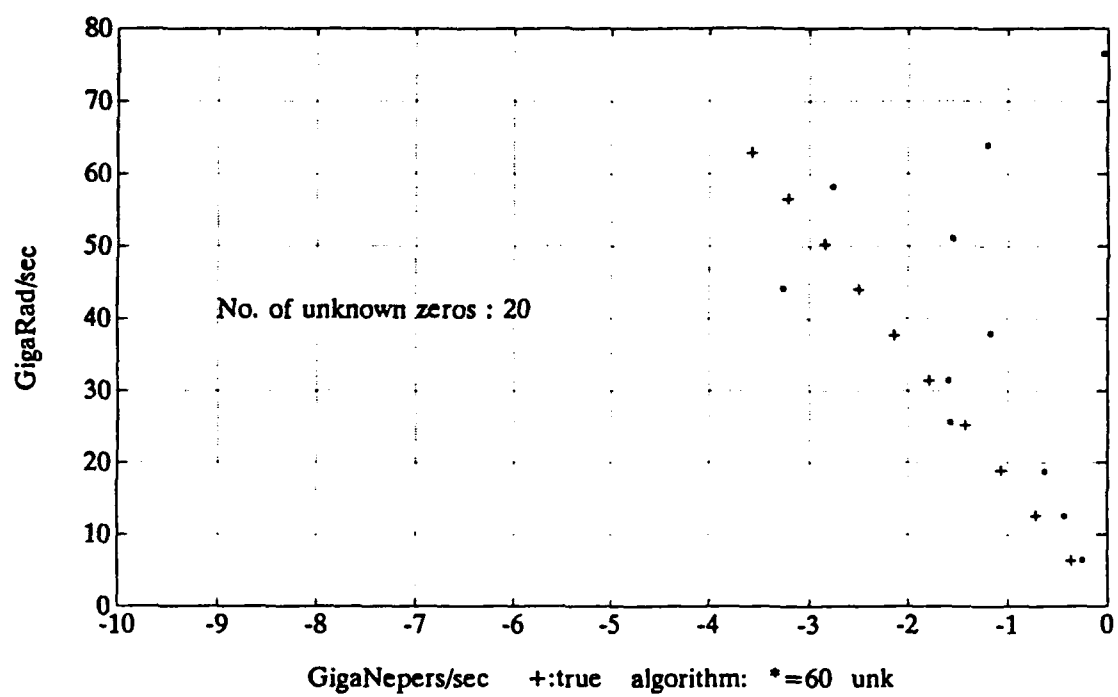The Cadzow-Solomon algorithm was also tested using thin wire measured scattering data. The results have been compared with the results obtained using time domain integral equation (TDIE) thin wire data. The poles obtained by processing the TDIE computed data were assumed to be correct, even though the program that computes the currents on the thin wire does not take into account the capacitance at the ends of the wire.

1. Thin Wire Integral Equation Computed Data

For the thin wire, the natural resonances may be determined by solving the integral equation that describes the current flowing on the wire. The result of this type of simulation is the response of the wire to a specified excitation field. Morgan [Ref. 14] developed a time-domain thin wire integral equation computer routine, based on the formulations of Sayre and Harrington [Ref. 15]. The wire used for this simulation had a length of 0.1 meter and a radius of 1.18 mm. The back-scattering response was computed at three different incident aspects, ranging from 30 to 90 degrees, with 90 degrees representing a broadside aspect. The excitation waveform used was the same double Gaussian as that used with the synthetic data, as illustrated in Figure 11. Figure 30 illustrates the position pole estimates obtained using Cadzow-Solomon algorithm and shows the aspect independence of the poles for three cases. The

five low frequency poles appeared exactly at the same position for all aspects. It should be noted that these results, as illustrated in Figure 30, appeared to be exactly the same, irrespective of any variations in the parameters (No. of points - No. of asking poles - No. of asking zeros) used in processing the signal. Note that for broadside illumination, only the odd-numbered poles appear. Because of the physical symmetry of both the thin wire and incident field, the even-numbered modes are prevented from being excited by the incident field. With illumination at 45 degrees aspect, a spectrum with adequate energy only within the bandwidth from 1 to 8 GHz was produced, as expected. At higher frequencies, backscattering is suppressed because most of the energy is reradiated near to the specular scattering directions. Therefore, only the five low frequency poles are accurately obtained for this case.

The TDIE program generated a response at 30 degrees aspect consisting of 255 points over 5 nsec, resulting in a sampling frequency of 50.8 GHz. In the case of 45 and 90 degrees aspect consisting of 240 points over 5 nsec, a sampling frequency of 47.8 GHz resulted. These sampling frequencies differ from the sampling frequency of 51 GHz used in the measured data.

When processing the TDIE thin wire data, points from 160 to 200 were used to run the algorithm starting at the point where the excitation starts. The number of asking poles

ranged from 28 (for the 90 degrees aspect) to 40 (for the 30 degrees aspect). The number of asking zeros or feed-forward order of the system was either the same as the number of asking poles or, was calculated by determining the length of early-time. This early-time was computed from the formula

$$t_e = \frac{L}{c} \cdot (1 + \cos\alpha) \qquad \text{(49)}$$

where,

- L is the length of the wire and

- α is the aspect angle from end-on orientation.

This value of time was then converted to the appropriate number of time points, as based on the sampling time interval of

$$n_b = integer\left[\frac{t_e}{T}\right] + 1 \qquad \text{(50)}$$

where,

- T is the sampling interval, and

- n_b is the feed-forward order of the system.

This value of n_b is the minimum number of asking poles that may be used, presenting the number of delays in the z-transform for the early-time of the system.

Another consideration in the processing of these data was the scaling of the excitation waveform and its position with respect to the computed response. Although the data were generated using a double Gaussian waveform with a 1 Volt peak

54

amplitude, the excitation waveform had approximately the same peak amplitude as the response waveform. Such scaling does not change the frequency contents of the exciting waveform and gives better results in the pole extraction due to minimization of some of the effects of ill-conditioning in the data matrix.

To position the driving waveform with respect to the response waveform, the time difference between the excitation of the first and last point of the wire may be computed. This time interval is represented as

$$t_{delay} = \frac{2L}{c} \cdot \cos\alpha, \qquad\qquad (51)$$

where α is the aspect angle. The maximum absolute value of the response occurs when the last point of the wire is being excited. The information derived from the time interval, t_{delay}, and the maximum absolute value of the response allows the excitation waveform to be positioned with the first point of the wire.

2. Thin Wire Measured Data

Measurements were performed in the Transient Electromagnetic Scattering Lab (TESL) to test the algorithm by using a thin wire with the same dimensions as the one used for the previous simulation. A detailed explanation of the procedure and the techniques used for measuring the scattering response from the thin wire, as well as other scale model

targets may be found in Morgan and McDaniel [Ref. 16] and Bresani [Ref. 17].

One measurement was available for each of the aspects at 30, 45 and 90 degrees. The scattering response waveforms obtained from the measurements are illustrated in Figures 24, 26 and 28. These waveforms were compared with the calculated waveforms obtained from the TDIE program. It can be seen from the figures that the natural modes between the calculated and the measured waveforms do not have exactly the same frequencies.

The spectrum of the measured response waveforms were also obtained, giving a distribution of energy within the bandwidth 1-12 GHz on eight frequencies, as shown in Table III:

Table III   DISTRIBUTION OF ENERGY WITHIN THE SPECTRUM OF THIN WIRE

Aspect [degrees]	Frequencies [GHz] with most energy	Frequencies [GHz] with less energy	Frequencies [GHz] with no energy
30	3,4.4,5.8, 7.2	1.6,8.6,10.2	11.6
45	3,4.4	1.6,5.6	7.2,8.6,10.2, 11.6
90	1.6,4.4	7.2	3,5.6,8.6, 10.2,11.6

Figures 25, 27 and 29 illustrate the spectrum of the measured thin wire scattering response for each aspect.

When the measured thin wire response was processed, the points used to run the algorithm were from 180 to 200, starting at the initial excitation point, while the number of asking poles ranged from 30 to 60. The best results were obtained when the number of asking poles approached 40. The feed-forward order of the system was either the same as the number of asking poles, or was calculated by determining the early-time length. The scaling of the driving waveform and the positioning of the excitation with respect to the response was computed, as previously described. Figure 30 illustrates the extraction of the poles from the TDIE response, while Figure 31 illustrates the extraction of the poles from the measured waveform for the combined aspects. Figures 32-37 illustrate the extraction of the poles from the measured waveform for each aspect separately. The pole results obtained using both the bias compensation method developed in this thesis and Cadzow-Solomon's bias compensation method have been plotted in Figures 32-37 along with the poles obtained without any bias compensation method, so that the results from the three types of methods may be compared.

solid : computed by TDIE   dashed : measured   dotted : excitation
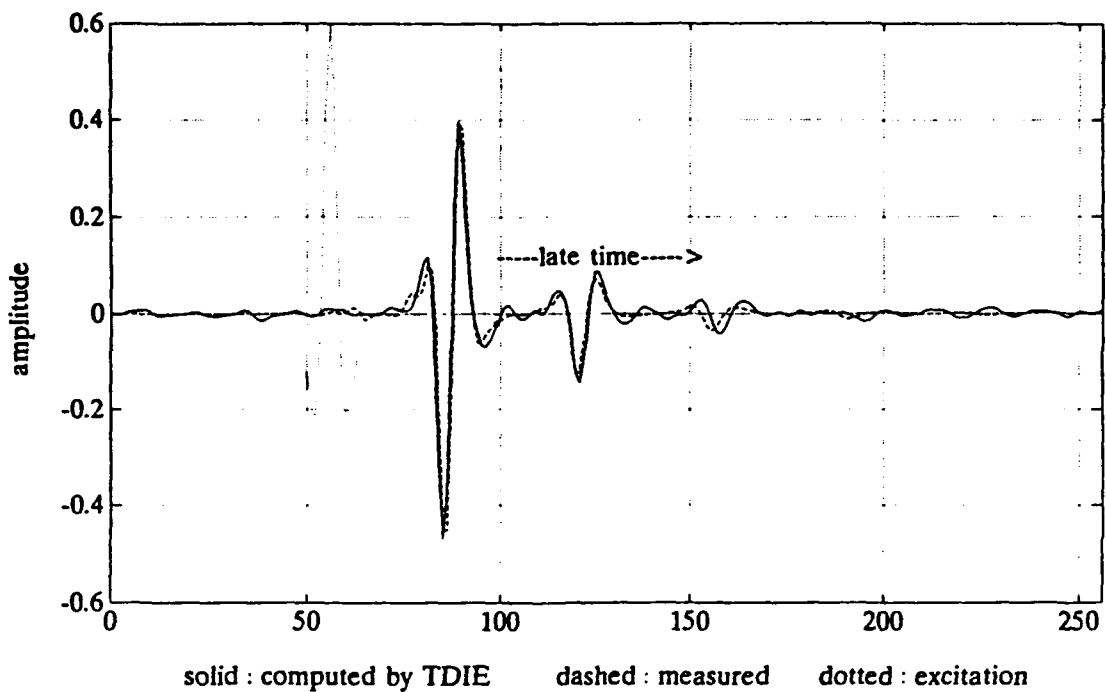
Figure 24 Thin wire TDIE & Measured Response, 30 deg aspect
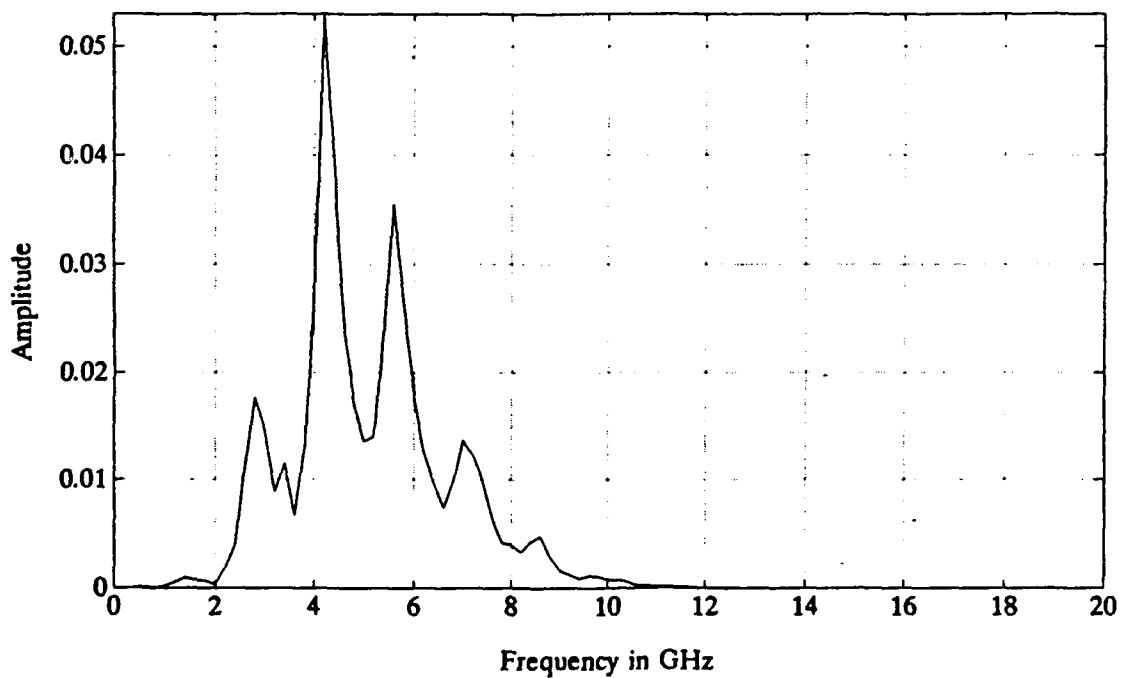
Figure 25 Spectrum of thin wire measured response, 30 deg

solid : computed by TDIE   dashed : measured   dotted : excitation
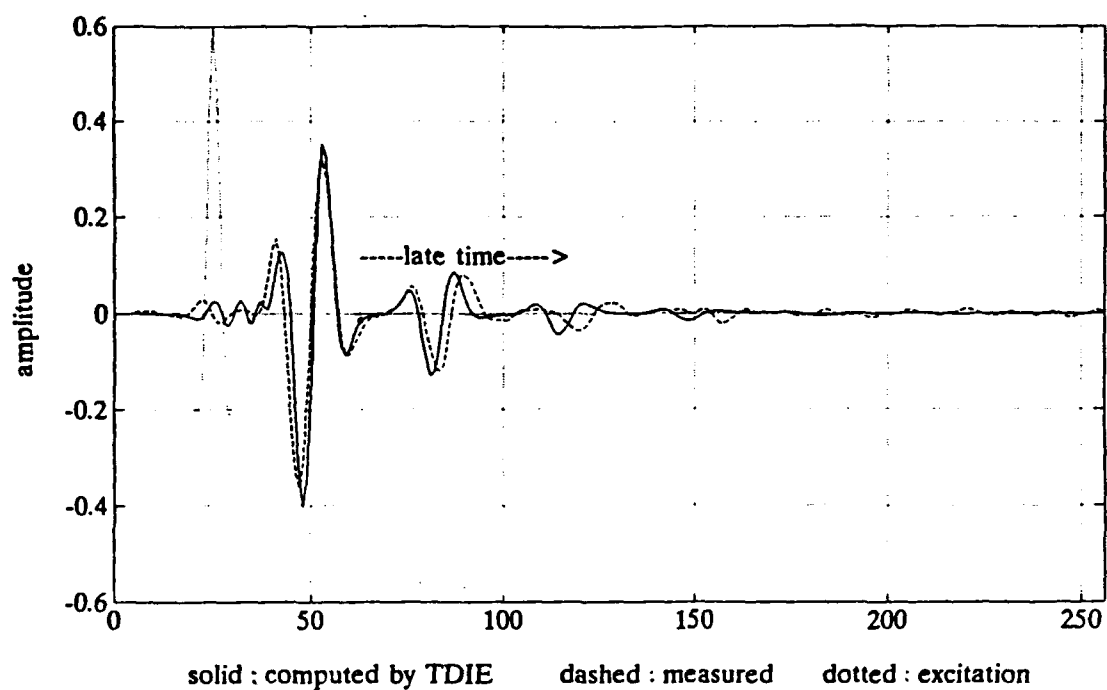
Figure 26   Thin wire TDIE & Measured Response, 45 deg aspect

Frequency in GHz
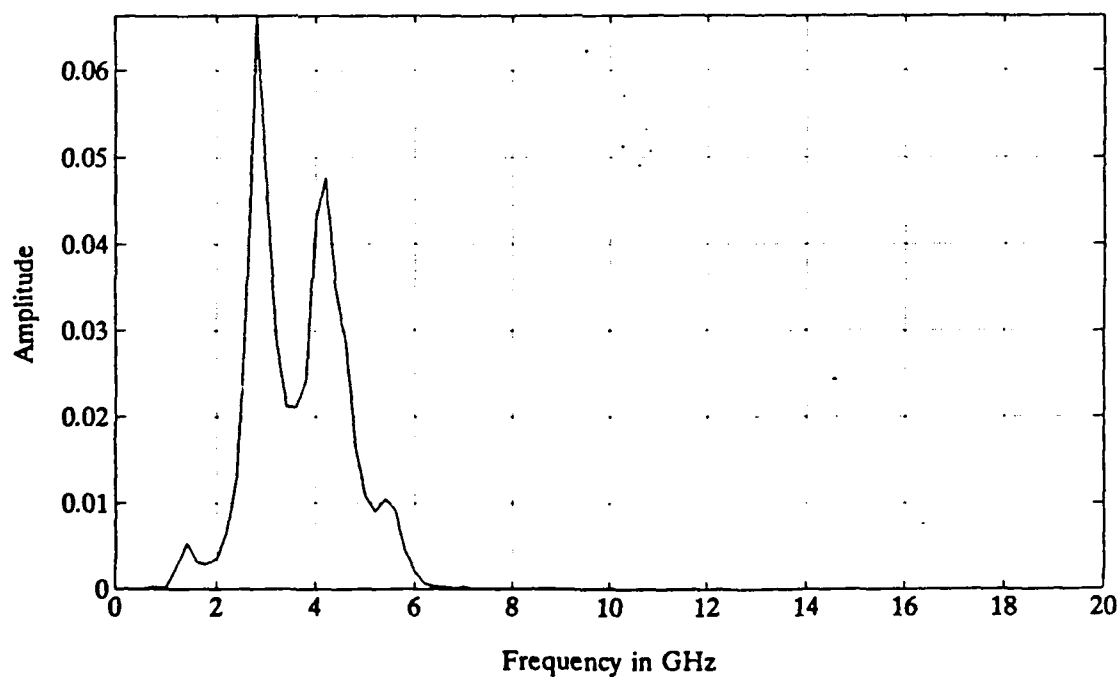
Figure 27   Spectrum of thin wire measured response, 45 deg

solid : computed by TDIE   dashed : measured   dotted : excitation
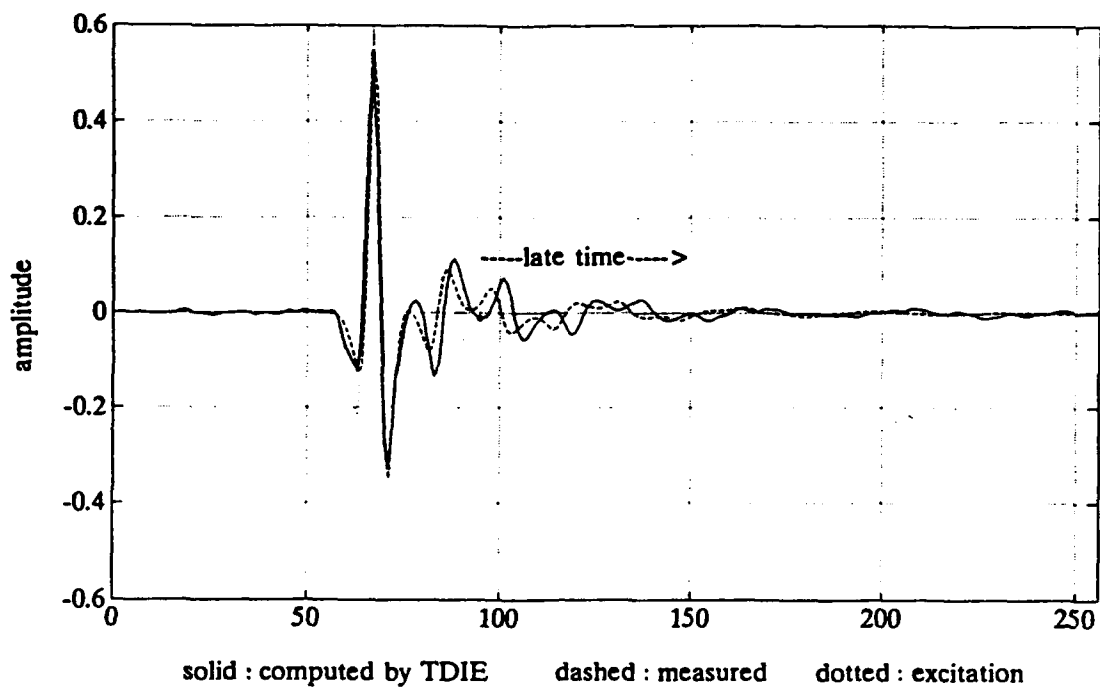
Figure 28   Thin wire TDIE & Measured Response, 90 deg aspect

Frequency in GHz
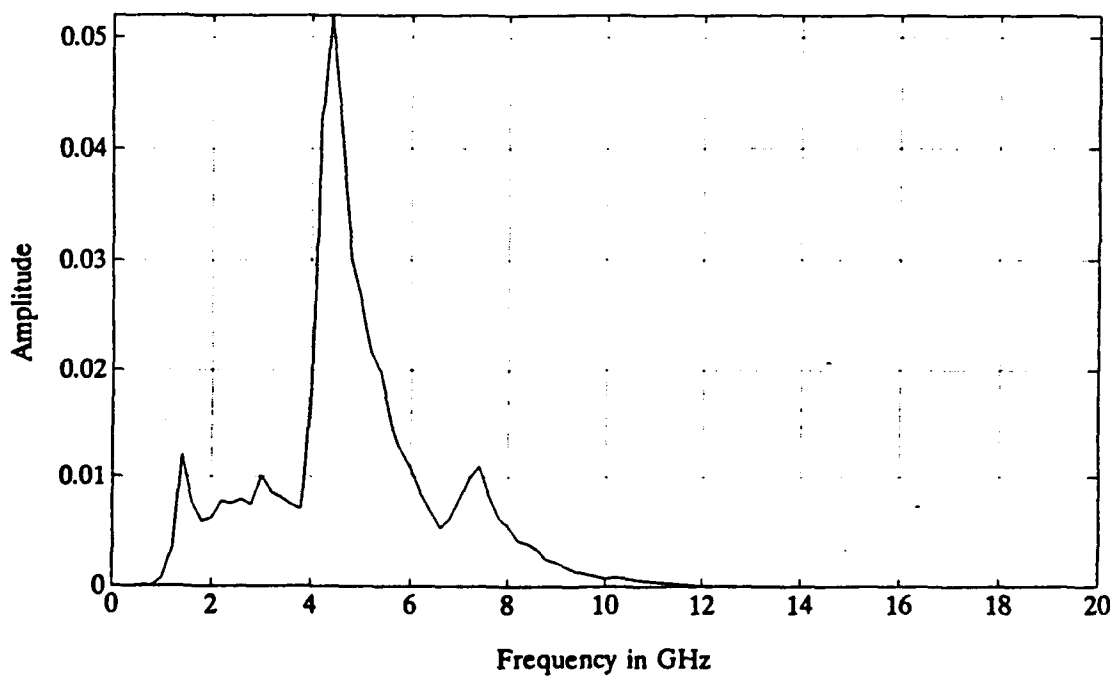
Figure 29   Spectrum of thin wire measured response, 90 deg

60

aspect: o : 30, x : 45, * : 90 deg
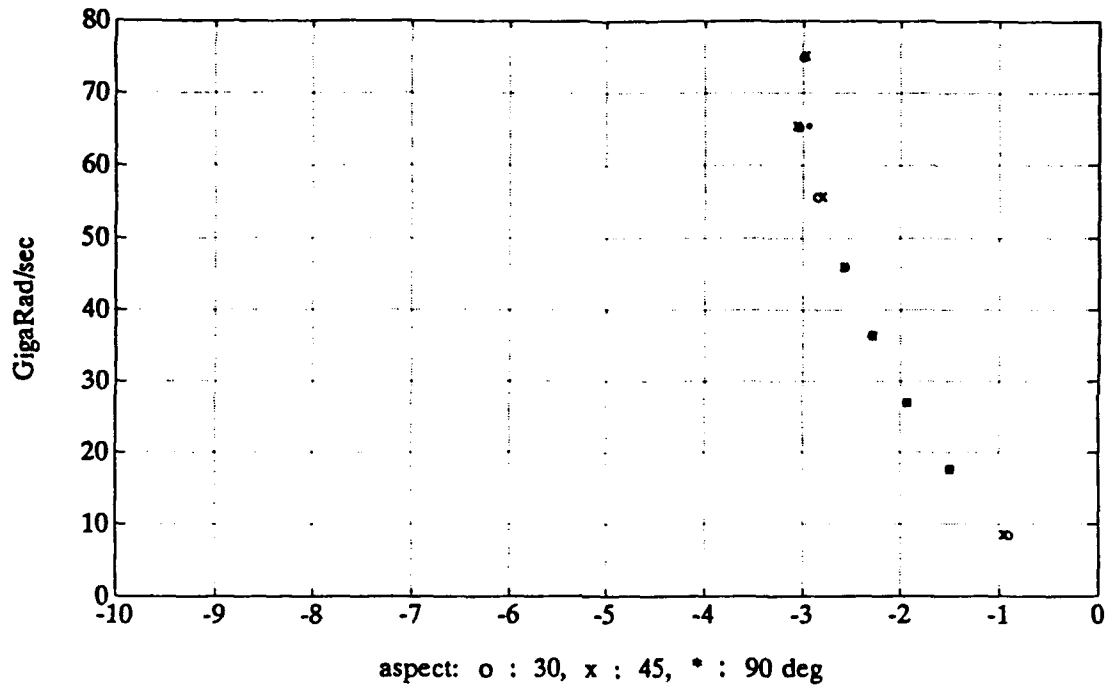
Figure 30   Poles extracted from TDIE response, all aspects

+ : TDIE response

Measured response
No bias compensation method

o : 30 deg, x : 45 deg, * : 90 deg
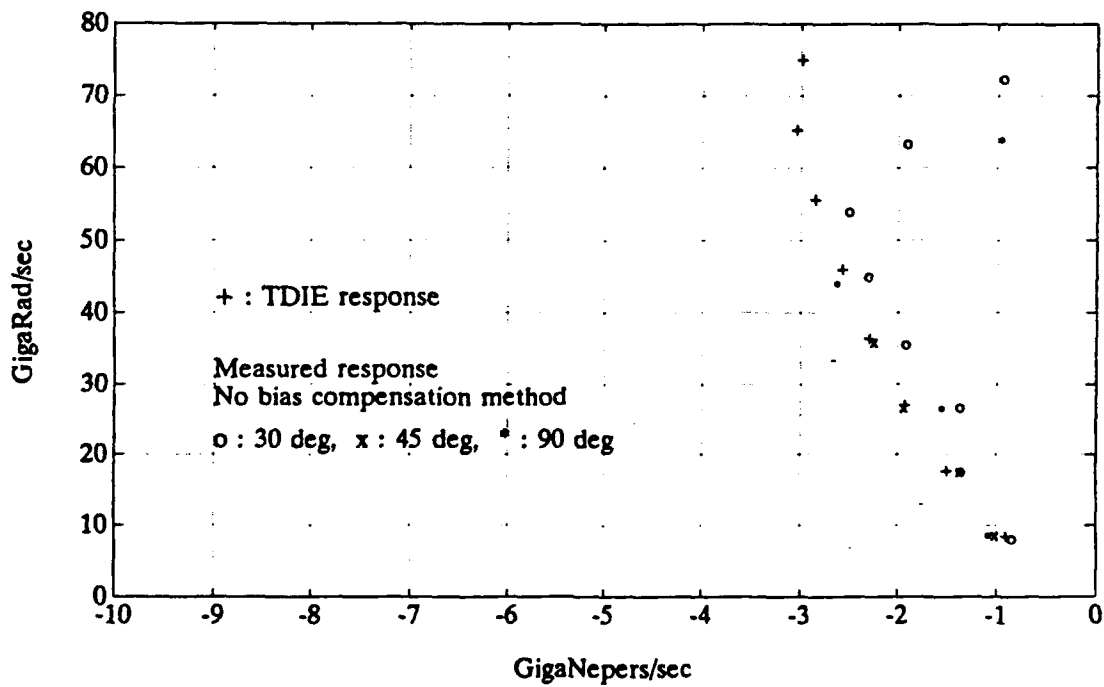
Figure 31   Poles from measured response, all aspects
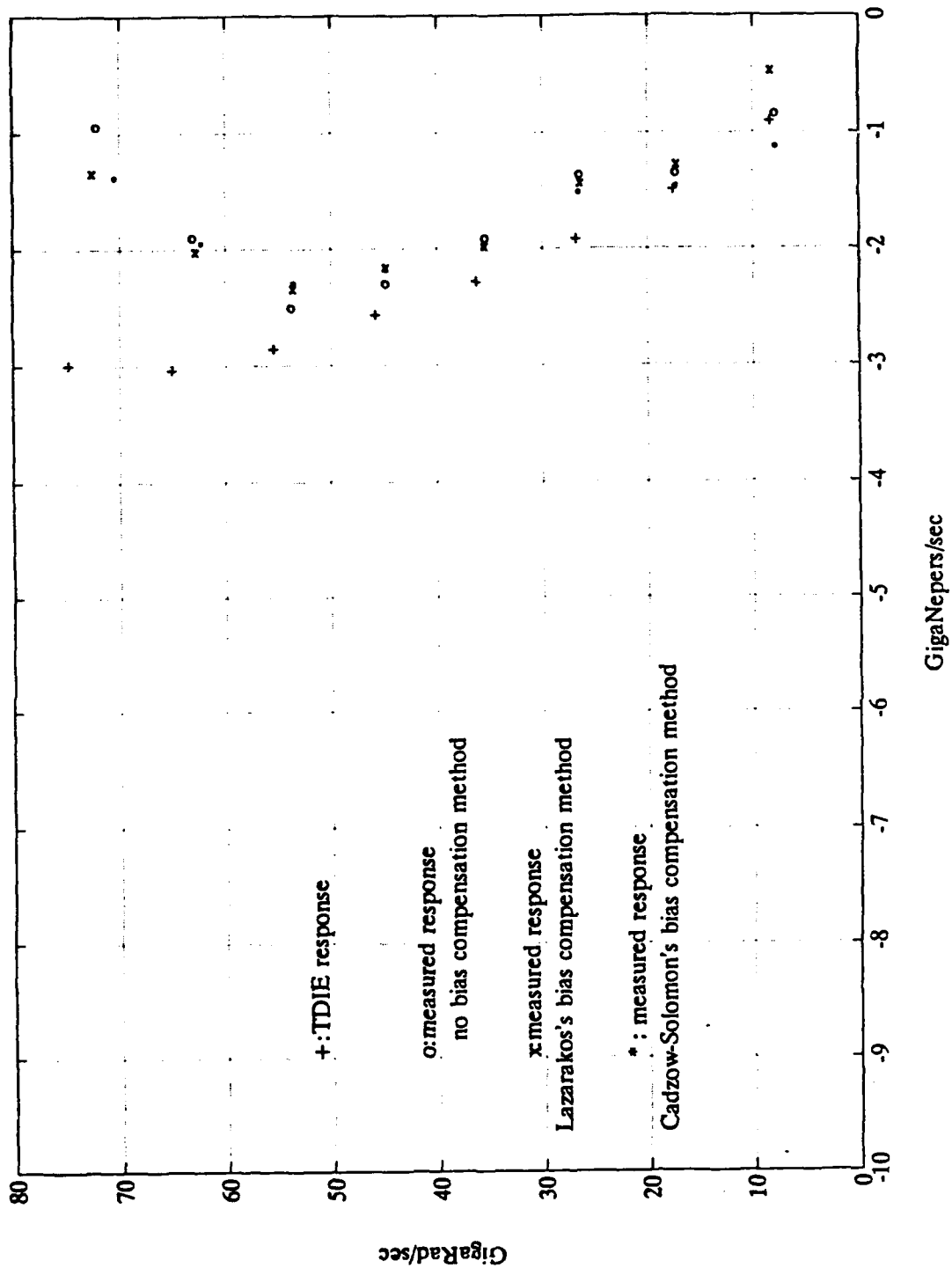
Figure 32 Poles extracted from measured response, 30 deg
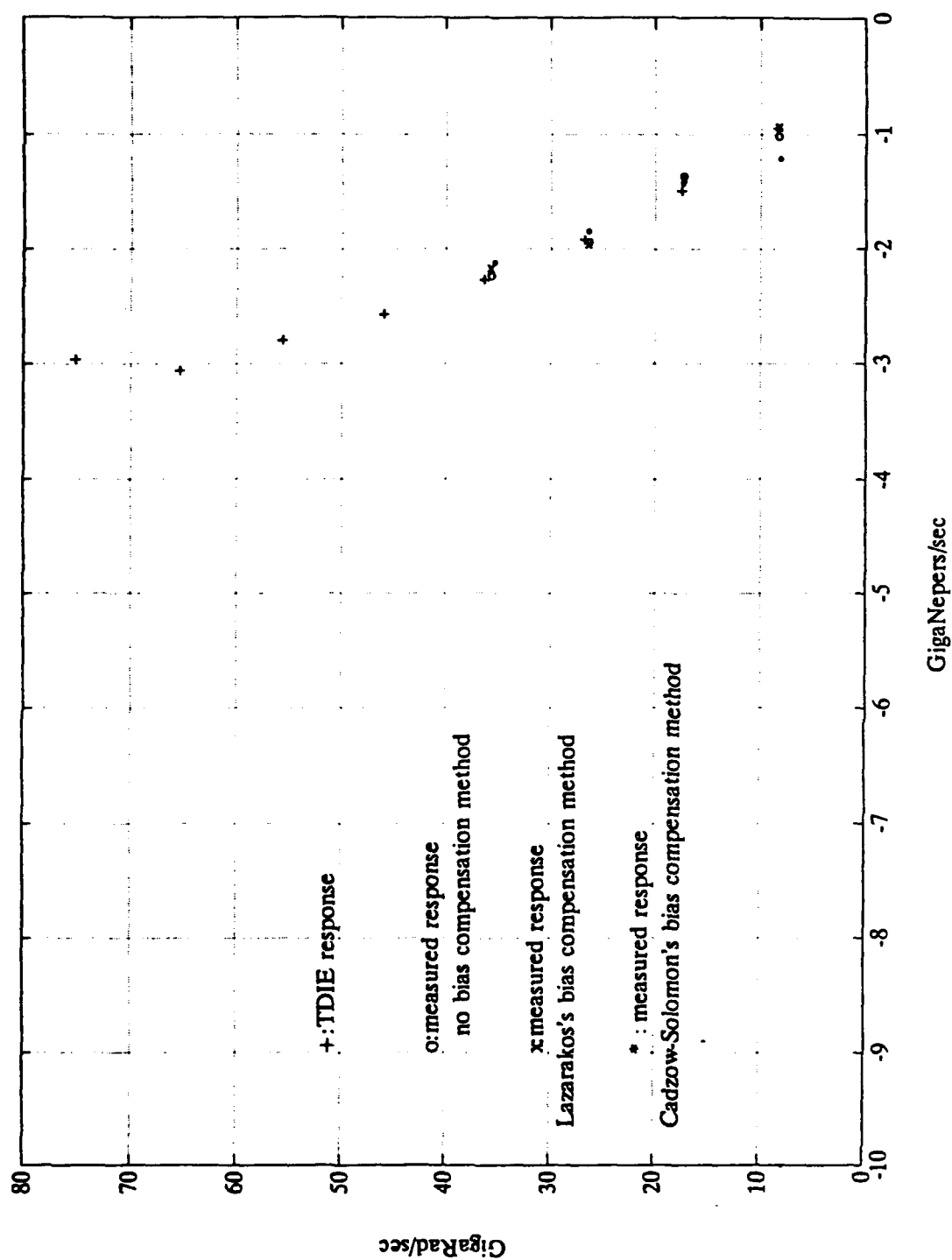
Figure 33   Poles extracted from measured response, 45 deg

63
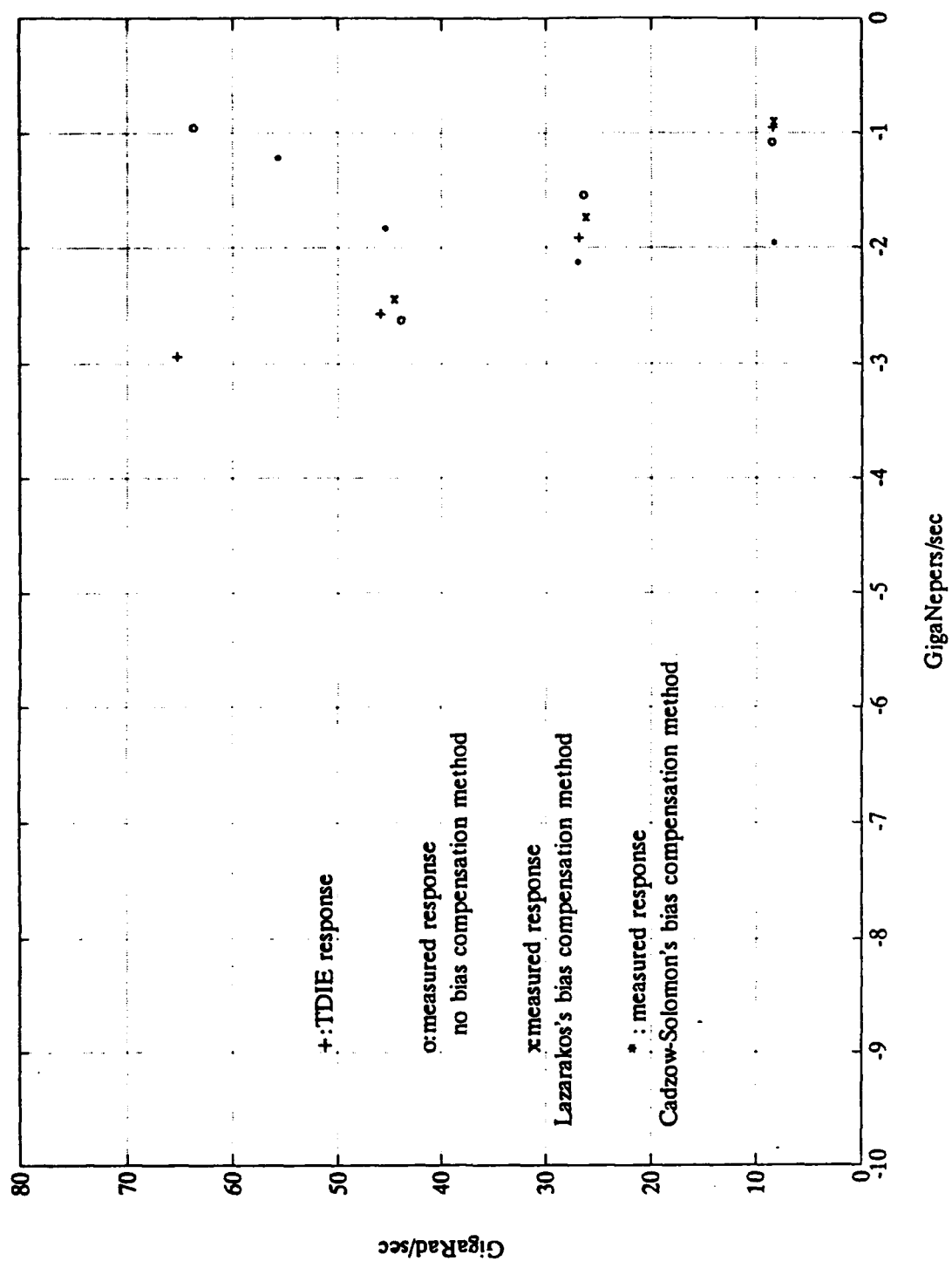
Figure 34 Poles extracted from measured response, 90 deg

The plot axes: horizontal axis labeled "GigaNepers/sec" ranging from 0 to -10; vertical axis labeled "GigaRad/sec" ranging from 0 to 80.

Legend:
+ :TDIE response

o: measured response
no bias compensation method

x measured response
Lazarakos's bias compensation method

* : measured response
Cadzow-Solomon's bias compensation method
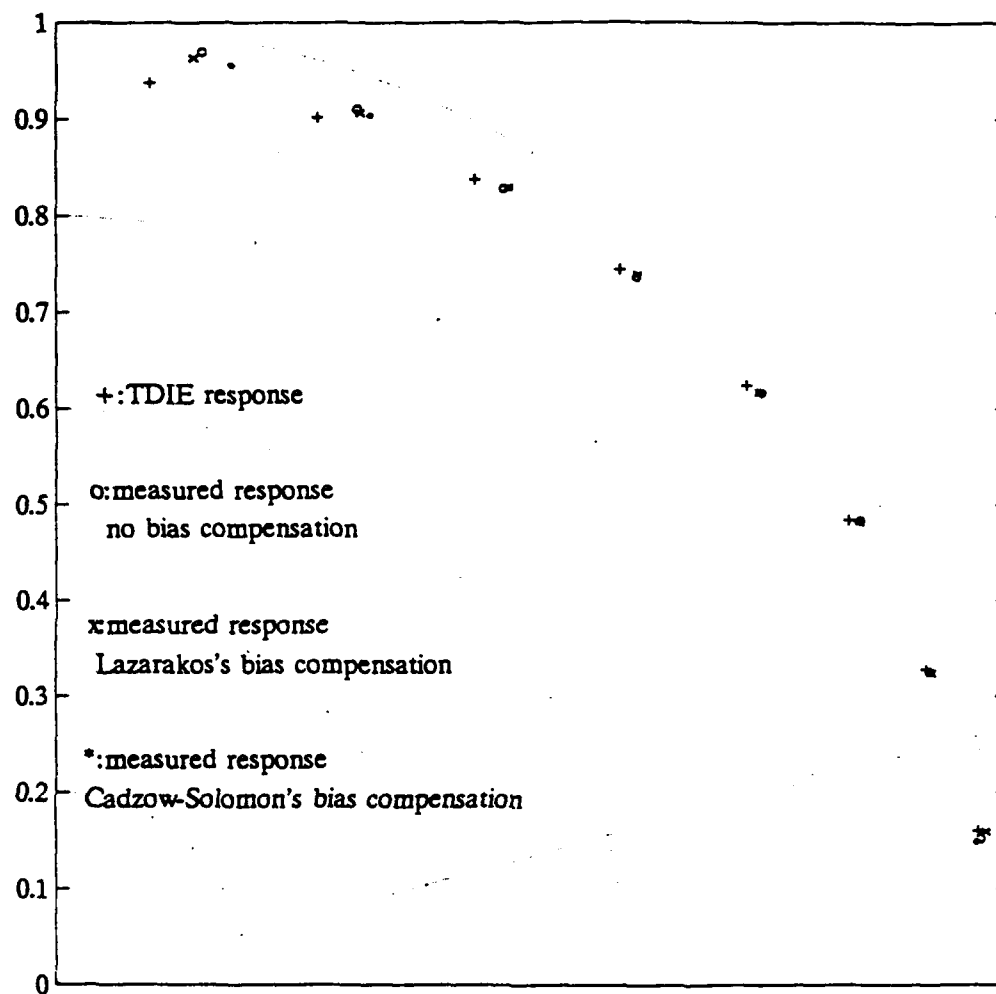
Figure 35   Poles at z-plane, 30 deg aspect

Legend within figure:

+:TDIE response

o:measured response
 no bias compensation

x:measured response
 Lazarakos's bias compensation

*:measured response
Cadzow-Solomon's bias compensation
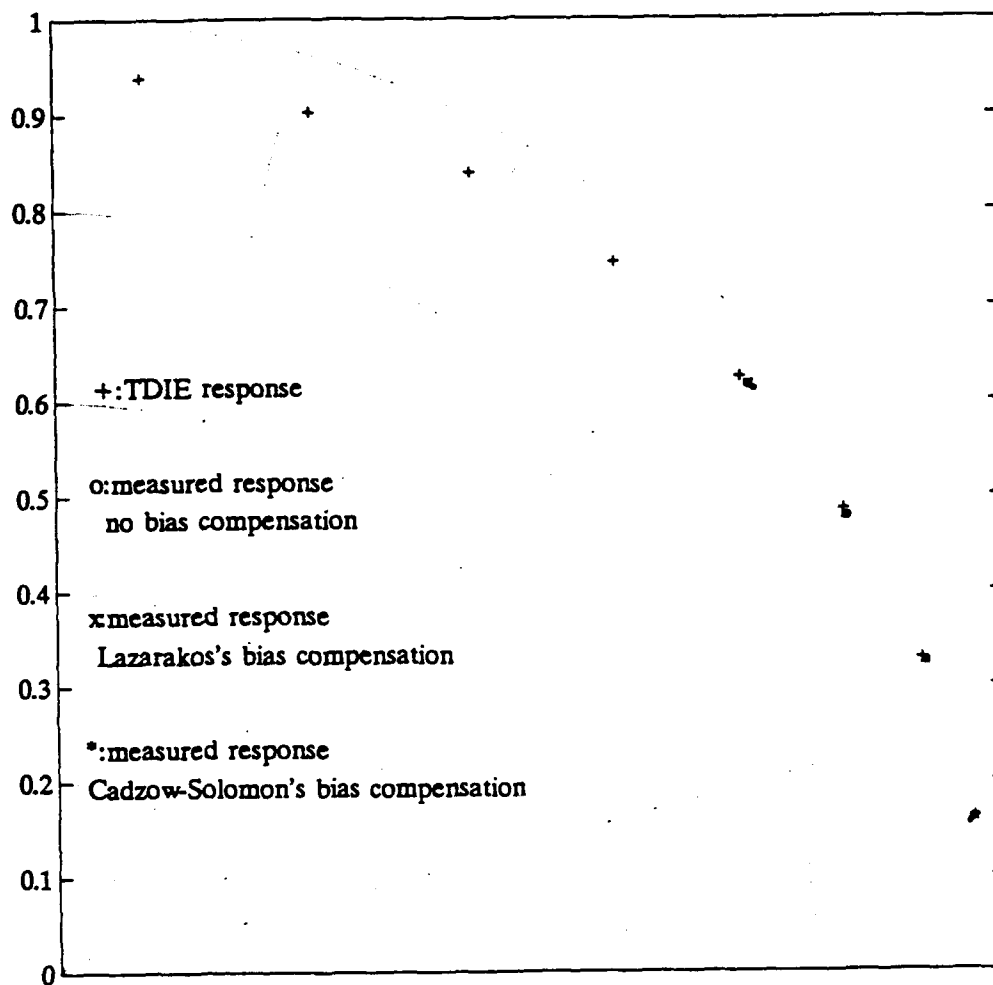
Figure 36   Poles at z-plane, 45 deg aspect
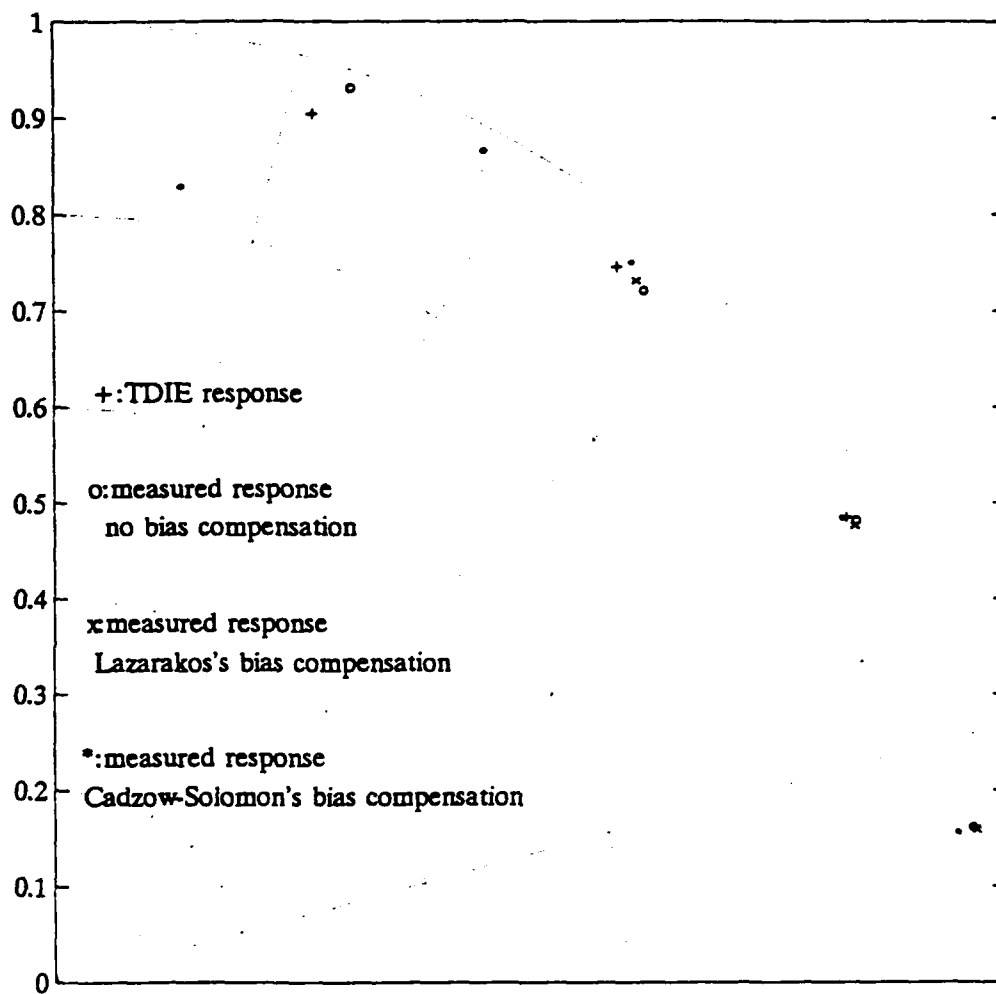
Figure 37   Poles at z-plane, 90 deg aspect

IV. POLES FROM SCALE MODEL AIRCRAFT

Scattering data for four different scale model aircraft targets were processed without bias compensation, using the Cadzow-Solomon algorithm. Poles were extracted from the measured scattering responses of the aircraft targets to double-Gaussian electromagnetic excitation incident at 0, 30, 90, and 180 degrees. The 0 degree aspect represents a nose-on measurement, while the 90 degree represents a broadside measurement. Signatures are shown in Figures 38-45 for targets 1 and 2.

The bandwidth of the TESL, 1-12 GHz, was matched to the scaling factor of the model aircraft targets. This scaling factor was 1/72 for all of the model aircraft targets used. Table IV contains the full scale, significant dimensions of these aircraft targets. The aircraft data was collected by Bresani [Ref. 17] at the four incident angles, as previously described.

Table IV   SCALED DIMENSIONS OF AIRCRAFT TARGETS

Target number	1	2	3	4
Overall length (cm)	26.5	22.5	23.6	26.2
Wingspan (cm)	19.8	19.0	16.4	16.0

A. DATA PROCESSING

The model aircraft scattering data was processed using a number of time points ranging from 200 to 240. The algorithm processing was started at the point of initial excitation.

The positioning of the excitation waveform was set up manually with respect to the response waveform from observations of the scattering data. Manual positioning for the driving waveform was required as no obvious condition existed for the model aircraft, as was the case for the thin-wire.

The number of asking poles was set to 60, as the value of 60 was found from previous experimentation to represent the most suitable results. The number of asking zeros was the same as the number of asking poles. This value was based on the fact that the computed early-time for the aircraft target is usually about $2L/c$. Conversion of this early-time to the appropriate number of time points (equal to the number of asking zeros) provides a number larger than the number of asking poles. However, the number of asking zeros may not be larger than the number of asking poles, the two values are set to be equal.

B. RESULTS FROM EXTRACTING THE POLES

The model aircraft scattering data showed that the poles were less likely to group than the thin-wire data. The highly complex nature of the aircraft scatterer combined with the

small number of significant data points (about 150) became a difficult problem for the algorithm to solve.

Figures 46-47 illustrate the spectrum of the data record for aircraft targets 1 and 2, for different incident angles.

Figures 48-51 illustrate the extraction of the poles from the same aircraft target for the combined aspects. To obtain an initial indication of the possibility of target identification by pole extraction, nose-on measurement results have been compared in Figures 52-53.

The thin wire data (Chapter III) indicated that the principle poles provided well defined clusters for all the incident angles examined, despite the use of a wide range of processing parameters. However, the scale model aircraft targets did not provide any well defined clusters under the limited attempts at pole estimation conducted here. The principle reason for this difference appears to be that the scale models have more complicated pole patterns than the thin wire targets and insufficient time was available to explore ideas for optimizing the performance of the estimation algorithm.

Processing the experimental scattering data for aircraft models, as performed herein, is only an initial attempt to demonstrate resonance estimation for real-world targets embodying complex configurations. Processing for this aircraft data was conducted for only one week at the end of the thesis research. It is recommended that this same data be used for a follow-on thesis.

solid:response   dash:excitation
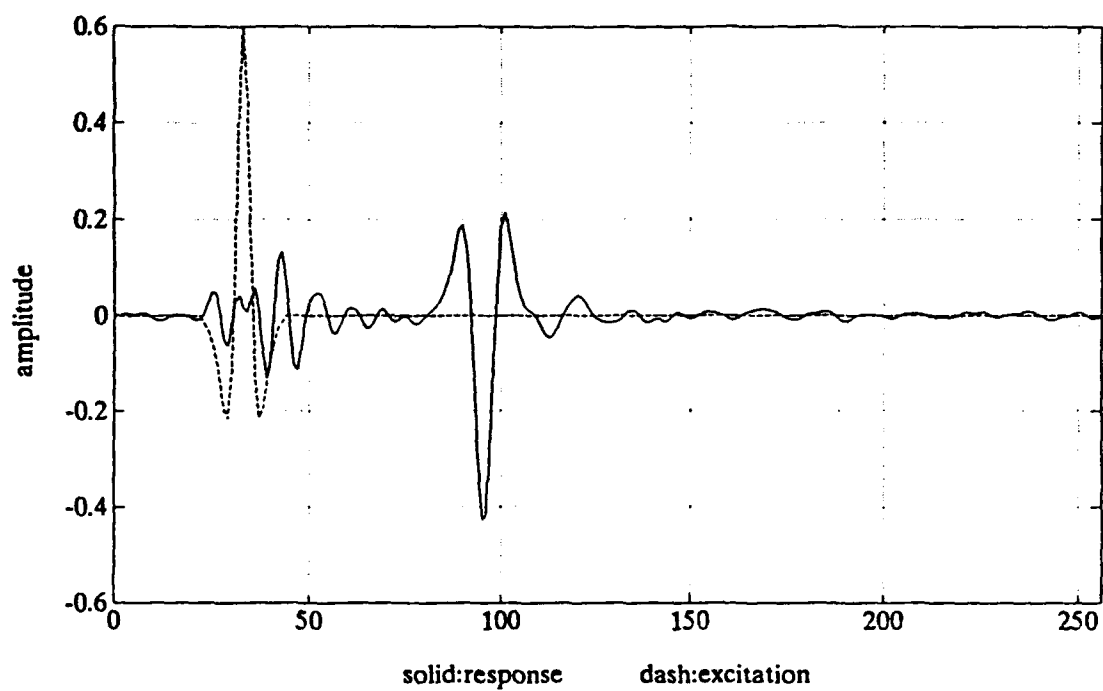
Figure 38   Measured response, model aircraft 1, 0 deg aspect

solid:response   dash:excitation
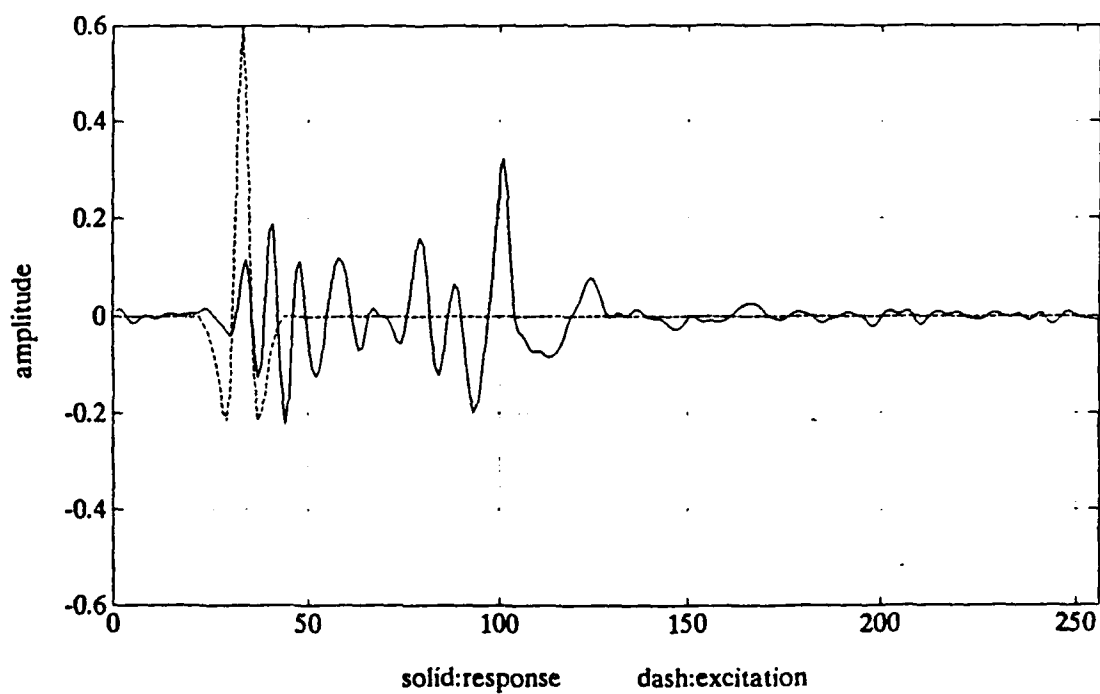
Figure 39   Measured response, model aircraft 1, 30 deg aspect

71

solid:response   dash:excitation
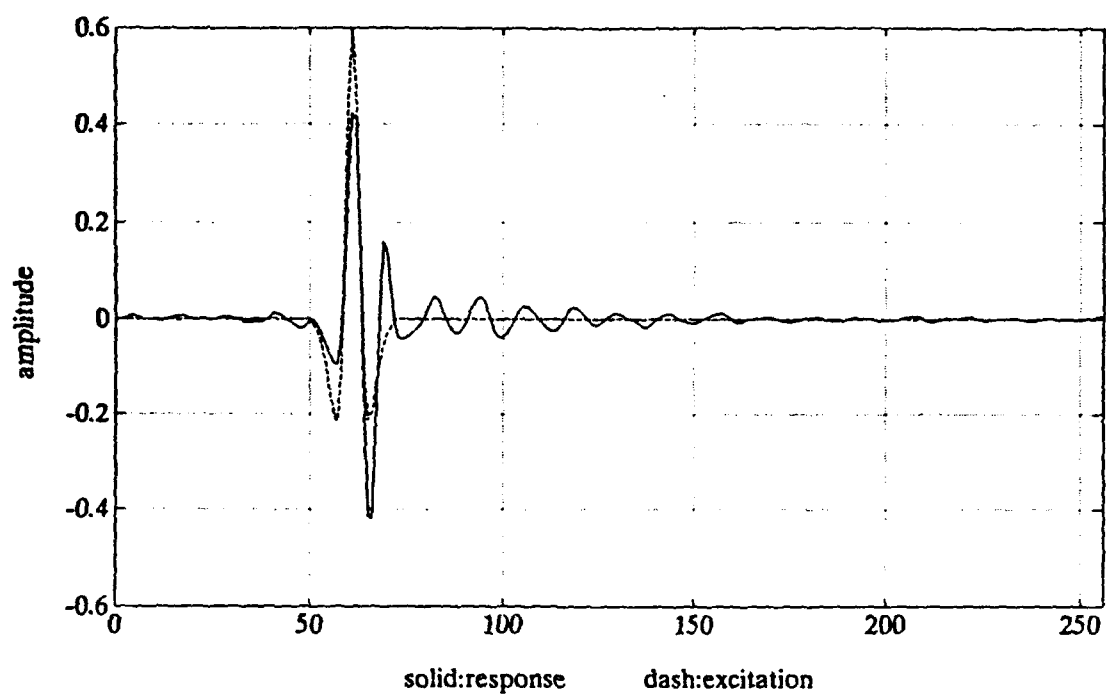
Figure 40   Measured   response,   model   aircraft   1,   90   deg
aspect

solid:response   dash:excitation
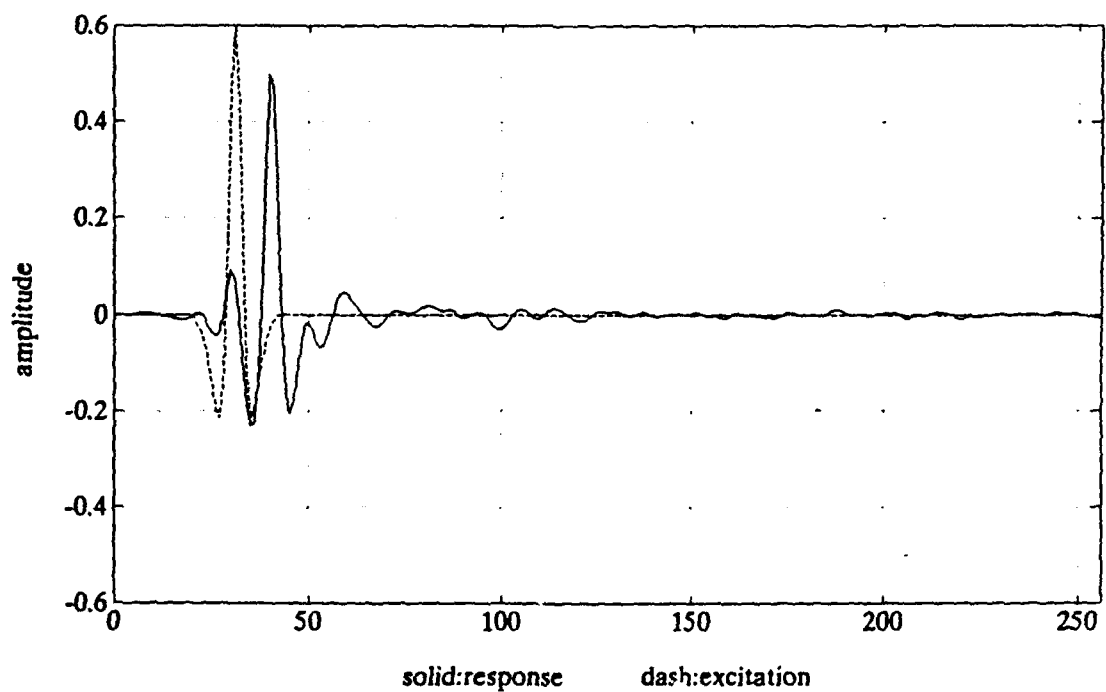
Figure 41   Measured   response,   model   aircraft   1,   180   deg
aspect

72

solid:response   dash:excitation
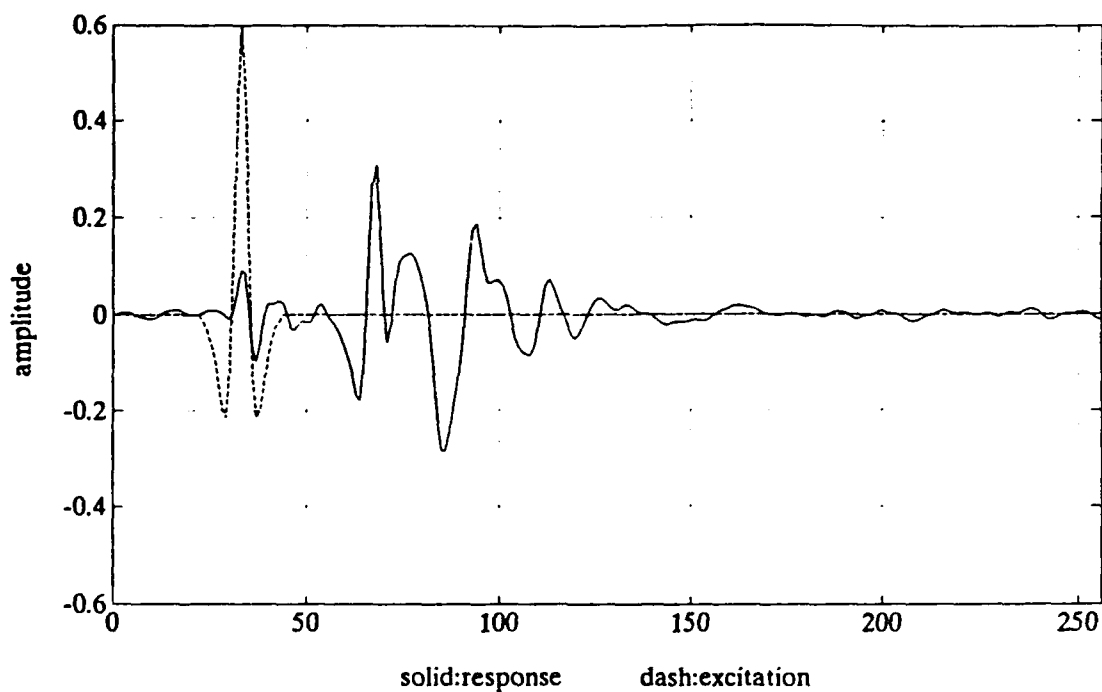
Figure 42   Measured response, model aircraft 2, 0 deg aspect

solid:response   dash:excitation
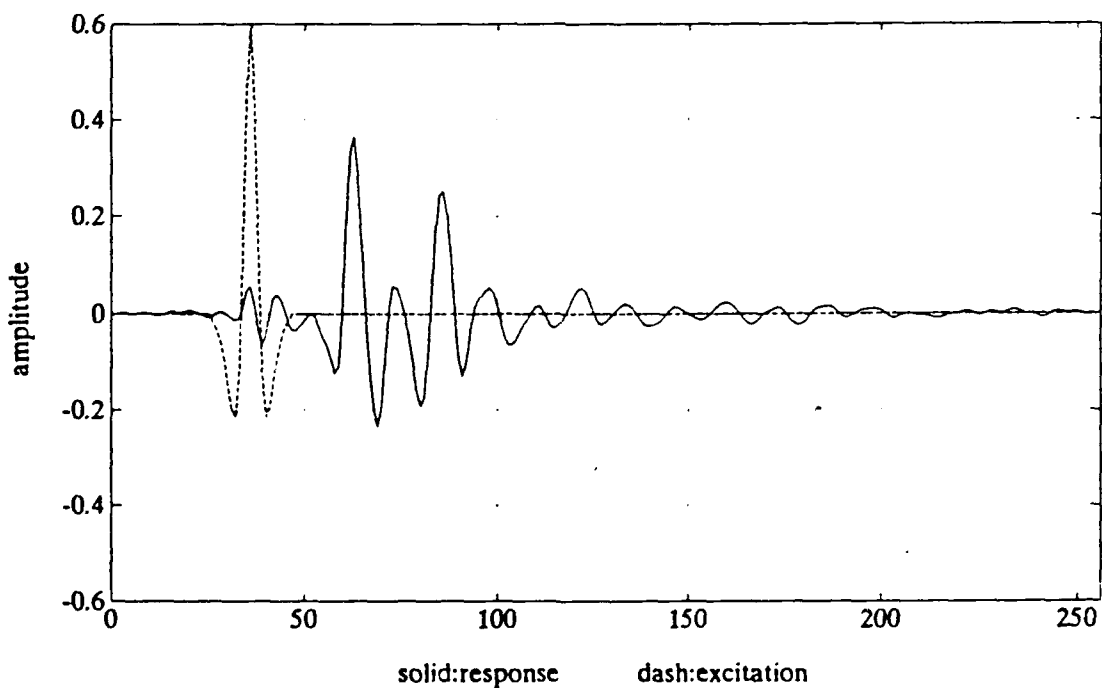
Figure 43   Measured response, model aircraft 2, 30 deg aspect

73

solid:response   dash:excitation
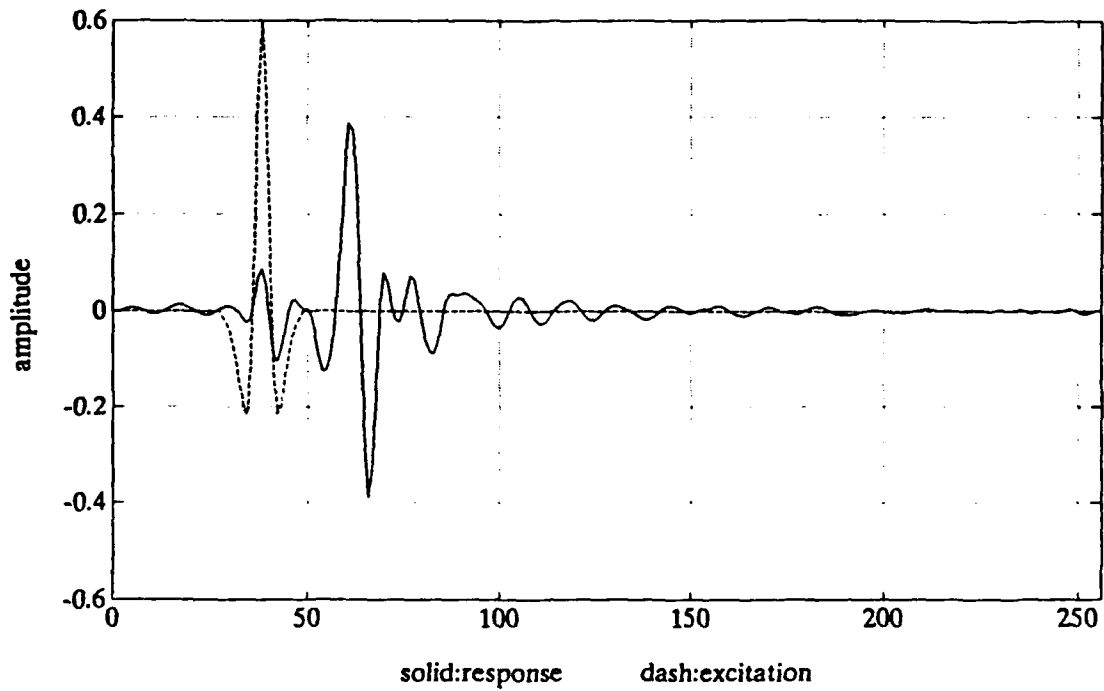
Figure 44   Measured response, model aircraft 2, 90 deg
aspect

solid:response   dash:excitation
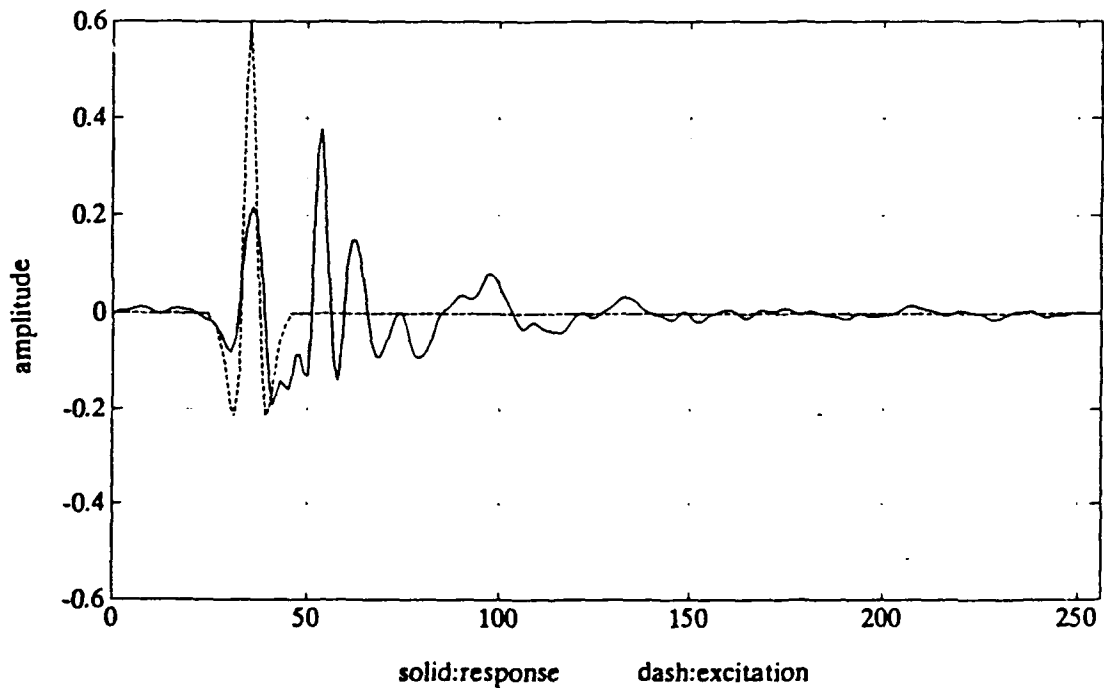
Figure 45   Measured response, model aircraft 2, 180 deg
aspect
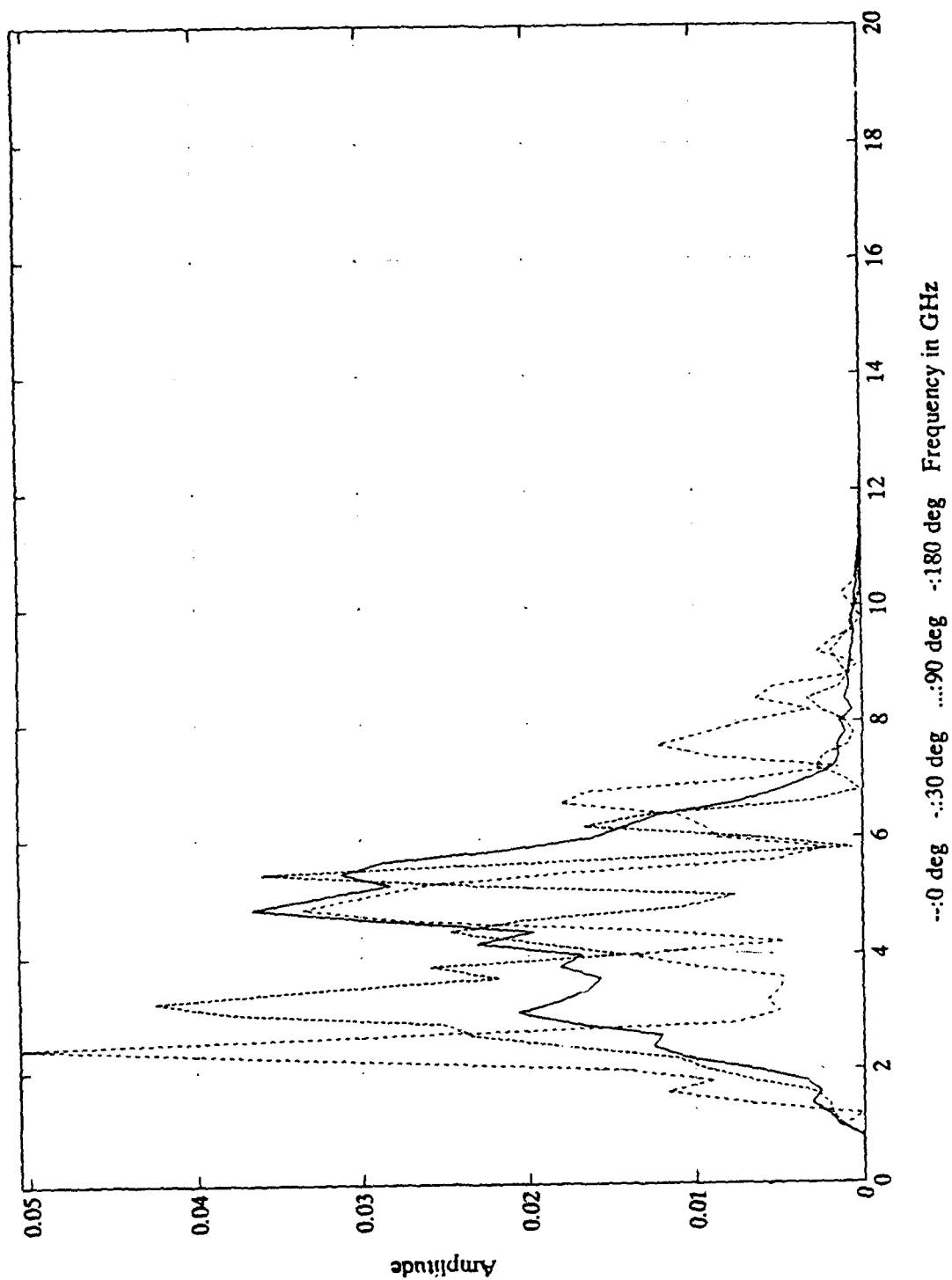
Figure 46 Spectrum of model aircraft 1 measured response, all aspects

75
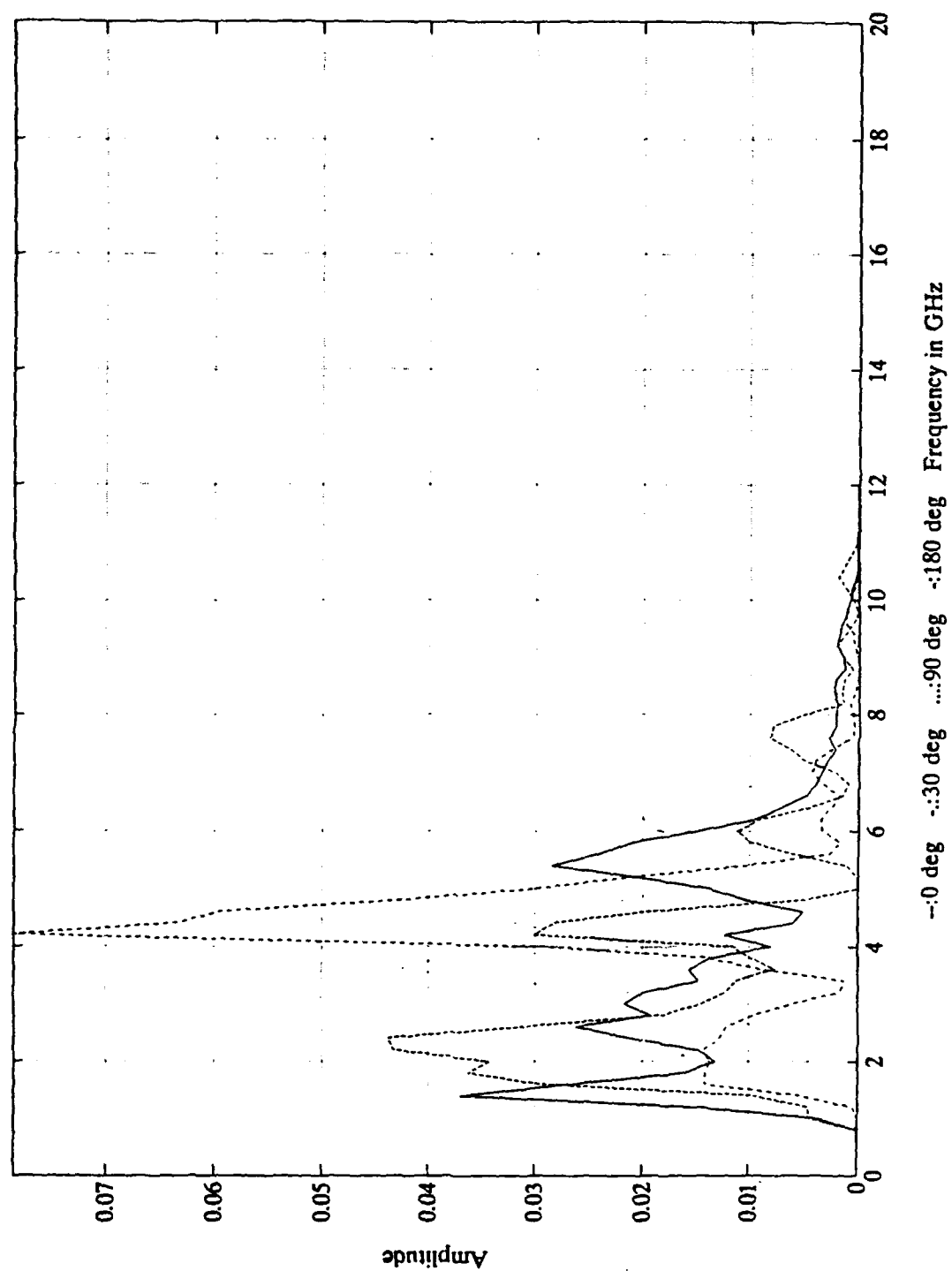
Figure 47   Spectrum of model aircraft 2 measured response, all aspects

76

Figure 48 Poles extracted from model aircraft 1 measured response in s-plane

77
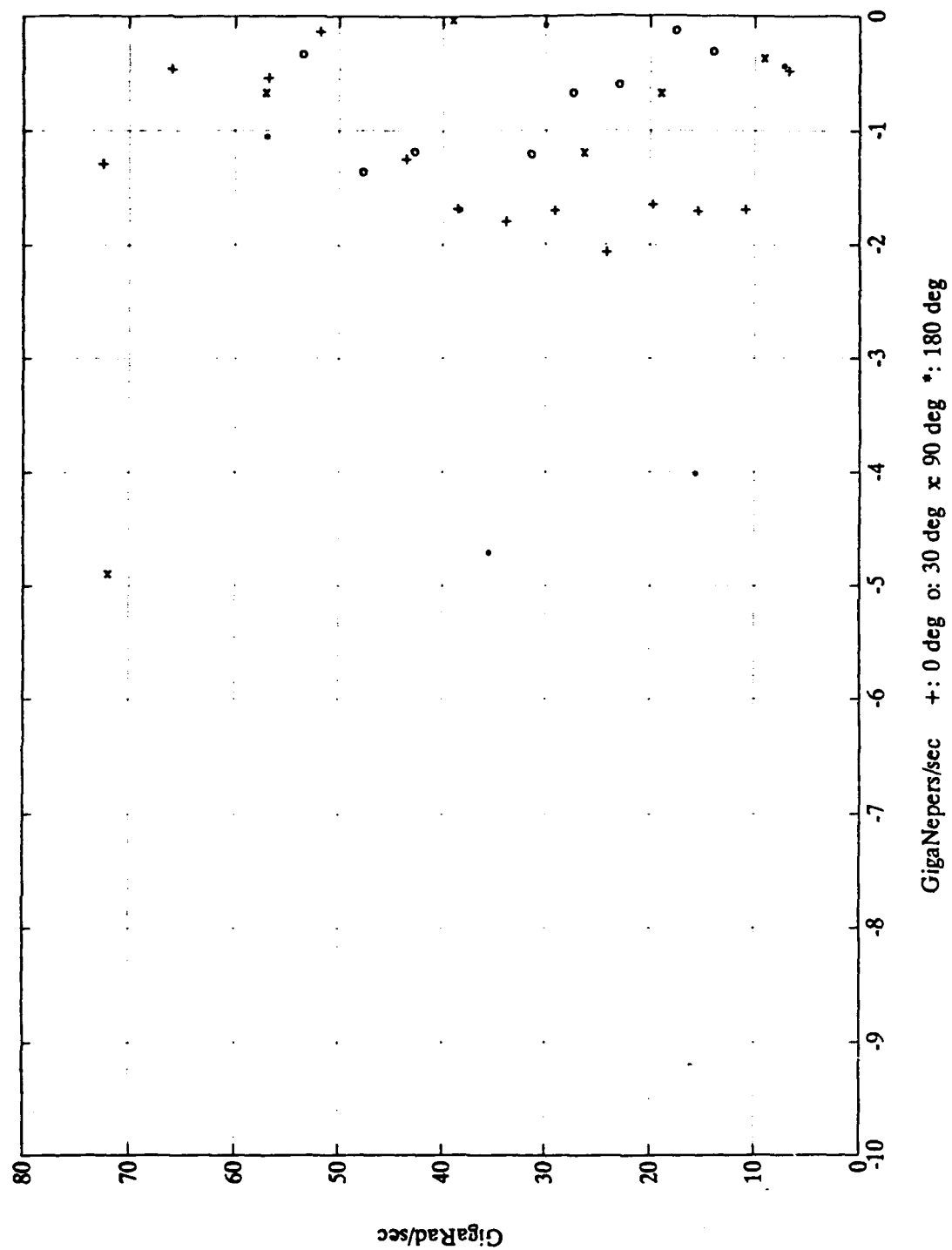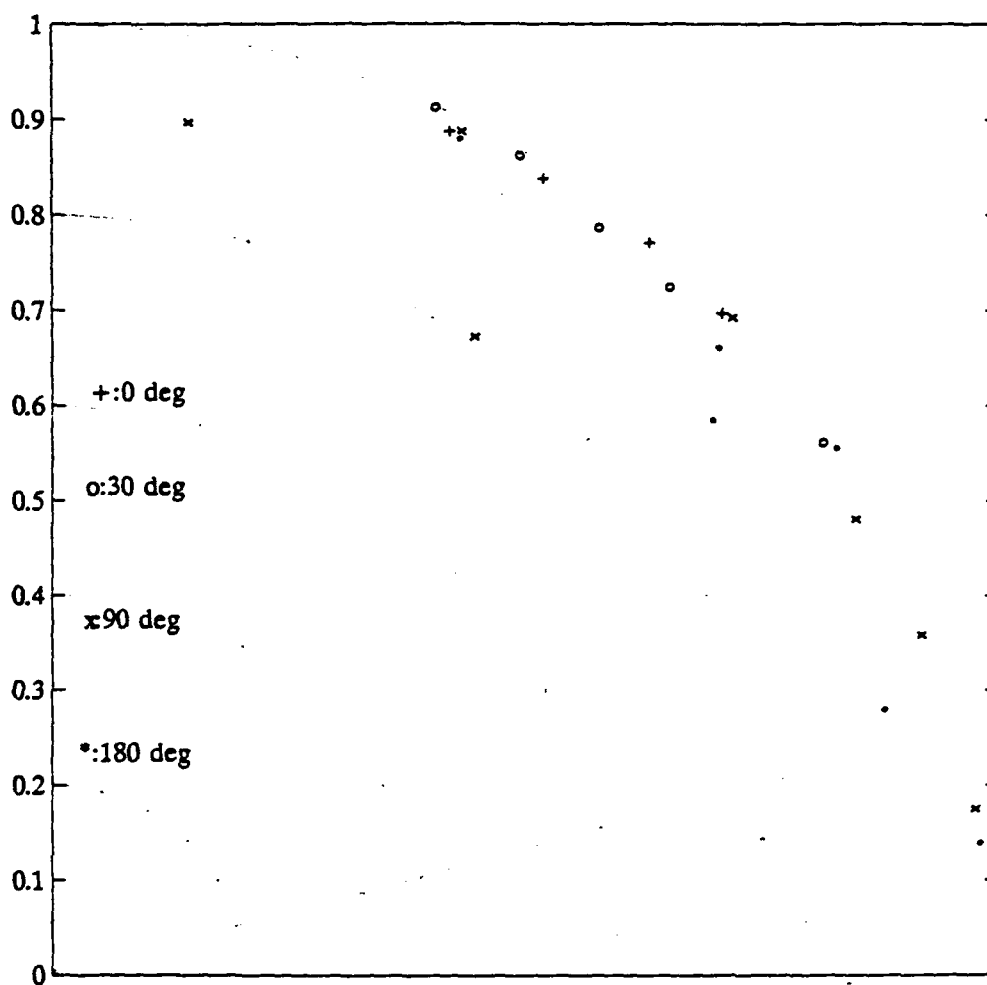
Figure 49 Poles extracted from model aircraft 1 measured response in z-plane

78
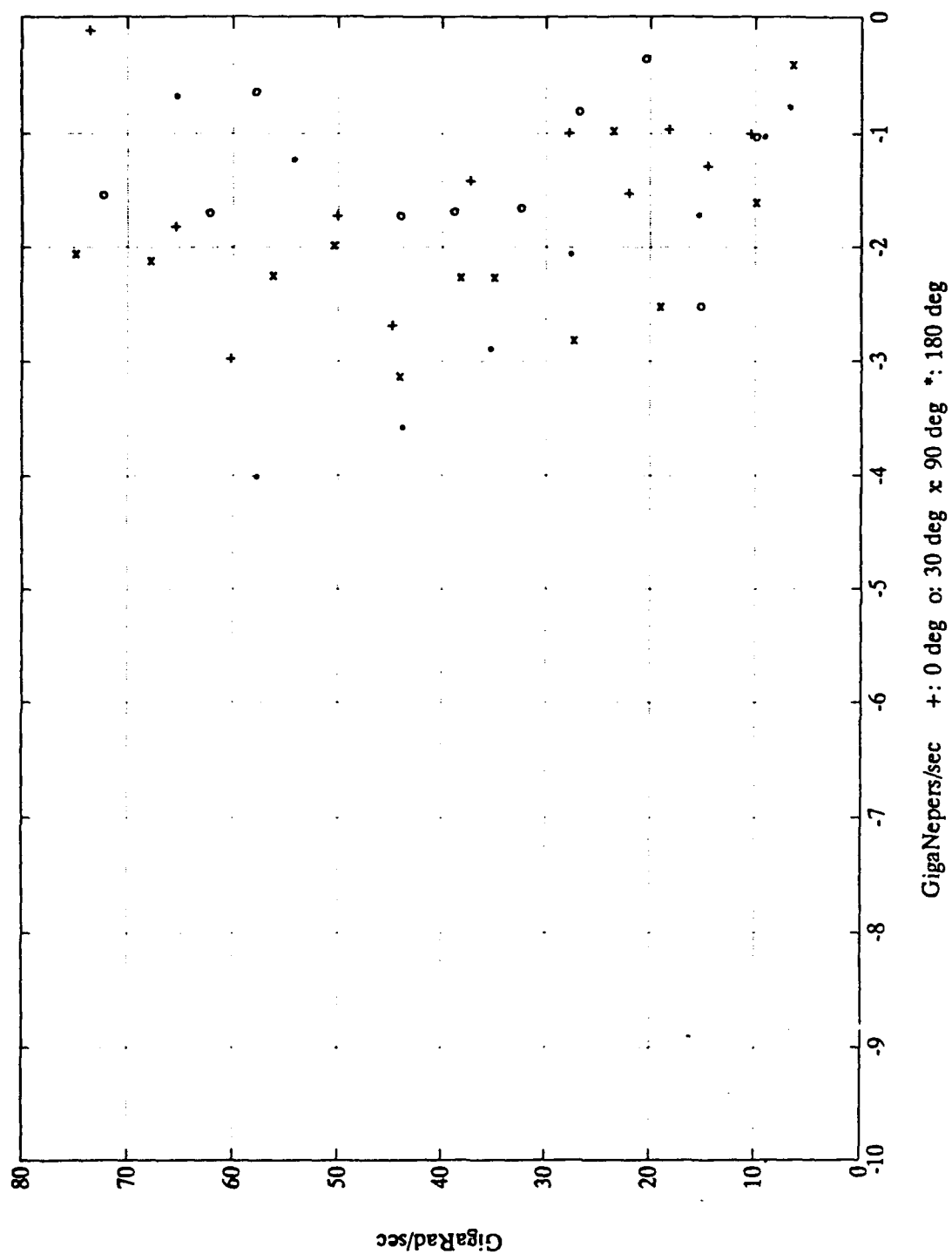
Figure 50 Poles extracted from model aircraft 2 measured response in s-plane

79
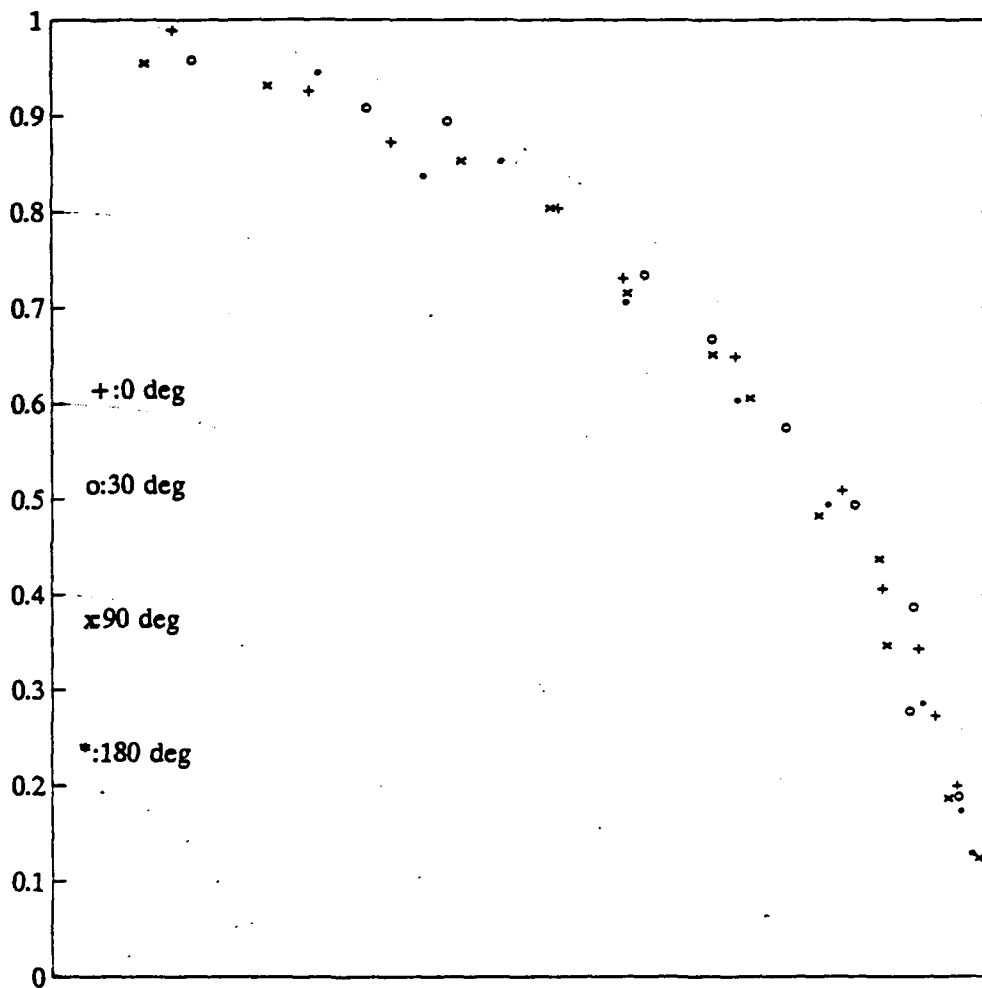
Figure 51 Poles extracted from model aircraft 2 measured response in z-plane

80
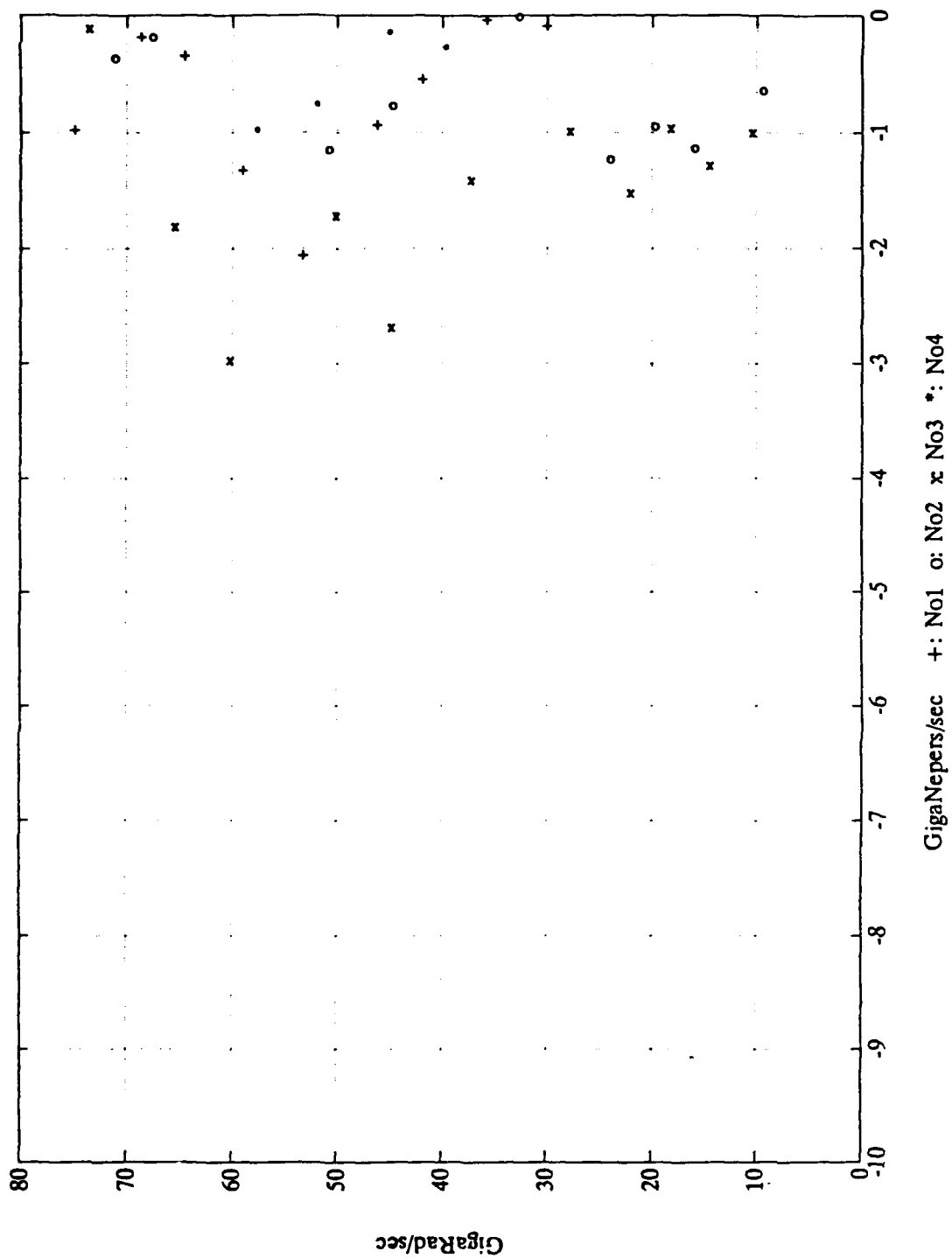
Figure 52 Poles extracted from four model aircraft in s-plane, nose-on
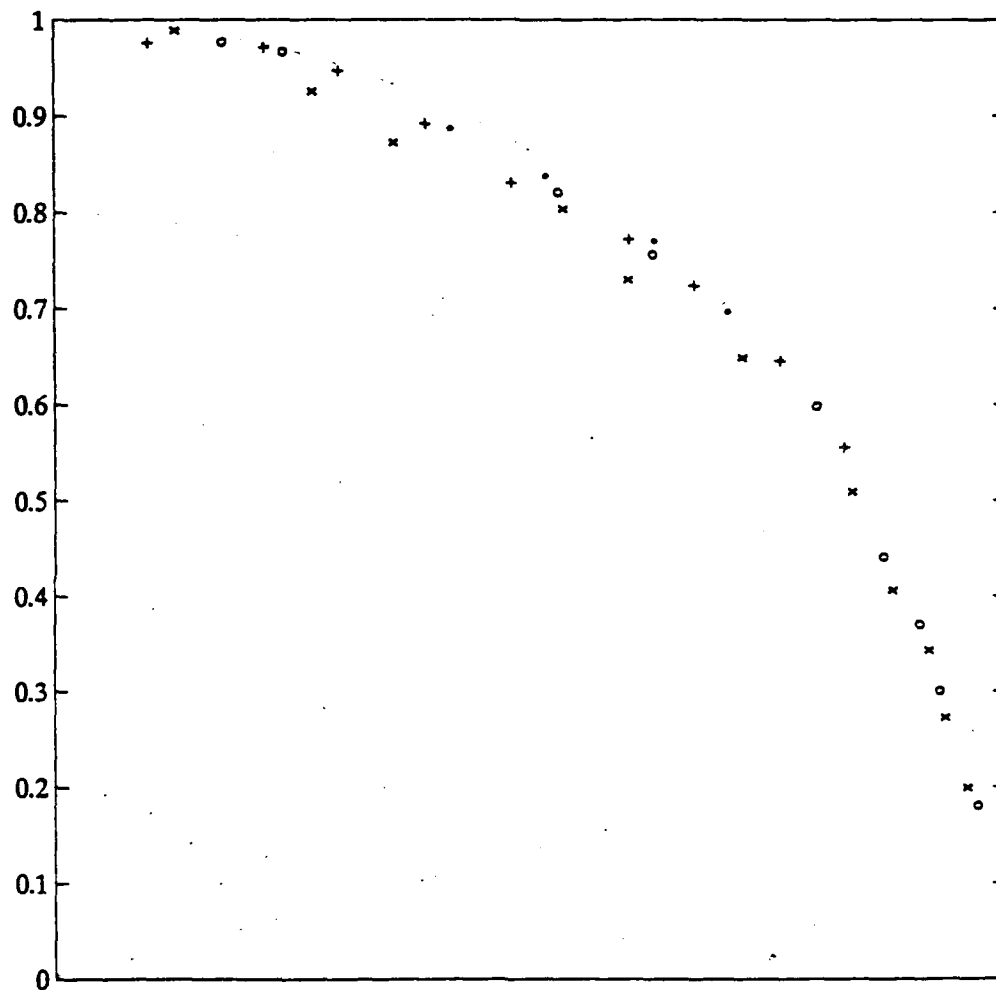
Figure 53 Poles extracted from four model aircraft in z-plane, nose-on

+ = No1   o = No2   x = No3   * = No4

V. SUMMARY AND CONCLUSIONS

A. SUMMARY

This thesis has attempted to demonstrate radar target identification by building on the earlier work of Norton [Ref. 11], Larison [Ref. 12] and Murphy [Ref. 13]. The largest portion of the work consisted of testing the Cadzow-Solomon algorithm using synthetic and thin wire measurement data.

Chapter I introduced the use of the Kumaresan-Tufts and the Cadzow-Solomon algorithms to locate target poles for a Non-Cooperative Target Recognition system. The resonance-based radar target identification problem was discussed and the transient electromagnetic scattering described.

Chapter II consisted of two parts. The first part discussed early methods used to solve target identification problems. This discussion included a description of Prony's method and also, Singular Value Decomposition on which the Kumaresan-Tufts and Cadzow-Solomon algorithms were developed. The Kumaresan-Tufts algorithm was developed in detail, including Norton's bias compensation method. The performance of the Kumaresan-Tufts algorithm was also demonstrated, as illustrated in Figures 3 through 10. The second part described the Cadzow-Solomon algorithm. Two bias compensation

methods were included: that of Cadzow-Solomon and that of the author.

Chapter III demonstrated the Cadzow-Solomon algorithm testing in two phases. The first phase of testing was performed with synthetic data, while the second phase was performed with thin wire measurement data. The thin wire data testing phase attempted to evaluate conditions appearing from a real target response. Results of the synthetic signal model testing are illustrated in Figures 13 through 23. The results of the thin wire scattering signature testing are illustrated in Figures 24 through 37.

Chapter IV considered an initial attempt at extraction of poles from scale model aircraft measurements obtained in the NPS Transient Electromagnetic Scattering Lab. Measurement data was processed using the Cadzow-Solomon algorithm and the unsuccessful results are illustrated in Figures 38 through 53.

Testing of both the Kumaresan-Tufts and the Cadzow-Solomon algorithms was performed using MATLAB programs. A sequence of programs was written to complete the demonstration of the target identification problem. Appendices A to E present only a part of this sequence of programs, including the theoretical models of the Cadzow-Solomon algorithm.

B. CONCLUSIONS

Both the Kumaresan-Tufts and the Cadzow-Solomon algorithms can effectively extract poles from the scattering response of simple high-Q targets such as thin wires. As the late-time portion of the response signal is weak (with low SNR) and the Cadzow-Solomon algorithm has the ability to use the early-time portion, this thesis concentrated mainly on the use of the Cadzow-Solomon algorithm.

The Cadzow-Solomon algorithm extracts poles of synthetically generated data, integral equation computed data, and thin wire measured scattering data with excellent results. A signal-to-noise ratio above 10 dB is required, depending on the damping rate of the data. The system order is intentionally overestimated. The excess order provides the flexibility to model the noise and improves the estimation of parameters of exponentially damped sinusoidal signals in noise. The Singular Value Decomposition method alleviates severe ill-conditioning of the data matrix. Backward prediction and SVD are used to separate the computed signal poles from spuriously computed noise poles introduced by the overestimated system order.

The most critical parameters required for the successful thin-wire processing were the selection of the appropriate starting point to begin the data processing and the appropriate system order. The best results were obtained with the starting point of the data processing set at the

excitation starting point, and with the processing system order at about 3 times the true system order.

The existence of noise in the target's response produces a bias in the positioning of the extracted poles. Thus, several bias compensation schemes may be developed.

Given a very limited initial effort, the Cadzow-Solomon algorithm was unable to extract poles of scale model aircraft scattering data with adequate accuracy. It is conjectured that the data points in the natural mode information response are too few for the algorithm to model both the target poles and the noise poles.

APPENDIX A. ARMA COEFFICIENT AND RECURSIVE SIGNAL GENERATOR

PROGRAM LISTING

```
%                        ARMAGEN1.M
%
%    Program generates a(k), b(k) coefficients of
%
%           b(0)+b(1)*z^-1+...+b(q)*z^-q
%    H(z) = -----------------------------
%              1 +a(1)*z^-1+...+a(p)*z^-p
%
%    given the s-plane poles, residues, number of time points
%    and time window.
%    Programed by Gregory Lazarakos, 5 Mar 1991.
%
!del temp.mat
case='synt';
    dt=t0./(notp-1);
    i=sqrt(-1);
    dm=exp((sigma+i*omega)*dt);
    alpha=ampl.*exp(i*phase);
    dm=dm';
    alpha=alpha';
    ['Please wait...']
    [b,a]=residue(alpha,dm,0);
    A=real(a);
    B=real(b);

%    Program generates time response of an ARMA system
%    via the equation
%             N                        L
%    y(n) = SUM A(k)*y(n-k+1) + SUM B(k)*x(n-k+1)  ,for n=1:notp
%           k=2                      k=1
%    given A(k), B(k) and input excitation record x(n).
%    Programed by Gregory Lazarakos, 10 Mar 1991.
    N=size(A);
    N=N(2);
    L=size(B);
    L=L(2);
    for j=2:N
        A(j)=-A(j);
    end
%
    ['Excitation is double Gaussian']
    excgen
```

```
%
    ['Please wait...']


    ye=zeros(1,notp);
    ye(1)=B(1)*x(1);
    energy=(ye(1)).^2;
    for n=2:notp
        ye(n)=0.0;
        Ln=[n;L];
        Lmax=min(Ln);
        for k=1:Lmax
            ye(n)=ye(n)+B(k)*x(n-k+1);
        end
        Nn=[n;N];
        Nmax=min(Nn);
        for k=2:Nmax
            ye(n)=ye(n)+A(k)*ye(n-k+1);
        end
        energy=energy+(ye(n)).^2;
    end
    rms=sqrt(energy);
    ic=zeros(1,notp);
    for n=1:notp
        ic(n)=ye(n)./rms;
    end
%
    axis([0 notp -0.4 0.8])
    plot(ic)
  title(['Generated  signal  w/o  noise,  medium  Q,  by
',int2str(nop),' poles']);
    xlabel('time points');
    ylabel('amplitude rms');
    grid;
    pause
    hard=input('Do you want a hardcopy for the plot? [n] :
','s');
      if hard=='y'
        plotfile=input('Enter filename : ','s');
        eval(['meta ',plotfile])
      end
```

88

APPENDIX B. DOUBLE GAUSSIAN SMOOTHING FUNCTION GENERATOR

PROGRAM LISTING

```
%                          EXCGEN.M
%
%    Program generates excitation record x(n) for a response
%    from TESL data and synthetic data,
%    via the equation of a double Gaussian waveform
%
%    x(n) = A1*exp(-a1*t^2) - A2*exp(-a2*t^2)
%
%    given the time window.
%    Program uses input values of the 10% height of the low
%    and high frequency ends of the double Gaussian frequency
%    response to determine the pulse widths in the time domain.
%    Programed by Gregory Lazarakos, 8 Apr 1991.
%    Last Revision August 6, 1991.
  if case=='meas'
     if filename(1)=='F'
         LENGTH=0.25;
     elseif filename(siz-1:siz)=='sp'
         LENGTH=eval(filename(3:4));
         LENGTH=LENGTH/100;
     else
         LENGTH=0.1;
     end
  end
     npts=notp;
     tmin=0.0;
     tmax=t0;
     DT=dt;
     T1=0.147;
     T2=0.314;
     thr=input('Enter   threshold   value   for   time   in   nsec
[1.25]:');
     if isempty(thr)
         thr=1.25;
     end
     a1=(4.0.*log(10))./(T1.^2);
     a2=(4.0.*log(10))./(T2.^2);
     A1=sqrt(a1)./(sqrt(a1)-sqrt(a2));
     A2=A1-1.0;
  if case=='synt'
     point=input('Which   to   be   the   point,   the   excitation
starts?');
     x=zeros(1,npts);
     for n=1:npts
```

```matlab
            t=(n-11-point).*DT;
            if t<=thr
                e1=A1.*exp(-a1.*t.^2);
                e2=A2.*exp(-a2.*t.^2);
                x(n)=e1-e2;
            else
                x(n)=0.0;
            end
    end
  elseif case=='meas'
    asprad=aspect*(pi/180);
  top=input('Do you want to position the excitation, auto or
manual ? (a,m) : ','s');
    if top=='a'
        [maxic,index1]=max(ic);
        [minic,index2]=min(ic);
        x=zeros(1,npts);
        tdel=cos(asprad)*(2*LENGTH/3e8);
        ndel=round(tdel/(dt*1e-9));
        if abs(maxic)>=abs(minic)
            point=index1-11-ndel;
            for n=1:npts
                t=(n-index1+ndel).*DT;
                if abs(t)<=10*DT
                    e1=A1.*exp(-a1.*t.^2);
                    e2=A2.*exp(-a2.*t.^2);
                    x(n)=e1-e2;
                else
                    x(n)=0.0;
                end
            end
            x=x*0.6;
        else
            point=index2-11-ndel;
            for n=1:npts
                t=(n-index2+ndel).*DT;
                if abs(t)<=10*DT
                    e1=A1.*exp(-a1.*t.^2);
                    e2=A2.*exp(-a2.*t.^2);
                    x(n)=e1-e2;
                else
                    x(n)=0.0;
                end
            end
            x=x*0.6;
        end
    end
    if top=='m'
        point=input('Which to be the point, the excitation
starts ? ');
        x=zeros(1,npts);
```

```
        for n=1:npts
            t=(n-11-point).*DT;
            if abs(t)<=10*DT
                e1=A1.*exp(-a1.*t.^2);
                e2=A2.*exp(-a2.*t.^2);
                x(n)=e1-e2;
            else
                x(n)=0.0;
            end
        end
        x=x*.6;
    end
    ltst=(1+cos(asprad))*(LENGTH/3e8);
    nltst=round(ltst/(dt*1e-9));
    ltimp=point+22+nltst;
else
  exit
end

if case=='synt'
    axis([0 notp -0.4 1])
    plot(x)
  title('Double-Gaussian Smoothing Function');
    xlabel('time points');
    ylabel('amplitude rms');
elseif case=='meas'
    plot(1:npts,x,'--',1:notp,ic,ltimp,ic(ltimp),'*')
    if filename(1)=='F'
  title(['Data response signal from aircraft',filename(1:3),',
aspect=',num2str(aspect),' deg ']);
    elseif filename(siz-1:siz)=='sp'
  title(['Data response signal from sphere',filename(3:4),'cm,
aspect=',num2str(aspect),' deg ']);
    else
  title(['Data     response     signal     from     thin     wire,
aspect=',num2str(aspect),' deg ']);
    end
    xlabel('solid=response          dash=excitation');
    ylabel('amplitude ');
    text(ltimp,0.1,'-----late time----->');
    if filename(1:2)=='et'
      text(100,0.4,'TDIE response');
    end
    grid;
else
    exit
end
    pause
    hard=input('Do  you  want  a  hardcopy  for  the  plot?
[n]:','s');
        if hard=='y'
```

```
            plotfile=input('Enter filename : ','s');
            eval(['meta ',plotfile])
        end
  if case=='meas'
      save temp ic energy x point dt t0 notp filename aspect siz
LENGTH
  end
```

APPENDIX C. SYNTHETIC NOISE GENERATOR

PROGRAM LISTING

```
%                          NOISEGEN.M
%
%     Synthetic Noise Generation
%     Programmed by Greg Lazarakos 20/2/91
%
      SN=input('How many db ? (7,10,20,30) [20]:');
      if isempty(SN)
          SN=20;
      end
      sn=SN./10;
      sn=10.^sn;
      en=0;
      for k=1:notp
          en=en+(ic(k)).^2;
      end
      ava=en./(notp.*sn);
      ava=sqrt(ava);
      rand('normal')
      w=rand(ic)*ava;
      ic=ic+w;
%
      save temp ic x point filename w ye energy dt dm notp omega
sigma t0        .
%
      axis([0 notp -0.4 0.8])
      plot(ic)
title(['Generated signal with noise S/N=',int2str(SN),' db']);
      xlabel('time points');
      ylabel('amplitude rms');
      grid;
      pause
      hard=input('Do  you  want  a  hardcopy  for  the  plot?
[n]:','s');
       if hard=='y'                        .
          plotfile=input('Enter filename : ','s');
          eval(['meta ',plotfile])
        end
```

APPENDIX D. SPECTRUM ESTIMATION

PROGRAM LISTING

```
%                         SPECTRUM.M
%
%    Programed by Gregory Lazarakos, 16 Apr 1991.
%    Last revision, 6 Aug 1991.
     df=1./((notp-1).*dt);
     IC=fft(ic,notp);
     f=(0:notp-1)*df;
     fmax=1./dt;
     axis([0 fmax -3 3])
     plot(f,IC)
     title('Fourier transform of the response signal');
     xlabel('Frequency in GHz');
     ylabel('Amplitude');
     grid;
     pause
     SIC=(abs(IC)).^2;
     SIC=SIC/notp;
     axis([0 20 0 max(SIC)])
     plot(f,SIC)
     if isempty(SN)
     title('Spectrum of the response signal ');
     else
     title(['Spectrum    of    the    response    signal    with
S/N=',int2str(SN),' db']);
     end
     xlabel('Frequency in GHz');
     ylabel('Amplitude');
     grid;
     pause
     hard=input('Do you want a hardcopy for the plot?
[n] : ','s');
        if hard=='y'
           plotfile=input('Enter filename : ','s');
           eval(['meta ',plotfile])
        end
```

APPENDIX E. THE CADZOW-SOLOMON POLE EXTRACTION ALGORITHM

PROGRAM LISTING

```
%                              CADSOL1.M
%
% Cadzow-Solomon's Algorithm for Extracting the Poles
% and Residues
% Version 1.0
% Programmed by Greg Lazarakos 3/16/91
%
% Set the first sample (kapa)
  if point>0
     kapa=point;
  else
     kapa=1;
  end
% Set the number of samples (CN)
  CN=input('How many samples to process ? (>120) [200]:');
  if isempty(CN)
     CN=200;
  end
% Compute the SNR for the processed time window
  en=0;
  nen=0;
  for k=kapa:CN
     en=en+(ic(k)).^2;
     nen=nen+(w(k)).^2;
  end
  SNR=en./nen;
  SNR=10.*log10(SNR);
% Set the number of poles (CL) > number of real poles (CM)
% CM <= CL and 2*CL <= CN-CL
  CL=input('How many unknown poles ? (>20) [60]: ');
  if isempty(CL)
     CL=60;
  end
% Set the number of expected zeros (CK)
  CK=input('How many expected zeros ? [No. poles]: ');
  if isempty(CK)
     CK=CL
  end
  ['Please wait...']
% Forming the matrix YI[(CN-CL)*CL] from the data ic(n)
     YI=zeros(CN-CL,CL);
  for j=kapa+1:CN-CL+kapa
     YI(j-kapa,:)=ic(j:j+CL-1);
  end
% Forming the matrix h[(CN-CL)*1] from the data ic(n)
```

```
      h=[ ];
      h=ic(kapa:CN-CL+kapa-1);
      h=h';
% Forming the matrix XI[(CN-CL)*CK] from the data x(n)
      XI=zeros(CN-CL,CK);
   for j=1:CN-CL
      XI(j,:)=x(j:j+CK-1);
   end
% Unify matrices YI and XI as I=[YI|XI]
   I=[YI XI];
% Set the tolerance
   tol=0.000001;
% Find the vector of backward prediction coefficients
   beta=pinv(I,tol)*[h];
% Set the coefficients of the prediction-error filter
polynomial
      ca=zeros(1,CL+1);
      ca(1)=1;
   for j=1:CL
      ca(j+1)=-beta(j);
   end
% Set the coefficients of the polynomial B(z)
      cb=zeros(1,CK);
   for j=1:CK
      cb(j)=beta(j+CL);
   end
% Find the residues and the poles
   [resid,d,gk]=residue(cb,ca);
% Find the signal poles
   s=log(d)/dt;
   k=0;
   l=0;
   for j=1:CL
      if real(s(j))>0,
         k=k+1;
         poles1(k)=-s(j);
         resid1(k)=resid(j);
      else
         l=l+1;
         nopol1(l)=-s(j);
         nores1(l)=resid(j);
      end
   end
   dm1=exp(poles1*dt);
   dm2=exp(nopol1*dt);
   alpha1=exp(resid1*dt);
   CM=k;
   ['The signal has the following ',num2str(CM),' real poles.']
   poles1
```

LIST OF REFERENCES

1. Air Force Weapons Laboratory Interaction Note 88, <u>On the Singularity Expansion Method for the Solution of Electromagnetic Problems</u>, by C.E.Baum, December 1971.

2. Moffatt, D.L. and Mains, R.K., "Detection and Discrimination of Radar Targets", <u>IEEE Trans. on Antennas and Propagation</u>, AP-23, pp. 358-367, May 1975.

3. Morgan, M.A., "Singularity Expansion Representations of Fields and Currents in Transient Scattering", <u>IEEE Trans. on Antennas and Propagation</u>, AP-32, pp. 466-473, May 1984.

4. Kumaresan, R. and Tufts, D.W., "Estimating the Parameters of Exponentially Damped Sinusoids and Pole-Zero Modeling in Noise", <u>IEEE Trans. on Acoustics, Speech and Signal Processing</u>, ASSP-30, pp. 833-840, December 1982.

5. Cadzow, J.A. and Solomon Jr., O.M., "Algebraic Approach to System Identification", <u>IEEE Trans. on Acoustics, Speech and Signal Processing</u>, ASSP-34, 3, pp. 462-469, June 1986.

6. Abstracts of 1986 National Radio Science Meeting, <u>Discrimination of Scatterers using Natural Resonance Annihilation</u>, by M.A. Morgan and J.B. Dunavin, Philadelphia, PA, June 1986.

7. Morgan, M.A., "Scatterer Discrimination Based upon Natural Resonance Annihilation", <u>Journal of Electromagnetic Waves and Applications</u>, vol.2, no.5/6, pp. 481-502, 1988.

8. Van Blaricum, M.L. and Mittra, R., "A Technique for Extracting the Poles and Residues of a System Directly from Its Transient Response", <u>IEEE Trans. on Antennas and Propagation</u>, AP-23, 6, pp. 777-781, November 1975.

9. Van Blaricum, M.L. and Mittra, R., "Problems and Solutions Associated with Prony's Method for Processing Transient Data", <u>IEEE Trans. on Antennas and Propagation</u>, AP-26, 1, pp. 174-182, January 1978.

10. Strang, G., <u>Linear Algebra and Its Applications</u>, 3d ed., pp. 442-452, Hancourt Brace Jovanovich, Inc., 1988.

11. Norton, S.A., <u>Radar Target Classification by Natural Resonances: Signal Processing Algorithms</u>, Master's Thesis, Naval Postgraduate School, Monterey, CA, March 1988.

12. Larison, P.D., <u>Evaluation of System Identification Algorithms for Aspect-Independent Radar Target Classification</u>, Master's Thesis, Naval Postgraduate School, Monterey, CA, December 1989.

13. Murphy, T.J., <u>Natural Resonanse Extraction and Annihilation Filtering Methods for Radar Target Identification</u>, Master's Thesis, Naval Postgraduate School, Monterey, CA, September 1990.

14. Morgan, M.A., <u>Thin-wire Integral Equation Program</u>, Naval Postgraduate School, Monterey, CA, 1988.

15. Sayre, E.P. and Harrington, R.F., "Time-domain radiation and scattering by thin wires", <u>Applied Science Res.</u>, v.26, pp.413-444, 1972.

16. Morgan, M.A. and McDaniel, B.W., "Transient Electromagnetic Scattering: Data Acquisition and Signal Processing", <u>IEEE Trans. on Instrumentations and Measurement</u>, v.37, 2, June 1988.

17. Bresani, A., <u>Performance Enhancement of the NPS Transient Electromagnetic Scattering Lab</u>, Master's Thesis, Naval Postgraduate School, Monterey, CA, September 1991.

INITIAL DISTRIBUTION LIST

No. Copies

1. Defense Technical Information Center   2
   Cameron Station
   Alexandria, Virginia 22304-6145

2. Library, Code 52   2
   Naval Postgraduate School
   Monterey, California 93943-5002

3. Group Chairman, Code EW   1
   Electronic Warfare Academic Group
   Naval Postgraduate School
   Monterey, California 93943-5100

4. Professor Michael A. Morgan, Code EC/Mw   6
   Department of Electrical and Computer Engineering
   Naval Postgraduate School
   Monterey, Californi. 93943-5000

5. Professor Jeffrey B. Knorr, Code EC/Ko   1
   Department of Electrical and Computer Engineering
   Naval Postgraduate School
   Monterey, California 93943-5000

6. Naval Attache   2
   Embassy of Greece
   2228 Massachusetts Ave. NW
   Washington, District of Columbia 20008

7. LTJG Gregory Lazarakos, HN   1
   12 Eftalioti St.
   Athens, 15126
   GREECE